Multi-temporal landsat images classification and change analysis of land cover in urban areas

	2012
URL	http://id.nii.ac.jp/1342/00001020/

Master's Thesis

MULTI-TEMPORAL LANDSAT IMAGES CLASSIFICATION AND

CHANGE ANALYSIS OF LAND COVER IN URBAN AREAS

September 2012

Graduate School of Marine Science and Technology

Tokyo University of Marine Science and Technology

Master's Course of Marine Technology and Logistics

NANG MYA MYA NWE

DECLARATION

I hereby declare that this dissertation has been composed by myself and is a result of my own investigation. It has never been accepted, nor submitted for any other degrees. All sources of information have been duly acknowledged.

Nang Mya Mya Nwe

TABLE OF CONTENTS

ACKNOWLEDGEMENT

ABSTRACT

Remotely sensed data have been widely used to map land cover which is an important parameter in the studies of natural resource management and sustainable development. This research work is to evaluate land cover change in urban areas and to analyze the impact of these changes on land surface temperature (LST) by using geographic information system (GIS) and remote sensing images. The study is also intended to provide accurate evaluation of land cover for managing natural resources and monitoring environmental changes.

In this study, a classification method has been developed for producing land cover maps from Landsat images (30m resolution) in two study areas, Hino city in Japan and Mandalay city in Myanmar. The method is simply based on training pixels collected from known locations referencing to maps of study areas. GIS data of Hino city was used to compare the result of classification accuracy. It is provided from local city office and developed from Ikonos image (1m resolution). Post classification was processed for change detection in both study areas between 1987 to 2011 and 1988 to 2009 respectively. The classification method was applied to images of Hino city study area first and it worked well to meet the accuracy of Hino city's GIS data. Then, the images of the study area-2, Mandalay city, were classified using the same classification method. Land surface temperatures were calculated from thermal bands of Landsat images for both study areas and the retrieved LSTs had been investigated with respect to classified data and normalized difference vegetation index (NDVI) which derived from visual and near infrared bands of Landsat. It was observed that green covers greatly decreased and built-up land increased in both study areas. And the concrete based land exhibits the highest surface temperature while the lowest surface temperature was observed in green cover areas.

In this study, the developed classification method worked well with Landsat images to solve the common problems in image classification, which are mixed pixel problem, shadows problem caused by topography, and problem of misinterpreted classes. The developed classification accuracy is a great potentially satisfied to the GIS data of Hino City, but more study in this regard and for Mandalay GIS data are required to improve classification results by utilizing very high resolution (VHR) satellite imagery with social economic survey in future.

LIST OF FIGURES

LIST OF TABLES

LIST OF ABBREVIATIONS

DN	Digital Number
TM	Thematic Mapper
ETM+	Enhanced Thematic Mapper
GIS	Geographic Information System
ENVI	Environment for Visualization of Images
GPS	Geographic Positioning System
GCPs	Ground Control Points
MSS	Multi Spectral Scanner
RS	Remote Sensing
USGS	United States Geological Survey
NDVI	Normalized Difference Vegetation Index
TIR	Thermal Infrared
NIR	Near Infrared
ROI	Region of Interest
ISO Data	Iterative Self-Organizing Data
UTM	Universal Trans Mercator
WGS	World Geodetic System

CHAPTER 1
INTRODUCTION

1.1. Background to the Study

Many studies have shown that there are only few landscapes remained on the Earth that are still in natural state. Due to anthropogenic activities, the Earth surface is being significantly altered in some manner and human's use of land has had a profound effect upon the natural environment thus resulting into an observable pattern in land cover over time. Land cover dynamics alter the availability of different biophysical resources including soil, vegetation, water, animal feed and others [02Aga]. Consequently, land cover changes could lead to a decreased availability of different products and services for human, livestock, agricultural production and damage to the environment as well. Land is becoming a scarce resource due to immense agricultural and demographic pressure. Hence, information on land cover and possibilities for their optimal use is essential for the selection, planning and implementation of land use schemes to meet the increasing demands for basic human needs and welfare.

Land cover change has become a central component in current strategies for managing natural resources and monitoring environmental changes. The advancement in the concept of vegetation mapping has greatly increased research on land cover change thus providing an accurate evaluation of the spread and health of the world's forest, grassland, and agricultural resources has become an important priority [06Zub]. Viewing the Earth from space is now crucial to the understanding of the influence of man's activities on his natural resource base over time. In situations of rapid and often unrecorded land use change, observations of the earth from space provide objective information of human utilization of the landscape. Over the past years, data from Earth sensing satellites has become vital in mapping the Earth's features and infrastructures, managing natural resources and studying environmental change.

In Japan, green Tokyo was started in 2007 to reconstruct metropolis Tokyo into a green-rich city, and to hand over precious greenery to the children who live in the next generation [4]. Although there are projects to build green environment in many places of Japan, only 2008/9/9 Ikonos data was developed for land cover study in Hino city. But many studies are needed to carry out for previous land cover and recently changes land cover. In Myanmar, the availability of natural resources as well as their dynamics and management vary considerably from area to area. For instance, different parts of the

Myanmar highlands receive between 300 and 600 mm of rainfall annually [8]. Besides high rainfall variability, also water shortages are prevalent in the Myanmar lowlands. For the coming decades, it is generally estimated that water withdrawal and consumption will increase as a result of increasing food needs by a growing population. Land cover study is highly needed in Myanmar to monitor the changes and manage the natural resources which become at risk due to human activities.

Remote Sensing (RS) and Geographic Information System (GIS) are now providing new tools for advanced ecosystem management. The collection of remotely sensed data facilitates the synoptic analyses of Earth-system function, patterning, and change at local, regional and global scales over time; such data also provide an important link between intensive, localized ecological research and regional, national and international conservation and management of biological diversity [96Wil].

Therefore, attempt will be made in this study to map out the status of urban area in two study areas, Hino city, western part of Japan and Mandalay city, in central part of Myanmar, with a view to detect land surface temperature and the changes that has taken place in this status particularly in forest land using both Geographic Information System and remote sensing data.

1.2. Problem Definition

To state problem, both study areas, Hino city and Mandalay city has witnessed remarkable expansion, growth and developmental activities such as building, road construction, deforestation and many other anthropogenic activities since 1980. It is therefore necessary for a study such as this to be carried out if the cities will avoid the associated problems of a growing and expanding city like many others in the world.

The application of remote sensing (RS) for extracting land cover information has been exploited since the advent of optical satellite systems. Various improvement and techniques have been developed through past decades with the development of RS technology. Many classification techniques have been developed and utilized by several research workers. Due to the importance of monitoring land cover change, research of classification techniques is an active field and several new methods are emerging regularly. Recent advancement of RS with wide-ranging spectral and higher spatial resolution of satellite images and repetitive coverage, this research field of classification RS image for change detection has been growing strongly. Coupled with the availability of historical RS data, the reduction in data acquisition and processing as well as higher spatial, spectral and

temporal resolution, the application of RS has great impact on growing development of image classification techniques for change detection [04Rog].

Successful use of RS for land cover change detection largely depends on an adequate understanding of the study area, the satellite imaging system and the various information extraction methods for change detection in order to fulfill the aim of the present study [02Yan]. Extracting meaningful land cover change information from satellite data using various techniques has been performed and established by a large number of authors. However, it is still sometimes appeared difficult in practice to select a good change detection method. Moreover, the choice of methods depends on the RS data available, the performed time limit and the objective of the study. The determination of suitable land cover change detection techniques from the various methods is a problem in the present research. There are a number of challenges in applying suitable set of techniques from change detection considering a series of dynamic factors ranging from selection of input data and their classification algorithm, to accuracy assessment to the ultimate aim of the study [04Lew].

However, change detection methods have their own merits (and demerits as well) and no single method has been proven as optimal to all cases. In the present study, investigating the efficiency of preferred classification methods for change detection, selected based on existing case studies, availability of resources and target of the work, to fulfill the objectives is one of the major challenges.

1.3. Aim and Objective

The aim of this study is to produce land cover maps of urban area by using Landsat images in order to detect the changes that have taken place particularly in the forest land and to analyze the impact of these changes on land surface temperature (LST). The following specific objectives will be pursued in order to achieve the aim above.

- To generate a land cover classification scheme and develop classification system.
- To identify the land cover changes in the study areas during the time periods of 1987 to 2011 for study area-1 and 1988 to 2009 for study area-2 using post-classification method.
- To derive land surface temperature (LST) from thermal bands of both study areas.

1.4. Scope of the Work

The present research is not completely free of limitation. First of all, considering

the technical aspects of the satellites images used are restricted to certain spatial and spectral resolution. The resolution has a great impact on the effectiveness of the classification method. Secondly, for accuracy assessment, a true high quality reference data or ground truth data with the same number of classes was not available. Thirdly, due to time limitations, the choice of data, aerial extent of study area and number of methodologies used are also restricted.

1.5. Thesis Outline

The thesis outline can be divided into five chapters. This chapter primarily gives the aim of the present research work. The rest of the thesis is arranged as follows:

Chapter 2 is for the literature review where related research work has been discussed. This chapter shows how the application of remote sensing is utilized for the land cover change study and briefly reviews various existing techniques and their advantages through several case studies.

After this chapter, a workflow has been proposed for the present work. Chapter 3 is allocated for the description data used for the whole work and illustrates the methodologies used in detail for image classification and deriving land surface temperature after image preprocessing and enhancement.

Chapter 4 adds to the present study a focus on the process of Landsat image classification and its accuracy assessment based on existing reference data.

Chapter 5 concludes the research work and recommends the future work.

CHAPTER 2
LITERATURE REVIEW

2.1. Remote Sensing for Land Cover Change

Remote Sensing (RS) is the science and art of obtaining information about an object, area, or phenomenon through the analysis of data acquired by a device that is not in contact with object, area, or phenomenon under investigation [80Byr]. It provides a large variety and amount of data about the earth surface for detailed analysis and change detection with the help of various space borne and airborne sensors (Figure 2.1). It presents powerful capabilities for understanding and managing earth resources. RS have been proven to be a very useful tool for land cover change detection.
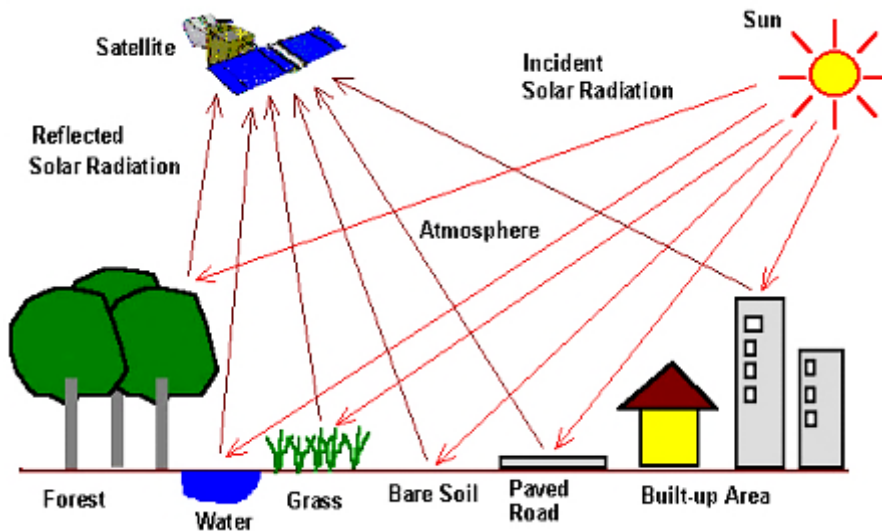
Figure 2.1. Principle of Remote Sensing [11]

Over the past decades, RS has played a large role in studying land cover change detection. With the availability of historical RS data, the reduction in data cost and increased resolution from satellite platforms, RS technology appears poised to make an even greater impact on monitoring land cover change [04Rog]. Change detection's studies of land cover are becoming demanding tasks with the availability of a suite of wide range sensors operating at various imaging scales and scope of using various techniques as well as increasing avenues for monitoring effective and accurate land cover change.

Considerable research has been directed at the various components of land cover change including the accuracy assessment which is drawing an equal attention by scientists nowadays [04Lew]. In general, change detection of land cover involves the interpretation

and analysis of multi-temporal and multi-source satellite images to identify temporal phenomenon or changes trough a certain period of time.

A RS device records response which is based on many characteristics of the land surface, including natural and artificial cover. An interpreter uses the element of tone, texture, pattern, shape, size, shadow, site and association to derive information about land cover. The generation of remotely sensed images by various types of sensor flown aboard different platforms at varying heights above the terrain and at different times of the day and the year does not lead to a simple classification system. It is often believed that no single classification could be used with all types of imagery and all scales. To date, the most successful attempt in developing a general purpose classification scheme compatible with RS data has been by Anderson et al which were also referred to as USGS (United State Geography Survey) classification scheme [76And]. Other classification schemes available for use with RS data are basically modification of the above classification scheme.

Ever since the launch of the first RS satellite (Landsat-1) in 1972, land cover studies were carried out on different scales for different users. For instance, waste land mapping of India was carried out on 1:1 million scales by NASA using 1980-82 Landsat multi spectral scanner data. About 16.2% of waste lands were estimated based on the study. Xiaomei Y, and Rong Qing L.Q.Y in 1999 noted that information about change is necessary for updating land cover maps and the management of natural resources. The information may be obtained by visiting sites on the ground and or extracting it from remotely sensed data [99Xia].

Land covers are distinct yet closely linked characteristics of the Earth's surface. The use to which we put land could be grazing, agriculture, urban development, logging, and mining among many others. While land cover categories could be cropland, forest, wetland, pasture, roads, urban areas among others. The term land cover originally referred to the kind and state of vegetation, such as forest or grass cover but it has broadened in subsequent usage to include other things such as human structures, soil type, biodiversity, surface and ground water [95Mey].

Land use affects land cover and changes in land cover affect land use. A change in either however is not necessarily the product of the other. Changes in land cover by land use do not necessarily imply degradation of the land. However, many shifting land use patterns driven by a variety of social causes, result in land cover changes that affects biodiversity, water and radiation budgets, trace gas emissions and other processes that

17

come together to affect climate and biosphere [94Rie].

Land cover can be altered by forces other than anthropogenic. Natural events such as weather, flooding, fire, climate fluctuations, and ecosystem dynamics may also initiate modifications upon land cover. Globally, land cover today is altered principally by direct human use: by agriculture and livestock raising, forest harvesting and management and urban and suburban construction and development. There are also incidental impacts on land cover from other human activities such as forest and lakes damaged by acid rain from fossil fuel combustion and crops near cities damaged by tropospheric ozone resulting from automobile exhaust [95Mey]. Hence, in order to use land optimally, it is not only necessary to have the information on existing land cover but also the capability to monitor the dynamics of land use resulting out of both changing demands of increasing population and forces of nature acting to shape the landscape.

Conventional ground methods of land use mapping are labor intensive, time consuming and are done relatively infrequently. These maps soon become outdated with the passage of time, particularly in a rapid changing environment. In fact according to Olorunfemi [03Bar], monitoring changes and time series analysis is quite difficult with traditional method of surveying. In recent years, satellite RS techniques have been developed, which have proved to be of immense value for preparing accurate land cover maps and monitoring changes at regular intervals of time. In case of inaccessible region, this technique is perhaps the only method of obtaining the required data on a cost and time-effective basis.

2.2. Satellite Image Processing

Satellite images were recorded in digital form and then processed by the computers to produce images for interpretation purposes [03Bar]. Images were available in two forms; photographic film form and digital form. Variations in the scene characteristics were represented as variations in brightness on photographic films. A particular part of scene reflecting more energy would appear bright while a different part of the same scene that reflecting less energy would appear black. Digital image consisted of discrete picture elements called pixels. Associated with each pixel was a number represented as digital number (DN) that depicts the average radiance of relatively small area within a scene. The size of this area effected the reproduction of details within the scene. As the pixel size was reduced more scene detail was preserved in digital representation. Digital image processing was a collection of techniques for the manipulation of digital images by computers. Digital

image processing encompassed the operations such as noise removal, geometric and radiometric corrections, enhancement of images, information extraction and image data manipulation and management.

Li, Zhang, Yu, Lin and Shihuosheng discussed a method to disintegrate digital remotely sensed image [04Zha]. By which the information in original remotely sensed data could be disintegrated point by point into three components--solar direct illuminance (SDI), sky-scattering illuminance (SSI) and atmospheric path radiance (APR). Because it was the result of the interaction of the natural spectral components with ground features and the atmosphere, the three components images played a more powerful role than the normal original remotely sensed data in the quantification inversion research of ground radiation energy, atmospheric environment condition, and satellite image pattern recognition.

The concept of image disintegration was widely used in remotely sensed digital image processing such as: to disintegrate panchromatic image into different band image according to spectral wavelength, to disintegrate image into high and low frequency parts by filter, to disintegrate image into the sum of wave element by Fourier transform and wavelet analysis Wavelet, and the mixed pixel disintegration etc. They are all effective method in remotely sensed image sensed image into three respective component images representing solar illuminance, sky-scattering illuminance and atmospheric brightness [99Mar].

2.2.1. Geometric Correction

Why does the geometric correction process seem to be more important today than before? In 1972, the impact of the geometric distortions was quite negligible for different reasons: [03Hua]

- the images, such as Landsat-MSS, were nadir viewing and the resolution was coarse (around 80-100 m);
- the products, resulting from the image processing were analog on paper;
- the interpretation of the final products was performed visually; and
- The fusion and integration of multi-source and multi-format data did not exist.

Now, the impact of distortions is less negligible although they are similar because:

- the images are off-nadir viewing and the resolution is fine (sub-meter level);
- the products resulting from image processing are fully digital;

- the interpretation of the final products is realized on computer;
- the fusion of multi-source images (different sensors) is in general use; and
- the integration of multi-format data (raster/vector) is a general tendency in geometrics.

Raw images usually contain such significant geometric distortions that they cannot be used directly with map base products in a geographic information system (GIS). Consequently, multi-source data integration (raster and vector) for applications in geometrics requires geometric and radiometric processing adapted to the nature and characteristics of the data in order to keep the best information from each image in the composite ortho-rectified products.

The processing of multi-source data can be based on the concept of terrain geo-coded images, a term originally invented in Canada in defining value-added products [03Hua]. Photogrammetric, however, prefer the term ortho-image. In referring to the unit of terrain geo-coded data, where all distortions including the relief are corrected. To integrate different data under the concept, each raw image must be separately converted to an ortho-image so that each component ortho-image of data set can be registered, compared, combined, etc. pixel by pixel but also with cartographic vector data in a GIS.

One must admit that the new data, the method and processing, the resulting processed data, their analysis and interpretation introduced new needs and requirements for geometric corrections, due to a drastic evolution with large scientific and technology improvements between these two periods. Even if the literature is quite abundant mainly in term of books and peer-reviewed articles, it is important to update the problems and the solutions recently adopted for geometrically correcting satellite images with the latest developments and research studies from around the world. The source of geometric distortions and deformations with different categorizations, the modeling of the distortions with different 2D/3D physical/empirical models and mathematical functions and the geometric correction method with the processing steps and errors were described [03Hua].

Comparisons between the models and mathematical functions, their applicability and their performance on different types of images (frame camera, Visible and Infra-Red (VIR) oscillating or push-broom scanners; side looking antenna radar (SLAR) or synthetic aperture radar (SAR) sensors; high, medium or low resolution) are also addressed. The errors with their propagation from the input data to the final results are also evaluated through the full processing steps.

2.2.2. Image Registration

Image registration was the process of overlaying two or more images of the same scene taken at different times, from different viewpoints, and/or by different sensors [03Bar]. It geometrically aligned two images-the reference and sensed images. The present differences between images were introduced due to different imaging conditions. Image registration was a crucial step in all image analysis tasks in which the final information was gained from the combination of various data sources like in image fusion, change detection, and multichannel image restoration. Typically, registration was required in RS (multispectral classification, environmental monitoring, change detection, image mosaicing, weather forecasting, creating super-resolution images, integrating information into GIS), in medicine (combining computer tomography (CT) and NMR data to obtain more complete information about the patient, monitoring tumor growth, treatment verification, comparison of the patient's data with anatomical atlases), in cartography (map updating), and in computer vision (target localization, automatic quality control), to name a few [94Kah].

Data Processing in Remote Sensing

Reconstruction/Correction
- Image Reconstruction
- Image Restoration
- Radiometric Correction
- Geometric Correction
- Mosaic

Transformation
- Image Enhancement
- Spatial Transformation
- Geometric Information
- Data Compression

Classification
- Learning
- Classification
- Segmentation
- Matching
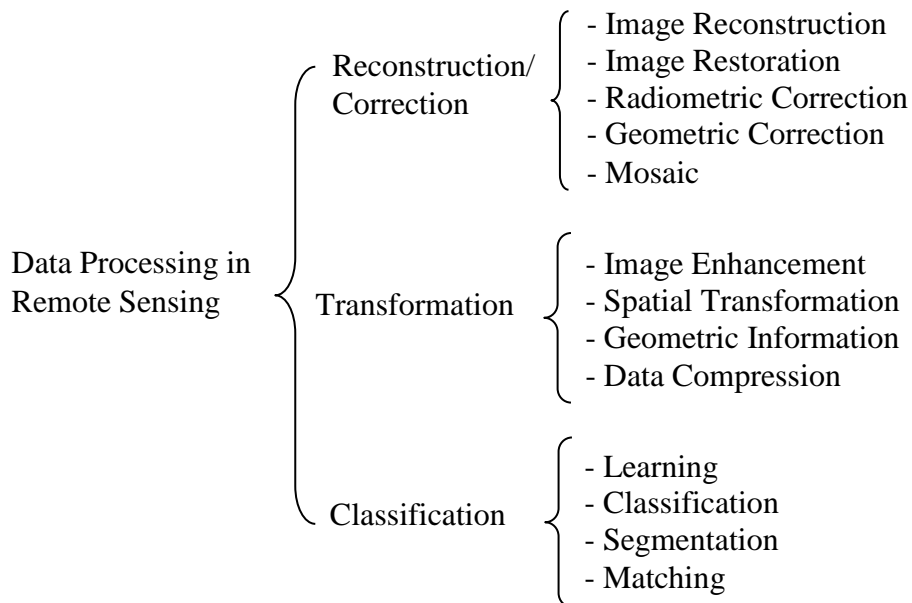
Figure 2.2. Data processing in Remote Sensing [94Kah]

Kahru described that frequent acquisition of remotely sensed data makes it possible to use the satellite images to determine type and extent of changes in the environment. Many digital change detection algorithms have been developed since the launch of ERTS-1 in 1972 to reveal changes. With the launch of new satellite generations with different

sensor characteristics and advancement in mathematical data processing algorithms, the use of new techniques to compare multi-resolution/multi-temporal image data in change detection procedure is required.

Hua-mei, Manoj and Pramod told that registration was a fundamental operation in image processing to align images taken at different times, from different sensors or from different viewing angles [03Hua]. Automatic image registration procedures are gaining importance to efficiently register large volumes of RS data available these days. In that paper, they investigated an automated mutual information based registration technique for RS data. Performance of a number of interpolation algorithms to compute mutual information for registration of multi-sensor and multi-resolution Landsat TM, Radarsat SAR and IRS PAN images was evaluated.

Satellite images are frequently used for a variety of tasks such as image fusion [98Poh], temporal change detection [98Lun] and integration of multi-source data in GIS. The basis of all these tasks is accurate image registration, though the requirement of registration accuracy may vary from one task to the other. For example, it has been reported that a registration accuracy of less than one-fifth of a pixel is required to achieve a change detection error within 10% [98Lun].

2.2.2.1. Mutual Information Based Image Registration

Having its roots in information theory, mutual information, *I (A, B)*, of two random variables *A* and *B* can be obtained from,

$$I(A, B) = H(A) + H(B) - H(A, B) \qquad 2.1$$

where *H (A)* and *H (B)* are the entropies of *A* and *B* and *H (A, B)* is their joint entropy [00Che]. Considering A and B as two images, the MI based registration criterion states that the images shall be registered when *I (A, B)* is maximal. The entropies and joint entropy can be computed from,

$$H(A) = \sum_a -p_A(a) \, log \, p_A(a)$$

$$2.2$$

$$H(B) = \sum_b -p_B(b) \, log \, p_B(b)$$

$$2.3$$

$$H(A,B) = \sum_{a,b} -p_{A,B}(a,b) \, log \, p_{A,B}(a,b)$$

<div align="right">2.4</div>

where p_A *(a)* and P_B *(b)* are the marginal probability mass functions, and $p_{A,\,B}$ *(a, b)* is the joint probability mass function. These probability mass functions can be obtained from,

$$p_{A,B}(a,b) = \frac{h(a,b)}{\sum_{a,b} h(a,b)}$$

<div align="right">2.5</div>

$$p_A(a) = \sum_b p_{A,B}(a,b)$$

<div align="right">2.6</div>

$$p_B(b) = \sum_a p_{A,B}(a,b)$$

<div align="right">2.7</div>

where *h* is the joint histogram of the image pair. It is a 2D matrix of the following form:

$$h = \begin{bmatrix} h(0,0) & h(0,1) & ... & h(o,N-1) \\ h(1,0) & h(1,1) & ... & h(1,N-1) \\ ... & ... & & ... \\ h(M-1,0) & (M-1,1) & ... & h(M-1,N-1) \end{bmatrix}$$

<div align="right">2.8</div>

Assuming the intensity value in the first image varies from **0** to **M-1** and in the second image from 0 to *N*-1. The value *h (a, b)* is the number of corresponding pairs having intensity value *a* in the first image and intensity value *b* in the second image. Thus, it can be seen from equations **1** to **7** that the joint histogram is the only requirement to determine the MI between two images. Different interpolation algorithms such as nearest neighbour [00Che], linear [00Hol], cubic convolution [81Key], and partial volume interpolation [97Mae] can be used to estimate the joint histogram of two images. In that paper, the performance of aforementioned interpolation algorithms had been evaluated by means of registration consistency.

2.2.3. Color Composition

A remote-sensing term is also referring to the process of assigning different colors to different spectral bands. The color picture formed by this process is called a "color composite" (a color image produced through optical combination of multiband images by projection through filters) and is produced by assigning a color to an image of the Earth's surface recorded in a particular waveband. For a Landsat color composite, the green waveband is colored blue, the red waveband is colored green and the infrared waveband is colored red. This produces an image closely approximating a false color photograph. Color composite images are easier to interpret than separate images recording different wavebands. US national experimental crop inventories are based upon visual interpretation of Landsat color composites [99Ser].

A multispectral image consists of several bands of data. For visual display, each band of the image may be displayed one band at a time as a grey scale image, or in combination of three bands at a time as a color composite image. Interpretation of a multispectral color composite image will require the knowledge of the spectral reflectance signature of the targets in the scene. In this case, the spectral information content of the image is utilized in the interpretation.

In RS, a thorough knowledge about colors is necessary for-
- visual interpretation of images printed on paper,
- interpretation of colors on screen,
- preparing color composites of processed data to make results readable,
- choosing the best possible printing of results on paper.

In order to establish comparisons between the objects that our eyes see and the color of these same objects on images or photographs, it is also necessary to understand the systems of color composition by our eyes, by computer monitors and by pigments. Colors in lights are called 'additive colors' and the color impressions obtained by means of pigments are known as 'subtractive' colors.

Color Composition is the result of combining three images: one of them is displayed in shades of red, others in shades of green and in shades of blue. After combining three images of different dates, one color composite multi-temporal image is obtained which suit for further analysis of colored objects. Color composition of multi-temporal images is used relatively widely, especially on the analysis of radar images, as it is a unique way to receive the color image from radar-images which by the nature only

black and white [95Nez].

Succeed in applying this technique depends on how sharply changing objects on study stand out against a background of an image in their brightness. So it is expedient to use images with a simplified brightness structure. For example, images of near infrared band are the most suitable for studying changes at coastal zone, since they are characterized with the most evident contrast between water and land or vegetation. Images taken in winter are the most proper on research of forests distribution changes, because dark forest-covered areas stand out against a background of snow covered woodless zone. Green growing vegetation of oases (dark tone at an image) contrasting with sand of desert (bright tone) gives a similar effect at the image in a visible range [06Kra].

Sometimes, it is advisable to simplify image structure executing quantification to 2-3 levels intensity of grey, as this procedure allows obtaining composite multi-temporal image with clear color separation of different changes. It is evident also that images acquired at different dates should be geometrically identical: geo-reference or mutual transforming and resampling should be done beforehand.

At color compositing, generally speaking, it is possible to use any order of multi-date images coloring by filters R, G, B, providing the best color division of investigated objects. But use of a uniform rule for applying Red, Green, Blue colors in order from earlier survey date to later one provides also uniform approaches to interpretation such color composite multi-temporal images, to decoding changes of brightness, "temporal signature an image". Consequently, one can define the character of replacement of objects basing on their color at a color composite multi-temporal image [06Kra].

2.3. Image Classification Method

Classifying the satellite images to extract the land cover theme is one of the major steps in this type of study. Classification is the process of assigning classes to the pixels in images. Moreover, successful utilization of remotely sensed data for land cover studies demands careful selection of an appropriate data set and image processing technique(s) [98Lun].

The most common image analysis for extracting land cover is digital image classification. Sabins explains that image classification techniques are most generally applied to the spectral data of a single-date image or to the varying spectral data of a series of multi-date images [97Sab]. The complexity of image classification techniques can range from the use of a simple threshold value for a single spectral band to complex statistically

based decision rules that operate on multivariate data. The purpose of image classification is to label the pixels in the image with the real information [01Jen]. Through classification of RS image, thematic maps such as the land cover can be obtained [01Tso]. Classification involves labeling the pixels as belonging to particular classes using the spectral data available.

There are two broad types of classification procedure and each finds application in processing of RS image. One is referred to as supervised classification and the other one is unsupervised classification. These can be used as alternative approaches but are often combined into hybrid methodologies using more than one method [06Ric]. Both the supervised and unsupervised classification methods used for classifying various multispectral images are based on so called traditional pixel-based method which has been played a great importance for classifying low resolution images. On the other hand, when using new generation images, characterized by a higher spatial and spectral resolution, it is still difficult to obtain satisfactory result [04Lew]. Figure 2.3 shows the procedures of classification.
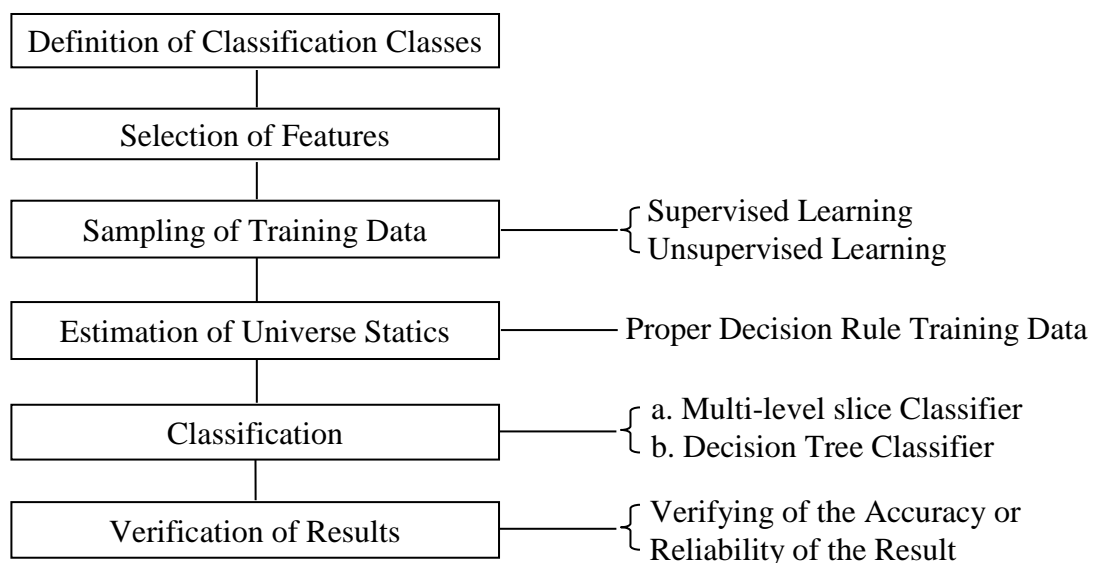
Figure 2.3. Procedures of Classification [04Lew]

2.3.1. Unsupervised Classification

Unsupervised Classification is the identification of natural groups, or structures, within multi-spectral data by the algorithms programmed into the software. The following characteristics apply to an unsupervised classification [01Jen].

- There is no extensive prior knowledge of the region that is required for unsupervised

26

classification unlike supervised classification that requires detailed knowledge of the area.

- The opportunity for human error is minimized with unsupervised classification because the operator may specify only the number of categories desired and sometimes constraints governing the distinctness and uniformity of groups. Many of the detailed decisions required for supervised classification are not required for unsupervised classification creating less opportunity for the operator to make errors.

- Unsupervised classification allows unique classes to be recognized as distinct units.

- Supervised classification may allow these unique classes to go unrecognized and could inadvertently be incorporated into other classes creating error throughout the entire classification.

2.3.2. Supervised Classification

Supervised classification was the process of using samples of known identity to classify pixels of unknown identity. The following characteristics apply to a supervised classification [01Jen].

- The analyst has control of a set, selected menu of informational categories tailored to a specific purpose and geographic region.

- Supervised classification is tied to specific areas of known identity, provided by selecting training areas.

- Supervised classification is not faced with the problem of matching spectral categories on the final map with the informational categories of interest.

- The operator may be able to detect serious errors by examining training data to determine whether they have been correctly classified.

- In supervised training, it is important to have a set of desired classes in mind, and then create the appropriate signatures from the data. You must also have some way of recognizing pixels that represent the classes that you want to extract.

2.3.2.1. Maximum Likelihood Classification

Maximum likelihood classification is based upon the assumption that there exist statistical models describing the distribution of the classes in the attribute space [78Mul]. Given these models, the class of a new object is determined by calculating which of the models is more likely to describe that object. In other words, the model with maximum likelihood is selected.

Maximum likelihood classification usually assumes multivariate normal (Gaussian) models. For a set of M n-dimensional objects, $(x_1,...,x_M)$ where $x_i = (x_{1,\ 1},...,x_{1,n})^T$, the Gaussian probability density function is defined to be:

$$g_{[m,C]} = \frac{1}{(\sqrt{2})^n \sqrt{\det(C)}} e^{\frac{-(x-m)^T C^{-1}(x-m)}{2}}$$

2.9

where the vector of means, m, is given by

$$m = \frac{1}{M} \sum_{i=1}^{M} x_i$$

2.10

and the covariance matrix, C, is given by

$$C = \frac{1}{(M-1)} \sum_{i=1}^{M} (x_i - m)(x_i - m)^T$$

2.11

The matrix C is positive semi-definite and symmetric by construction. Hence, it is possible to diagonals the matrix and calculate the eigenvalues and eigenvectors. In the case where the attribute space is two-dimensional, the eigenvalues and eigenvectors provide a useful means for displaying the two-dimensional Gaussian as an ellipse in the attribute space. By writing,

$$C = (e_1, e_2) \begin{bmatrix} \lambda_1 & 0 \\ 0 & \lambda_2 \end{bmatrix} \begin{pmatrix} e_1 \\ e_2 \end{pmatrix}$$

2.12

where e_1 and e_2 are the Eigen basis vectors, and λ_1 and λ_2 are the eigenvalues of C. Then the ellipse which marks all points in the attribute space that are two standard deviations away from the mean is given by

$$\left\{ x \in \Re^2 : x = m + (e_1, e_2) \begin{bmatrix} \lambda_1 & 0 \\ 0 & \lambda_2 \end{bmatrix} \begin{pmatrix} e_1 \\ e_2 \end{pmatrix} \begin{pmatrix} \cos(t) \\ \sin(t) \end{pmatrix}, t \ \varepsilon \ [0,2\pi] \right\}$$

2.13

2.3.3. Post-classification Technique

In the post-classification approach, images belonging to different dates are

classified and labeled individually. Later, the classification results are compared directly and the area of changes extracted [96Jen]. Individual classification of two image dates minimizes the problem of normalizing for atmospheric and sensor differences between two dates [89Sin]. Accuracy dependency of the classifications results is the main disadvantage of this method. Poor classification accuracy of individual classification leads to propagation of uncertainties in the change map, which results in inaccurate information of land-use changes.

Shi and Ehlers described the uncertainty sources in change detection as error of the source image, classification methods, and determination of changes [89Sin]. They explained three main error sources in Maximum Likelihood (ML) classification-based change detection:

- the process of training data collection is subjective;
- the ML classifier assumes that the probability distribution of each class is normal,
- method used to determine changes (based on amount of uncertainties).

Confusion matrix (error) is the common method to describe the uncertainty in a classified satellite image. Several error indicators can be derived from confusion matrix, such as error of commission, error of omission, total accuracy of classification, and Kappa coefficient. These indicators represent the classification accuracy (for the whole classification and for each category), but do not indicate the classification uncertainty for each pixel, which is required to determine change detection uncertainties [89Sin]. They suggested an approach to determine uncertainties and their propagation in dynamic change detection of classified remotely sensed data. In this approach first the probability vectors created during ML classification were assessed as uncertainty indicators. In the next step they described the uncertainty propagation of classified multi-date images using mathematical language. They concluded that the uncertainty propagation of change maps was much higher than the uncertainty of individual ML classification, and that assessment of individual classification uncertainty is not enough to quantify accurately the change detection uncertainty.

2.4. Remote Sensing As a Tool for Change Detection

Change detection is the process of identifying differences in the state of an object or phenomenon by observing it at different times [89Sin]. Change detection is an important process in monitoring and managing natural resources and urban development because it

provides quantitative analysis of the spatial distribution of the population of interest. Macleod and Congalton [98Mac] list four aspects of change detection which are important when monitoring natural resources:

- Detecting the changes that have occurred
- Identifying the nature of the change
- Measuring the area extent of the change
- Assessing the spatial pattern of the change

The basis of using RS data for change detection is that changes in land cover result in changes in radiance values which can be remotely sensed. Techniques to perform change detection with satellite imagery have become numerous as a result of increasing versatility in manipulating digital data and increasing computer power [98Mac].

A large number of change detection techniques have been developed since the advent of the orbital system [72Lil]. Weismiller et al. [77Wei] have used various RS techniques for evaluating change detection for coastal zone environments. In 1980, Byrne, Crapper and Mayo have shown that Landsat multispectral data can be used to identify land cover changes very effectively [80Byr].

Change detection and monitoring involve the use of several multi-date images to evaluate the differences in land cover due to various environmental conditions and human actions between the acquisition dates of images [89Sin]. Successful use of satellite RS for land cover change detection depends upon an adequate understanding of landscape features, imaging systems, and methodology employed in relation to the aim of the analysis [02Yan]. Various RS data products over time have often been incorporated into historical land use information [96Ace]; [02Cla]; [90Mea]. RS data are the primary source for change detection in recent decades and have made a greater impact on urban planning agencies and land management initiatives [99Yeh]; [02Yon]; [04Rog].

A wide variety of digital change detection techniques have been developed over the last two decades. Singh [89Sin] and Coppin & Bauer [96Cop] summarize eleven different change detection algorithms that were found to be documented in the literature by 1995 [95Cop]. These include:

- Mono-temporal change delineation.
- Delta or post classification comparisons.
- Multidimensional temporal feature space analysis.
- Composite analysis.

- Image differencing.

- Multi-temporal linear data transformation.

- Change vector analysis.

- Image regression.

- Multi-temporal biomass index

- Background subtraction.

- Image ratioing

In some instances, land cover change may result in environmental, social and economic impacts of greater damage than benefit to the area [99Mos]. Therefore data on land use change are of great importance to planners in monitoring the consequences of land use change on the area. Such data are of value to resources management and agencies that plan and assess land use patterns and in modeling and predicting future changes.

Shosheng and Kutiel investigated the advantages of RS techniques in relation to field surveys in providing a regional description of vegetation cover. The results of their research were used to produce four vegetation cover maps that provided new information on spatial and temporal distributions of vegetation in this area and allowed regional quantitative assessment of the vegetation cover [94Sho].

Arvind C. Pandy and M. S. Nathawat [06Arv] carried out a study on land cover mapping of Panchkula, Ambala and Yamunanger districts, Hangana State in India. They observed that the heterogeneous climate and physiographic conditions in these districts has resulted in the development of different land cover in these districts, an evaluation by digital analysis of satellite data indicates that majority of areas in these districts are used for agricultural purpose. The hilly regions exhibit fair development of reserved forests. It is inferred that land cover pattern in the area are generally controlled by agro – climatic conditions, ground water potential and a host of other factors.

It has been noted over time through series of studies that Landsat Thematic Mapper is adequate for general extensive synoptic coverage of large areas. As a result, this reduces the need for expensive and time consuming ground surveys conducted for validation of data. Generally, satellite imagery is able to provide more frequent data collection on a regular basis unlike aerial photographs which although may provide more geometrically accurate maps, is limited in respect to its extent of coverage and expensive; which means, it is not often used.

In 1985, the U.S Geological Survey carried out a research program to produce

1:250,000 scale land cover maps for Alaska using Landsat MSS data [87Fit].The State of Maryland Health Resources Planning Commission also used Landsat TM data to create a land cover data set for inclusion in their Maryland Geographic Information (MAGI) database. All seven TM bands were used to produce a 21- class land cover map [92EOSAT]. Also, in 1992, the Georgia Department of Natural Resources completed mapping the entire State of Georgia to identify and quantify wetlands and other land cover types using Landsat Thematic Mapper ™ data [92ERDAS]. The State of southern Carolina Lands Resources Conservation Commission developed a detailed land cover map composed of 19 classes from TM data [94EOSAT]. This mapping effort employed multi-temporal imagery as well as multi-spectral data during classification.

An analysis of land cover changes using the combination of MSS Landsat and land use map of Indonesia reveals that land cover change were evaluated by using RS to calculate the index of changes which was done by the superimposition of land cover images of 1972, 1984 and land use maps of 1990 [95Dim]. This was done to analyze the pattern of change in the area, which was rather difficult with the traditional method of surveying as noted by Olorunfemi in 1983 when he was using aerial photographic approach to monitor urban land use in developing countries with Ilorin in Nigeria as the case study.

Daniel et al [02Dan], in their comparison of land cover change detection methods, made use of 5 methods;
-   traditional post-classification cross tabulation,
-   cross correlation analysis, neural networks,
-   knowledge-based expert systems
-   image segmentation, and
-   Object-oriented classification.

A combination of direct T1 and T2 change detection as well as post classification analysis was employed. Nine land cover classes were selected for analysis. They observed that there are merits to each of the five methods examined, and that, at the point of their research, no single approach can solve the land use change detection problem.

Also, Adeniyi and Omojola, in their land cover change evaluation in Sokoto-Rima Basin of North-Western Nigeria based on Archival Remote Sensing and GIS techniques, used aerial photographs, Landsat MSS, SPOT XS/Panchromatic image Transparency and Topographic map sheets to study changes in the two dams (Sokoto and Guronyo) between

1962 and 1986 [99Ade]. The work revealed that land cover of both areas was unchanged before the construction while settlement alone covered most part of the area. However, during the post - dam era, land cover classes changed but with settlement still remaining the largest.

Although coarse-spatial resolution meteorological satellite data have been available since the 1960s, civilian RS of the Earth's surface from space at medium spatial resolutions (i.e. <250 m) only began in 1972 with the launch of the first of a series of Landsat Satellites [04Rog]. Since then a large numbers of change detection techniques have been developed after the launching of Landsat orbital system as described in the article titled "Techniques for Change Detection" by Lillestrand in 1972. Many methods of change detection have been developed to detect land cover change [97Lam], [89Sin], but by far the most popular has been the utilization of post classification comparison method. In spite of the numerous evaluations of these techniques [77Wei], [89Sin], no standard techniques have yet been adopted [98Mac] for all cases. Although the development of RS technology has been developed dramatically within last few years, examples of effective land cover change detection studies remain relatively rare [02Lov]; [04Rog].

Numerous researchers have addressed the problem of accurately monitoring land cover change in wide applications with greater success [94Muc]. One of the most definite reasons is that a wide variety of digital change detection techniques and algorithm have been developed and manipulated over last few decades commensurate with the fast-pace advancement of RS technology with spatial, spectral, thematic and temporal properties. They can be broadly divided into two which are pre-classification spectral change detection or post-classification methods [88Pil], [89Sin]. The simplest rule separates land cover changes that are categorical versus those that are continuous [99Abu]. Basically, the detection of categorical and continuous changes are also known as post-classification and pre-classification method respectively.

In case of post classification change detection, two multi-temporal images are classified separately and labeled with proper attributes. The area of change is then extracted through the direct comparison after obtaining the classification results [81Col], [81How]. With the post-classification methods basic issues are the accuracies of the component classifications and more subtle issues associated with the sensors and data preprocessing methods [99Kho]. Though it avoids the difficulties in change detection, it has significant limitations because the comparison of land cover classifications for temporal images does not allow the detection of subtle changes within land cover classes

[99Mac]. Owojori and Xie have shown the example of post classification in the study demonstrated the potential for accurate land cover change assessment with advanced atmospheric correction and object-oriented image analysis using medium resolution satellite data, Landsat TM [05Owo].

Pre-classification technique, where changes occur in the amount or concentration of some attribute that can be continuously measured [96Cop]. Image differencing (one of the most common pre-classification methods) is the most commonly used change detection algorithm [89Sin]. It involves subtracting one date of imagery from a second date that has been precisely registered to the first. According to recent research, image differencing emerges to perform generally better than other methods of pre-classification change detection [96Cop]. Maryna Rymasheuskaya in recent study has proved that both image differencing and post-classification comparison confirms their ability to be used for detecting land cover changes over northern Belarusian landscapes. The presented study allows estimating the amount of changes occurred at the study area [07Rym].

Spectral change detection technique is also considered as pre-classification category where the conception is about spectral signature change of the affected land surface through certain period of time. The largest number of change-detection techniques was considered as spectral change category, such as image differencing, image ratioing, vegetation index differencing, and principal component analysis (PCA) and change vector analysis (CVA) [08Den]. Despite many factors affecting the selection of suitable change-detection methods, image differencing, PCA, and post-classification are, in practice, the most commonly used methods [04Lew]. Principal component analysis (PCA) has been proven as efficient and basic economical technique for change detection in most cases [80Byr]; [88Fun].

According to Byrne *et al.*, PCA has provided an effective way of identifying areas in which change has occurred between two four-channel multispectral images [02Mal]. In 2005, Deng *et al.* adopted the technique of combining PCA with interactive supervised classification to detect changes. The method of combining PCA and supervised classification is common practice to detect temporal changes with satisfying results [05Den].

Other not so common change detection techniques in the category of spectral change detection are Change vector analysis and composite analysis. Change vector analysis (CVA) involves the calculation of two change features (magnitude and direction of change) based on a multi-temporal dataset. Composite analysis (CA) is often performed

in change detection applications [80Mal]. This approach involves compositing all desired bands into a multi-date layer stack (the layer stack may contain raw or enhanced image data). Supervised or unsupervised classification is then performed on the data set to obtain the desired number of output classes [04Rog].

2.5. Land Surface Temperature from Thermal Band

In the recent years, thermal environment has been paid great attention including the greenhouse effect and global warning. It not only refers to the air temperature, but also the land surface temperature (LST) [06Zha]. Remotely sensed thermal infrared (TIR) data have been widely used to retrieve LST [99Qua], [04Wen]. The LST is an important parameter in the studies of urban thermal environment and dynamics [08Wen]. The LST of urban surface correspond closely to the distribution of land cover characteristics [01Wen], [04Wen].

The integration of RS and GIS has been widely applied and been recognized as a powerful and effective tool in detecting urban land cover change [90Ehl]. The different studies carried out in different contraries about UHI and its relationship with land cover changes. Nichol carried out a detailed study using TM thermal data to monitor microclimate for housing estates in Singapore [94Nic]. Weng examined LST pattern and its relationship with land cover in Guangzhou and in the urban clusters in the Zhujiang Delta, China [01Wen]. Nichol et al. investigated the influence of land use on the urban heat island in Singapore. Nowadays, land cover changes due to changes in surface temperature cause to the urban managers to estimate the urban temperature and its surrounding for management and urban planning.

LST which is controlled by the surface energy balance, atmospheric state, thermal properties of the surface, and subsurface mediums, is an important factor controlling most physical, chemical, and biological processes of the Earth [90Bec]. In spite of the great importance in modeling and application of LST, confusions exits in both the use of the term and its determination with satellite thermal data. Numerous factors need to be quantified in order to assess the accuracy of the LST retrieval from satellite thermal data, including sensor radiometric calibrations [89Wuk], atmospheric correction [89Coo], surface emissivity correction [90Nor], characterization of spatial variability in land cover, and the combined effects of viewing geometry, background, and fractional vegetative cover. In estimation of LST from satellite thermal image, the digital number (ND) of image pixels needs to be converted into spectral radiance using the sensor calibration data

[86Mar].

However, the radiance converted from digital number does not represent a true surface temperature but a mixed signal or the sum of different fractions of energy. These fractions include the energy emitted from the ground, upwelling radiance from the atmosphere, as well as the down welling radiance from the sky integrated over the hemisphere above the surface. Therefore, the effects of both surface emissivity and atmosphere must be corrected in the accurate estimation of LST.

Thematic Mapper (TM) data, sensor on board the Landsat 5 satellite, are one of the most used for environmental studies. TM is composed by seven bands, six of them in the visible and near infrared, and only one band located in the thermal infrared region. Band 1 (with central wavelength of 0.49 μm) is used for coastal water studies, TM2 (0.56 μm) is used for crops identification and vegetation stage studies, TM3 and TM4 (0.66 and 0.83 μm, respectively) are used to calculate vegetation indexes, as the Normalized Difference Vegetation Index (NDVI), TM5 and TM7 (1.65 μm and 2.22 μm, respectively) can be used for clouds, ice, snow and geological formations discrimination, and finally band TM6 (with an effective wavelength of 11.457 μm) is used for LST retrieval. The fact of possessing only one thermal band is an important limitation in order to obtain LST, it does not allow to apply a split-window method [96Sob] neither a temperature/ emissivity separation (TES) method [98Gil] and therefore to obtain information about the emissivity spectrum of natural surfaces. For these reasons, band TM6 has not been used for environmental studies as the other bands have.

Thermal RS is recognized to be a major source of quantitative and qualitative information on land surface processes and for their characterization, analysis, and modeling [99Qua], [04Qua]. The launch of the Landsat series has allowed the acquisition of a historical database (from 1982 to present) of thermal imagery at medium spatial resolution suitable for different environmental studies, for example, evapotranspiration and energy balance component estimations or water resource studies. Thermal-infrared (TIR) data have been collected through band 6 (B6) of the Thematic Mapper (TM) instrument onboard Landsat-4 (L4B6) and Landsat-5 (L5B6) platforms and the enhanced TM plus instrument onboard the Landsat-7 (L7B6) platform.

LST is maintained by the incoming solar and long wave irradiation, the outgoing terrestrial infrared radiation, the sensible and latent heat flux, and the ground heat flux. Therefore, LST is a good indicator of the energy balance at the Earth's surface. LST is also strongly influenced by the ability of the surface to emit radiation (i.e. surface emissivity).

36

Surface emissivity (ε) is the ratio of energy emitted from a natural material from an ideal blackbody at the same temperature and emissivity from thermal infrared RS data which is important for the study of urban planning, water and energy balances, climate models, lithological mapping and resource exploration, and etc. [02Sob].

2.6. Summary

The studies from various literature of related work revealed that the use of RS application is a key instrument for studying land cover change detection. However, a careful selection of RS data has to be stipulated considering the scope and type of actual work. With rapid advancement of RS techniques, a bunch of classification techniques have been developed as well. Those can be primarily grouped into two broad types which are tradition pixel based method and advance object oriented method. The preference of employing them is fairly driven by the resolution of RS data. Evolution of RS technology also accelerated the growing development of various change detection techniques which are implemented through case studies. The case studies in this regard have greatly influenced the development of new techniques. However, it has not been established any single technique as optimum and best. Every techniques are useful and having a balance between pros and cons. Because of impacts of complex factors and objectives, different researchers often arrived at different conclusion about which the efficacy of various methods. LST derivation is also a part of good change detection research work. Moreover, it can be mentioned that LST estimation itself is an active field of research nowadays.

CHAPTER 3
RESEARCH METHODOLOGY

3.1. Study Area and Procedure

This chapter describes the area and data used for the study. At first, a short description of the study area is given to demonstrate the characteristics of the area in terms of geography, land cover and general narrative. Then, it illustrates about the technical details of the various data used for the proposed study.

The study area-1(Hino city) is approximately in the center of Tokyo Metropolis (Figure 3.1). It locates on north latitude between 35°38'20" and 35°41'30", and on east longitude between 139°21'40" and 139°26'40". The area is about 27.53 km^2. The southern part is Tama hill in an area from 150 meters above sea level to approximately 200 meters. And there is an alluvion of the Tama River of the eastern part from the northern part. On November 3, 1963, Hino was elevated to city status. Hino is largely a regional commercial center and bedroom community for central Tokyo [9]. As it combines different land covers, it was chosen as one of study areas.
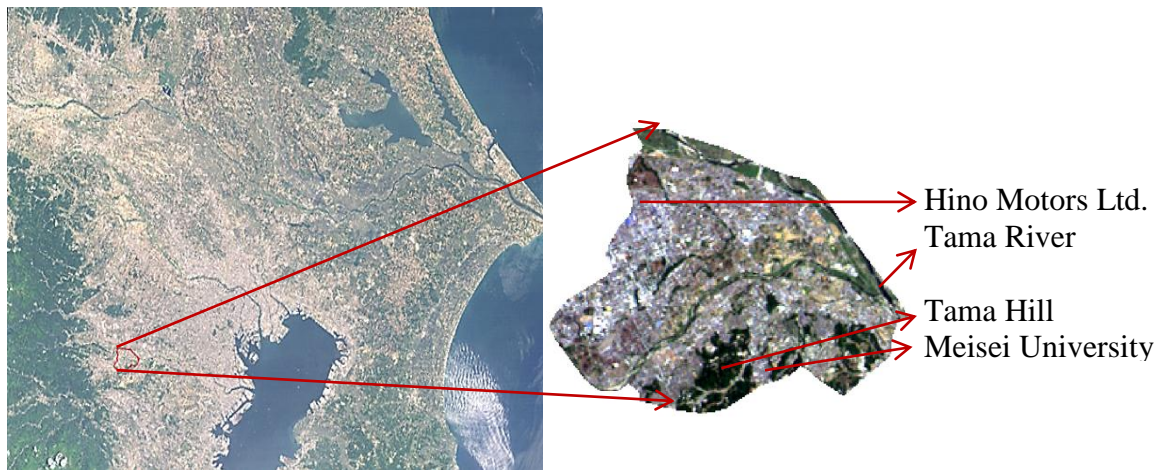
Figure 3.1. Hino City Location in Tokyo Region

Japan is an island country comprising of more than three thousand islands and thus, the Japan climate is not same everywhere. The climate of Hino city is in the humid subtropical climate zone, with hot humid summers and generally mild winters with cool spells [07Pee]. The region, like much of Japan, experiences a one-month seasonal lag, with the warmest month being August, which averages 27.5°C, and the coolest month being January, averaging 6°C. Annual rainfall averages nearly 1529.08 mm, with a wetter

summer and a drier winter. Snowfall is sporadic, but does occur almost annually [10]. Hino city also often sees typhoons each year, though few are strong.

The study area-2 (Mandalay city) is the capital of Mandalay State (Figure 3.2). It is located on latitude 21° 58' 30" North and 96° 5' 0" East with an area of about 507.54 km^2. Being situated in the transitional zone; between the mountain and the lowlands region of Myanmar and it serves as to be the main cultural, educational and economic hub of Upper Myanmar. The landscape of the region (Mandalay) is relatively flat, this means it is located on a plain and is surrounded by two large rivers, Irrawaddy and Myitnge in western and south part, and two small rivers in northern part [7].
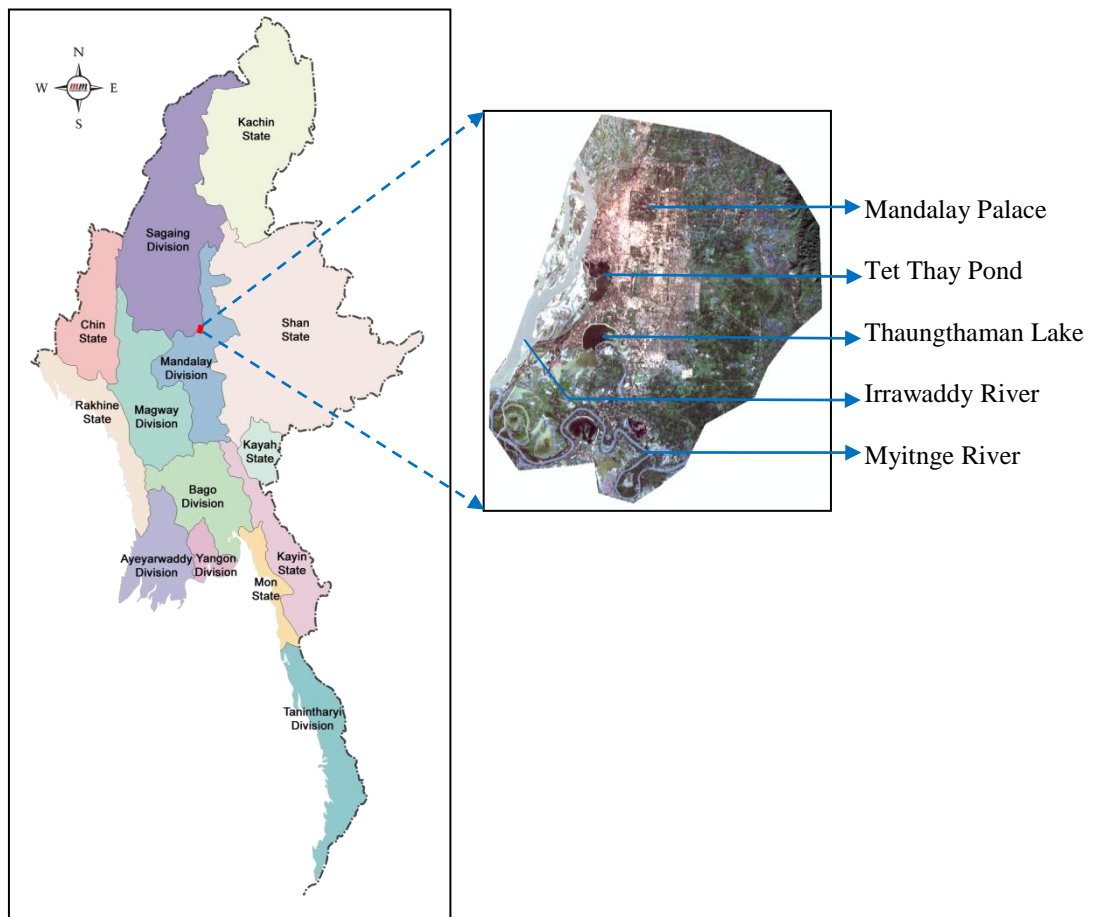
Figure 3.2. Mandalay Location in Region

The climate is humid tropical type and is characterized by summer, rain and cold seasons. The summer season begins towards the end of February and ends in July. A raining season in the city begins in August and ends in October. The rest months are so called cold season but the temperature is uniformly high throughout the year though it will fall at early morning during cold season. The mean monthly temperature of the city for the

39

period of 1961-1990 varies between 21°C and 32°C with the months of April and May having about 38°C [8]. The vegetation is characterized by dry lowland rainforest vegetal cover.

In this chapter, a general sketch of the methodology adopted has been described in figure 3.3 and GIS data of Hino city was used instead of ground control data. The present research is a framework of digital image processing using a case study to meet the expected result in order to solve the specified research problems.
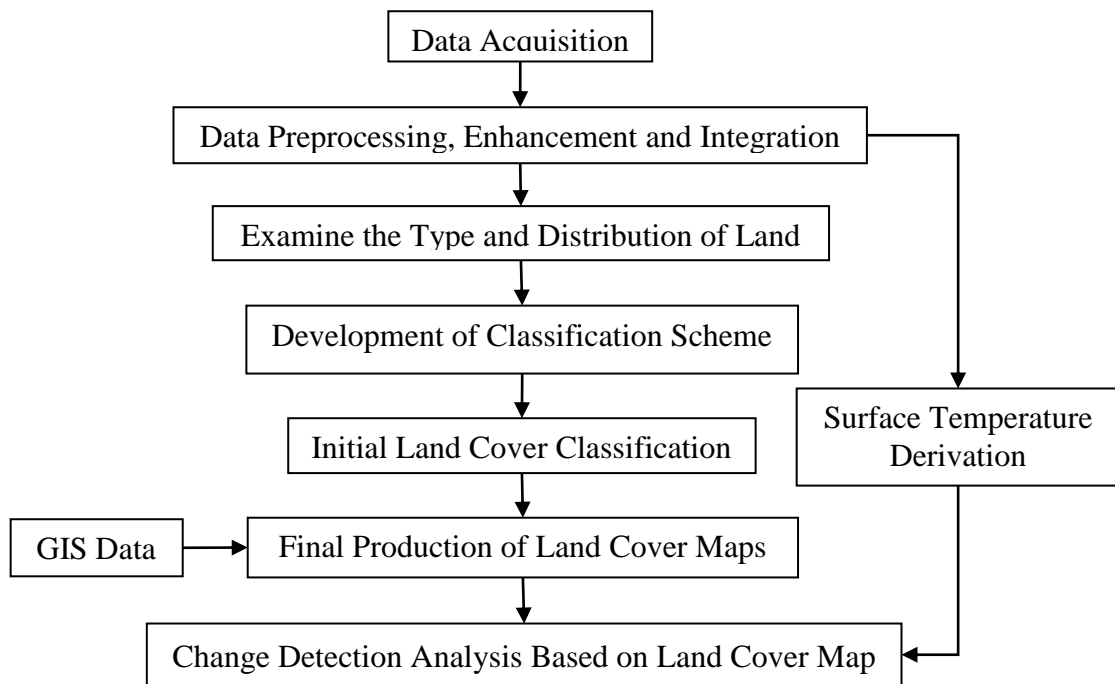
Figure 3.3. Flowchart of the Study

Towards this approach, information extraction using digital image processing using remote sensing (RS) data has been adopted. There are several techniques exist for improved information extraction from various sources of RS from simple visual interpretation of aerial photographs to complex automatic digital interpretation using various developed classification procedures. These techniques are directly influenced by several technical factors resolution and type of the image, target information to be extracted, objective of the study and accuracy requirements are worthy mentioned. A method for image classification along with required preprocessing; enhancement and post-classification analysis for change detection have been utilized for the whole study. As follow, the procedure adopted in this research work forms the basis for deriving statistics of land cover dynamics and subsequently in the overall, the findings.

40

3.2. Data Acquired and Source

In order to cover the intended period of study, different type of images originating from different types of sensors were used. Hence, Landsat Multispectral Scanner (MSS) and Thematic Mapper (TM) were used for both land cover change study areas (Table 3.1). Landsat satellite images of Hino city for this study were taken on 1987, 1996, 2001 and 2011 about 10:05 o'clock in the morning. Images of Mandalay city used in this study were acquired on 1988, 1996 and 2009 about 10:18 o'clock in the morning. All images were obtained from the Earth Resources Observation and Science Center (EROS), the United State Geography Survey (USGS) [6]. The GIS data of Hino city which was provided from Hino city office was used as a ground truth data for this study. It is also important to state that Myanmar Administrative map which was used to carve out Mandalay and its environs was obtained from local government. These were brought to Universal Transverse Mercator (UTM) projection in zone 47.

Table 3.1. Data Source

Study Area	Data Type	Date of Production	Scale	Source
Hino City	Landsat image	1987/5/21	30m^{TM}	USGS
	Landsat image	1996/4/27	30m^{TM}	
	Landsat image	2001/4/1	30m^{ETM+}	
	Landsat image	2011/4/5	30m^{TM}	
	Map of GIS Data (IKONOS-1m)	2008/9/9	1:56,424 (view scale)	Hino City
Mandalay City	Landsat image	1988/12/31	30m^{TM}	USGS
	Landsat image	1996/1/12	30m^{TM}	
	Landsat image	2009/1/15	30m^{TM}	
	Map of Mandalay	2005	1:9,196,429 (view scale)	City Office

3.2.1. Landsat Data

As described in Table 3.1, the Landsat images were available from two Landsat operations. Landsat TM imagery are part of Landsat 5 mission, launched in March 1, 1984 by NASA and Landsat ETM+ images are part of Landsat 7 mission, launched on April 15, 1999. The technical details of Landsat TM and Landsat ETM+ bands have been provided in the table 3.2 [5].

Table 3.2. Bands of Landsat TM (left) and ETM+ (right)

Band	μm	Resolution	Band	μm	Resolution
1	0.45-0.52	30	1	0.45-0.515	30
2	0.52-0.60	30	2	0.525-0.605	30
3	0.63-0.69	30	3	0.63-0.69	30
4	0.76-0.90	30	4	0.75-0.90	30
5	1.55-1.75	30	5	1.55-1.75	30
6	10.4-12.5	120	6	10.4-12.5	60
7	2.08-2.35	30	7	2.09-2.35	30
	-	-	8	0.52-0.9	15

3.3. Software Used

Basically, three softwares were used for this research.

(1) ArcGIS Desktop 10 - A geographic information system (GIS) is a database that links information to location, allows seeing and analyzing data in new and useful ways. ArcGIS uses intelligent GIS data models for representing geography and provides all the tools necessary for creating and working with the geographic data [1]. It is used for -

- creating and using maps
- compiling geographic data
- analyzing mapped information
- sharing and discovering geographic information
- using maps and geographic information in a range of applications and
- managing geographic information in a database.

ArcGIS Desktop includes a suite of integrated applications.

- **ArcMap:** (the central application in ArcGIS desktop and used for all map-based tasks including cartography, map analysis and editing)
- **ArcCatalog:** (to organize and manage GIS data and includes browsing and finding geographic information, recording, viewing and managing metadata, quickly viewing any dataset and defining the schema structure for geographic data layers)
- **ArcTool box:** a simple application containing many GIS tools for geoprocessing.

Using these three applications together, any GIS task can be performed simple to advanced, including mapping, data management, geographic analysis, data editing, and geoprocessing. In this study, ArcGIS was used for the carving out of Mandalay city region

from the whole Mandalay division imagery using both the admin and local government maps. Moreover, it makes faster for the development of land cover classes and subsequently for change detection analysis of the study areas.

(2) Envi 4.3 - ENVI (**Environment** for Visualizing Images) is the premier software solution for processing & analyzing geospatial imagery. It is used by image analysts, GIS professionals, scientists and researchers. This software was used in this study to preprocess the images such as, registering, geometric correction, and color composition. It is also useful for enhancement quality of images [2].

(3) remo10 - This software was developed by Dr. Sugimura (Remote Sensing Technology Center of Japan) and Land Surface Temperature (LST) derivation was done by this software [3].

3.4. Pre-processing

Before performing the classification of the RS data, it is important to pre-process the data to correct the error during scanning, transmission and recording of the data. It refers to the functions which are frequently performed to improve geometric and radiometric qualities of the images.

Typically, the pre-processing steps are-
- Radiometric correction to compensate the effects of atmosphere
- Geometric correction i.e. registration of the image to make it usable with other maps or images of the applied reference system, and
- Noise removal to remove any type of unwanted noise due to the limitation of transmission and recording processes.

3.4.1. Radiometric Correction

In this study, the radiometric correction has not been adopted due to the following reasons:
- The data for this study were already corrected to some extent. From the histogram (x= number of pixels, y=pixels values), it is noticed that all bands have 'offsets' from zero (shown by red line) which is acceptable except for the case of Band 6 which will be exploited for estimation of LST (Figure 3.4).
- For radiometric correction or normalization, calibrated data is required to achieve the

higher accuracy. Most importantly;

- Radiometric correction is obligatory only when image differencing is used for change detection analysis [09Tan].
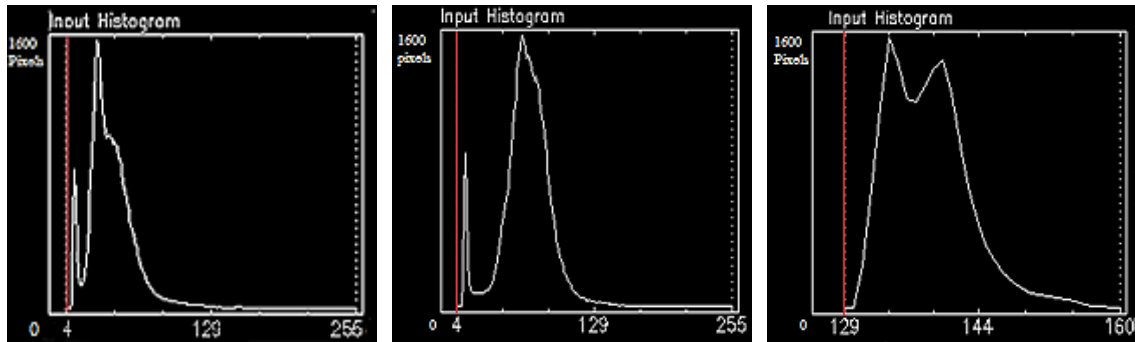
Figure 3.4. Band 5, 7& 6 Respectively with Histograms of Image (2001/11/17)

3.4.2. Geometry Correction

Raster data is commonly obtained by scanning maps or collecting aerial photographs and satellite images. In order to use these types of raster data in conjunction with other spatial data, it is often needed to georeference it to a map coordinate system. Image geometry correction (often referred to as Image Warping) is the process of digitally manipulating image data such that the image's projection precisely matches a specific projection surface or shape. It compensates for the distortion created by off-axis projector or screen placement or non-flat screen surface, by applying a pre-compensating inverse distortion to that image in the digital domain.

In present study all the datasets were geometrically corrected by the source in UTM-54N projection for study area-1 and UTM-47N projection for study area-2. The 1996 Landsat TM images for both study areas have been geo-referenced to the other datasets in UTM WGS 84 system using image to image registration method. The Landsat ETM+ image has been used as a reference image in this case. During registration, initially 4 ground control points (GCP) were used from the Landsat image but finally 8 GCPs have been used to improve the positional accuracy and the root mean square was 0.0010 for both study areas (Figure 3.5). The GCP have been collected from the image itself as it has some cross-points with known latitude/longitude value.

After examination of all the datasets and the statistics and histograms of images, there were no noise or image pixel dropout, primarily because those might be removed by the data center who delivered the data to the source. However, all the images have been

enhanced its quality in terms of visual appealing which is described in the next section under image enhancement.

	Base X	Base Y	Warp X	Warp Y	Predict X	Predict Y	Error X	Error Y	RMS	
#1+	1523.00	484.00	722.00	230.00	720.4674	229.1985	−1.5326	−0.8015	1.7295	
#2+	2835.00	2253.00	1373.00	1113.00	1376.1266	1115.1865	3.1266	2.1865	3.8152	
#3+	413.00	5877.00	165.00	2929.00	165.1980	2929.4740	0.1980	0.4740	0.5136	
#4+	3069.00	4728.00	1495.75	2357.25	1493.6615	2354.1624	−2.0885	−3.0876	3.7276	
#5+	4738.75	3528.00	2326.80	1752.50	2328.1184	1753.6599	2.1184	1.1599	2.4152	
#6+	4051.00	5747.00	1985.75	2863.50	1985.1625	2864.2045	−0.5875	0.7045	0.9173	
#7+	6368.00	1367.00	3142.25	673.25	3141.0162	672.6133	−1.2338	−0.6367	1.3894	
#8+	6714.00	4218.00	3316.14	2099.10	3316.1395	2099.1009	−0.0005	0.0009	0.0010	

Figure 3.5. Image to Image Registration (1996 Wrap Image and 2009 Based Image)

3.4.3. Color Composition

For visual display, each band of the image may be displayed one band at a time as a grey scale image (Figure 3.6 & 3.7 shows the visual bands and NIR in grey scale, respectively for Hino city and Mandalay city), or in combination of three bands at a time as a color composite image. In displaying a color composite image, three primary colors (red, green and blue) are used. When these three colors are combined in various proportions, they produce different colors in the visible spectrum.

Associating each spectral band (not necessarily to be a visible band) to a separate primary color results in a color composite image. If band 1 is displayed in the blue color, band 2 is displayed in the green color, and band 3 is displayed in the red color, is known as visual RGB composite and the resulting images are fairly close to realistic (Figure 3.8-a & 3.9-a). The color is resampled closely what would be observed by the human eyes as in photograph. But that are also pretty dull - there is little contrast and features in the images are hard to distinguish. If band 2 is displayed in blue, band 3 is displayed in green, and band 4 is displayed in red, it is known as a false color composite image (Figure 3.8-b & 3.9-b). The color in the displayed images does not have any resemblance to its actual color.

45

This false color composite scheme allows vegetation to be detected readily in the images and vegetation appears in different shades of red depending on the types and conditions of the vegetation, since it has a high reflectance in the near infrared (NIR) band.
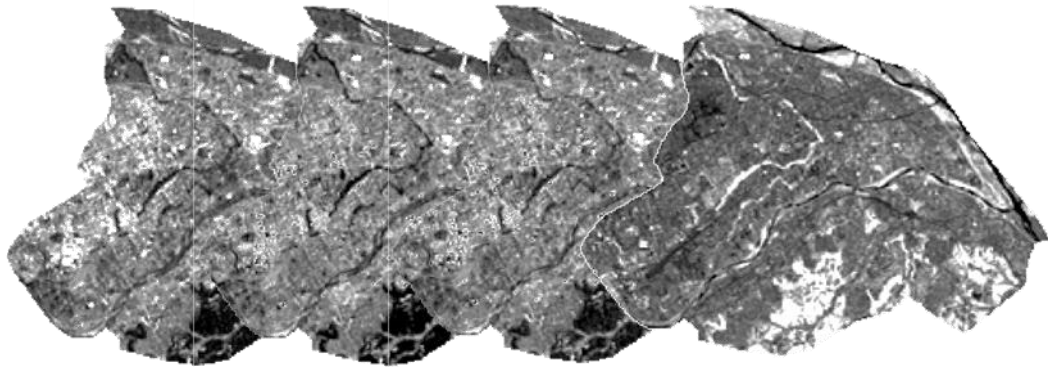

Figure 3.6. Visual and Infrared Bands of Satellite Image (Hino City-1987/5/21)
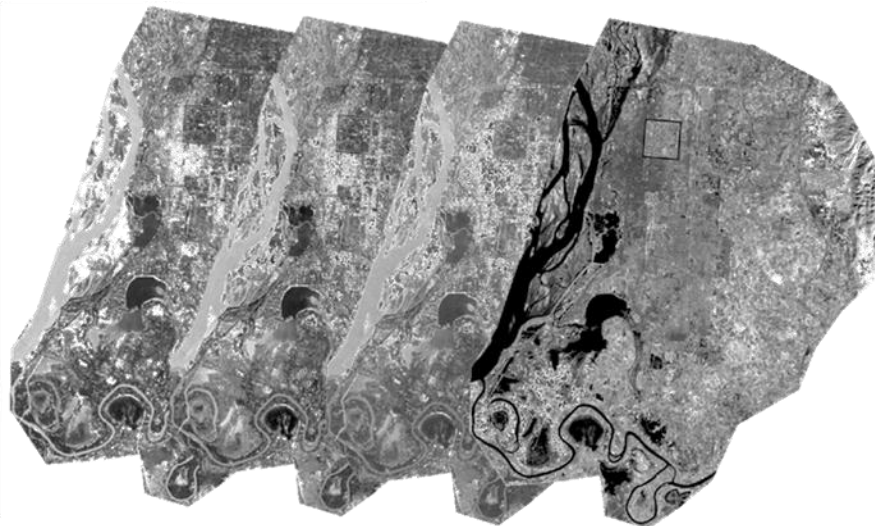

Figure 3.7. Visual and Infrared Bands of Satellite Image (Mandalay City-2001/11/17)
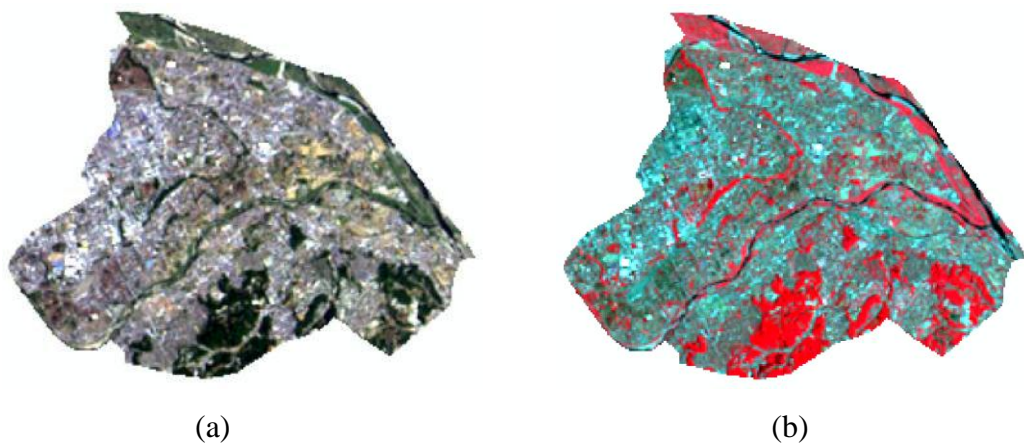

| (a) | (b) |

Figure 3.8. (a) True Color and (b) False Color of Hino City (1987/5/21)

(a)   (b)
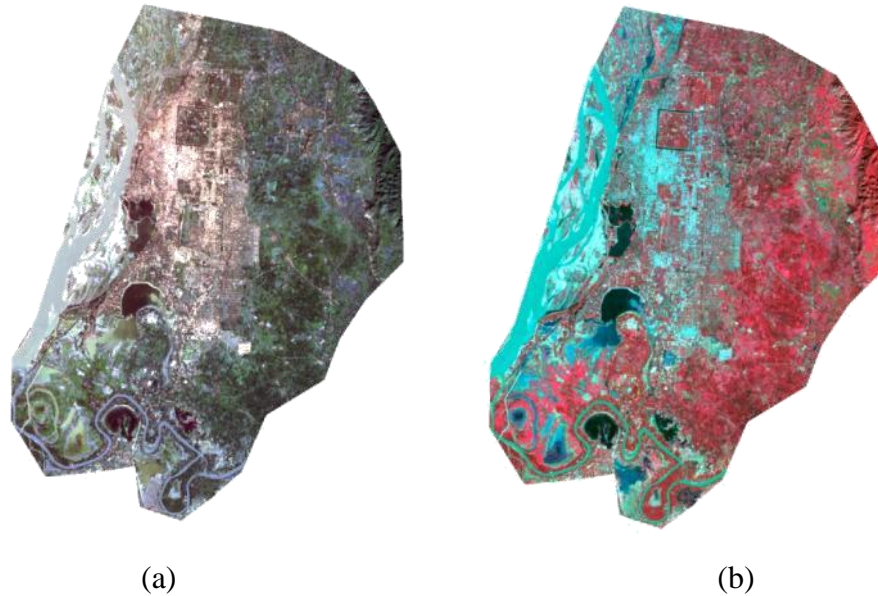
Figure 3.9. (a) True Color and (b) False Color of Mandalay City (2001/11/17)

3.4.4. Image Enhancement

Image enhancement involves the technique to increase the visual distinction of the features or classes in the image. This step alters the pixel value of the image and therefore image enhancement is followed after the pre-processing step is completed. The choice of enhancement technique depends upon the features to be used for extracting from the image. The most commonly used one is the simple contrast stretching which has also been adopted in this study. This step has been considered and proved to increase effectively the overall contrast of the image elements by accomplishing few simple steps.

In order to aid visual interpretation, visual appearance of the objects in the image can be improved by image enhancement techniques such as contrast stretching to improve the contrast and spatial filtering for enhancing the edges. Contrast stretching (often called normalization) is a simple image enhancement technique that attempts to improve the contrast in an image by stretching the range of intensity values it contains to span a desired range of values, e.g. the full range of pixel values that the image type concerned allows. Unlike histogram equalization, contrast stretching is restricted to a linear mapping of input to output values. The result is less dramatic, but tends to avoid the sometimes artificial appearance of equalized images. There are several methods for contrast stretching as well. After performing those methods on the complete dataset, it has been found that linear stretching and histogram equalization are the suitable ones for this purpose.

The first step is to determine the limits over which image intensity values will be extended. These lower and upper limits will be called **"a"** and **"b"**, respectively (for

standard 8-bit grayscale pictures, these limits are usually 0 and 255). Next, the histogram of the original image is examined to determine the value limits (lower= **"c"**, upper= **"d"**) in the unmodified picture. If the original range covers the full possible set of values, straightforward contrast stretching will achieve nothing, but even then sometimes most of the image data is contained within a restricted range; this restricted range can be stretched linearly, with original values which lie outside the range being set to the appropriate limit of the extended output range. Then for each pixel, the original value **"r"** is mapped to output value **"s"** using the function of linear mapping, so get equation of a straight line,

$$s = (r - c)\left[\frac{b-a}{d-c}\right] + a$$

3.1

As a result the 'enhancement' is less harsh and the results of applying the linear stretch are shown in the following image in figure 3.10. Although the contrast of the images has been improved, it was not visibly distinguishable. After that, histogram equalization was applied which improved the images significantly as in figure 3.11.

The same methods were followed for rest of datasets. It has been decided to use histogram equalization method for enhancement since it is supposed to be best for this case study. A histogram equalization stretch assigns the image values to the display levels on the basis of their frequency of occurrence [72Lil]. As it can be easily seen from the figure 3.10 & 3.11, more display values are assigned to the frequently occurring portion of the histogram which consequently increased the radiometric quality of the image.
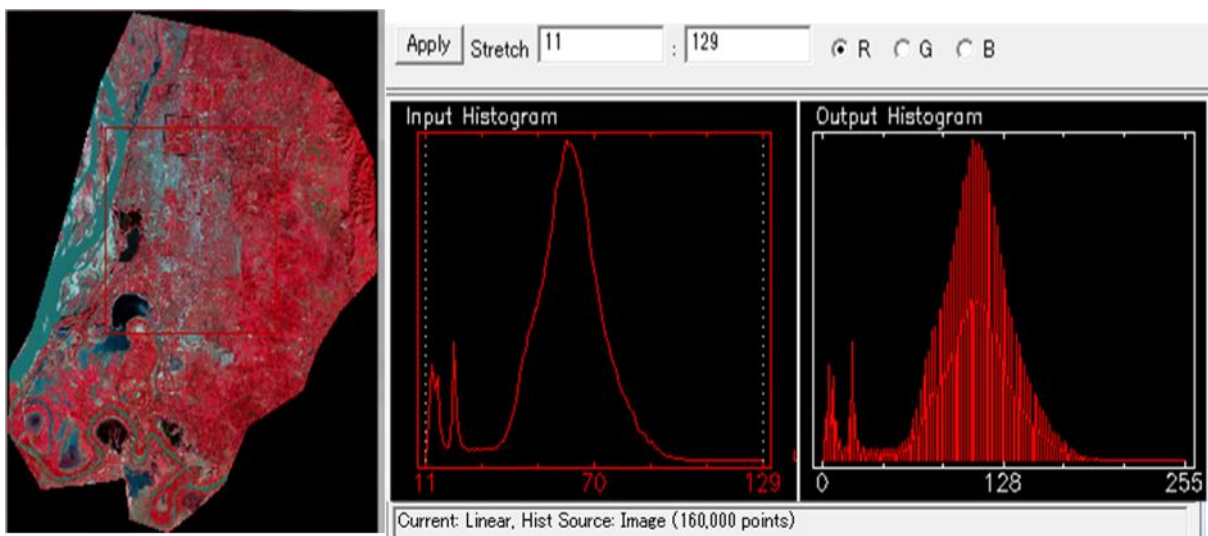
Figure 3.10. Input Image with Histogram after Contrast Stretching (Linear 2%)
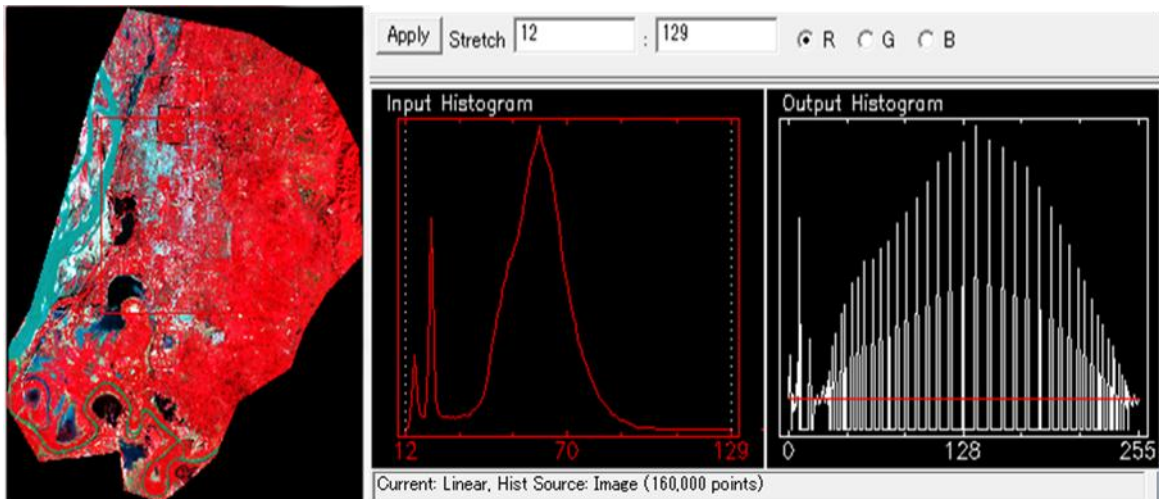
Figure 3.11. Histogram after Contrast Stretching (Histogram Equalization)

3.5. Development of a Classification Scheme

Based on the priori knowledge of the study area and a brief reconnaissance survey, a classification scheme was developed for both study areas with differences in class 4 depends on landscapes of study areas, where "Bare Ground" is set for study area-1 and "Agriculture mixed land" is set for study area-2. The limited possibility of classes for Landsat images was also considered as the images have 30m resolution which is too large to classify other classes of small areas. The developed classification scheme gives a rather broad classification where the land cover was identified by a single digit and the source to be used for classification (Table 3.3).

Table 3.3. Land Cover Classification Scheme

Class	Land cover categories	Classified Source
1	Forest	Infrared Composite
2	Lawn/Grass	Infrared Composite
3	Water	Infrared Composite
4	Bare Ground/Agriculture Mixed Land	RGB or Visual
5	Built-up and other land	RGB or Visual

3.5.1. Forest

Forest includes most riverside areas, highlands and also some steep slopes. In this study, vegetated areas are classified in two general classes, as either open or dense, and

comparison of their relative greenness values using the Normalized Difference Vegetation Index (NDVI) value was employed to make a distinction between them.

3.5.2. Lawn or Grass

Lawn/grass land was found very little areas in both study areas. Lawn/grass land is seemed well maintained in Hino city. In Mandalay city, area closure is not practiced, even though the district announces it to be one of the activities they are currently working at. Hence, vegetated areas are not well protected and are being accessed freely to serve as grazing land.

3.5.3. Water

The category of water encompasses Tama and Asa river in study area-1; Irrawaddy and Myintnge river and those areas located in southern part of Mandalay city which experience frequent immersion by water.

3.5.4. Bare Ground and Agriculture Mixed Land

Bare ground is found mostly around the rivers' side in study area-1especially in April as lawn areas are still being affected by drier winter. Agriculture mixed land is where various food crops are grown, either on a rain-fed basis or using irrigation. Irrigation is commonly practiced in eastern part of study area-2. They are covered by any type of crops, grass or any other shrub or tree species. Accordingly, in such areas, growing various tree and shrub species as live fences, boundary plants, or woodlots has been observed to be a common practice. It is also apparent that various agricultural crops like cereals, fruit trees, and sometimes vegetables are grown in the homesteads, depending on the availability of water supply.

3.5.5. Built-up and Other Land

In addition to the land cover classes described above, it is also apparent that there are areas that serve as built up area, most of which are made of up of corrugated metal roofs, scattered around and traditional huts. The category of built up land denotes areas that are without any vegetation cover at the time of satellite image acquisition but could be categorized in one of the land cover types mentioned above. Built land meant to include those areas with exposed sand/soil, bare ground and exposed rock as well. Because it was not possible to easily identify settlements features in the satellite images and due to the

relative small size of the study areas, the decision was made not to consider settlements among the land cover classes.

3.6. Methods of Image Classification

Image classification is the most widely used technique in various remote sensing applications for extraction of target thematic information. In the context of present study, the land cover is the main 'theme' which is to be extracted using a suitable classification method for land cover change detection. Basically, image classification is a mapping process to generalize the image pixels into meaningful groups each resembling different land category [01Jen]. The process requires an optimum and specifically designed classification algorithm for precise application purpose because it largely varies depending upon the type and objective of the work.

Typical method for RS image classification is so called pixel based method in which the classifier considers different pixel values and group them into classes solely based on their spectral properties. In general, some pixels from known locations will be collected by referencing to GIS map or other sources. These pixels are called training pixels as it has to collect many times to match with the actual data. After collecting training pixels, the range of training pixel values for each class (minimum, maximum, mean etc.) was computed to determine the membership of the pixels to the class. Then, each pixel is assigned to the class to which its value is within the range of that class.

This training is based on conventional statistical techniques such as supervised and unsupervised classification where the classes are supervised by analyst and are not supervised (i.e. fully automatic based on spectral values) respectively. In unsupervised classification, the ArcGIS automatically groups pixels with similar spectral characteristics (means, standard deviations, covariance matrices, correlation matrices, etc.) into unique classes according to some statistically determined criteria [00Bru]. The analyst then re-labels and combines the spectral classes into information classes (Figure 3.12).

In supervised classification, identify known a priori through a combination of fieldwork, map analysis, and personal experience as training sites; the spectral characteristics of these sites are used to train the classification algorithm for eventual land cover mapping of the remainder of the image [01Jen]. Every pixel both within and outside the training sites is then evaluated and assigned to the class of which it has the highest likelihood of being a member (Figure 3.13). This study is mainly used supervised classification based on the knowledge of GIS map and other source of maps.
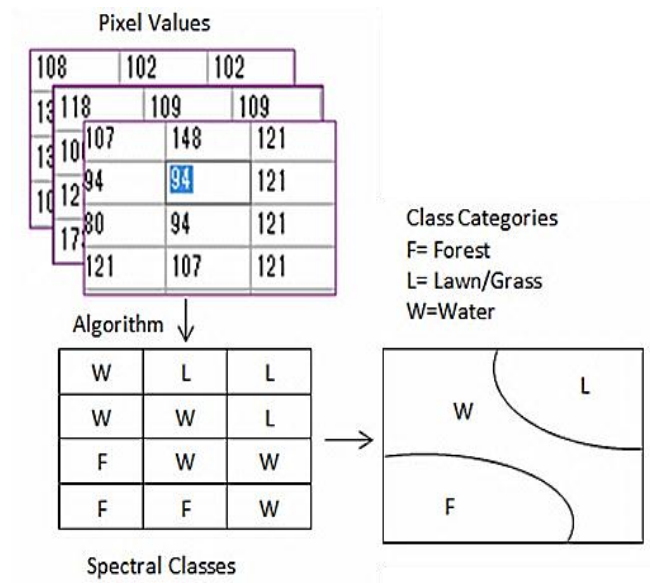
Figure 3.12. Process of Unsupervised Classification
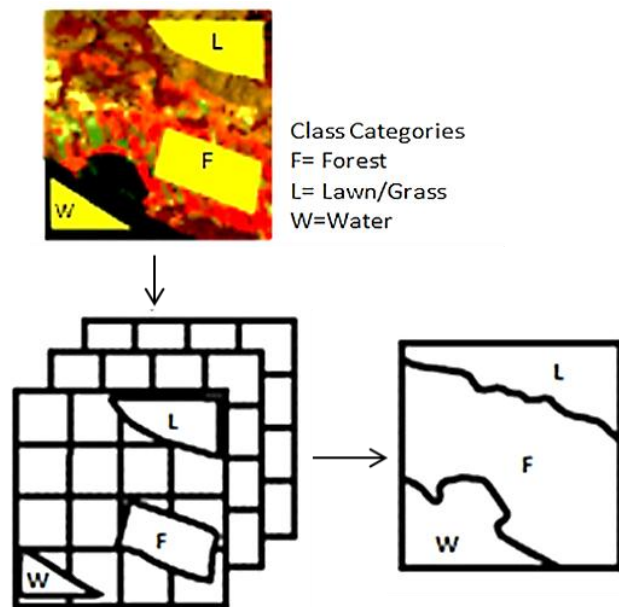
Figure 3.13. Process of Supervised Classification

Both classification algorithms typically use hard classification logic to produce a classification map that consists of hard, discrete categories (e.g., forest, agriculture). Unsupervised classification uses statistical techniques to group n-dimensional data into their natural spectral clusters, and uses the iterative procedures (Figure 3.14). Then certain clusters are labeled as specific information classes. There are two iterative procedures; K-mean and ISO DATA (Iterative Self-Organizing) and the later was used in this study. In ISO DATA procedure, for the first iteration arbitrary starting values (i.e., the cluster

properties) have to be selected. These initial values can influence the outcome of the classification.
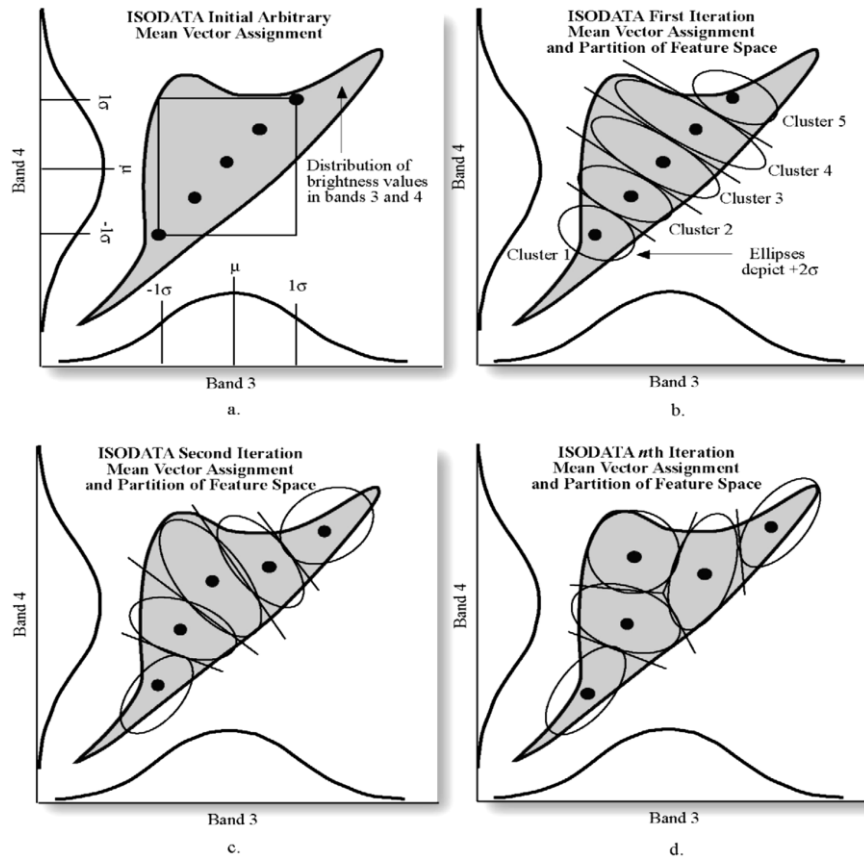
Figure 3.14. Process of ISO DATA Iteration

In general, this method assigns first arbitrary initial cluster values. The second step classifies each pixel to the closest cluster. In the third step the new cluster mean vectors are calculated based on all the pixels in one cluster. The second and third steps are repeated until the "change" between the iteration is small. The "change" can be defined in several different ways, either by measuring the distances of the mean cluster vector have changed from one iteration to another or by the percentage of pixels that have changed between iterations. This algorithm has some further refinements by splitting and merging of clusters. Clusters are merged if either the number of members (pixel) in a cluster is less than a certain threshold or if the centers of two clusters are closer than a certain threshold. Clusters are split into two different clusters if the cluster standard deviation exceeds a predefined value and the number of members (pixels) is twice the threshold for the minimum number of members. The example of ISO DATA classification is shown in figure 3.15, which were classified 5 classes and 10 classes respectively.

(a)   (b)
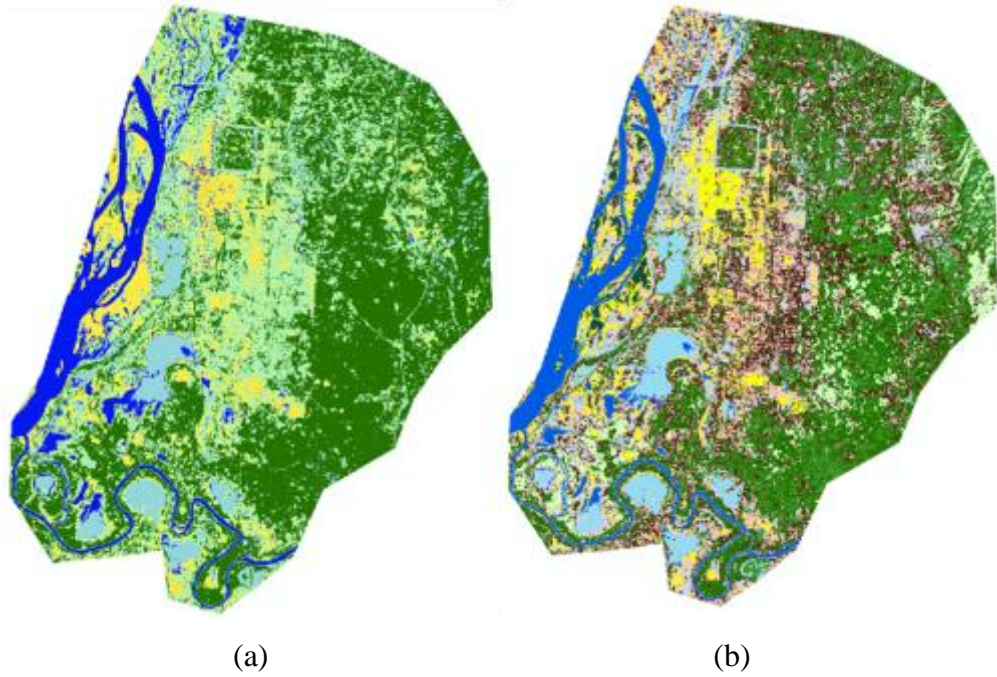
Figure 3.15. ISO DATA Unsupervised Classification (a) 5 classes (b) 10 classes

■ Forest

□ Cotton

■ Grass

■ Fallow
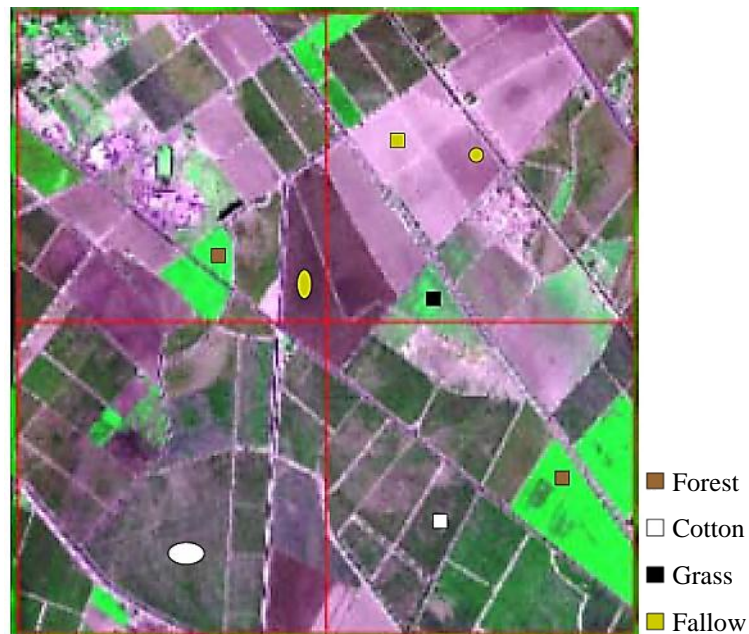
Figure 3.16. Example of On-screen Selection of Polygonal Training Data

Various supervised classification algorithms may be used to assign an unknown pixel to one of impossible classes. The choice of a particular classifier or decision rule depends on the nature of the input data and the desired output. Maximum likelihood classification algorithm was commonly used which its decision rule is based on probability instead based on training class multispectral distance measurements [78Mul]. Maximum

likelihood assumes that each training class in each band are normally distributed (Gaussian). Training data with bi- or n-modal histograms in a single band are not ideal. In such cases the individual modes probably represent unique classes that should be trained upon individually and labeled as separate training classes. The probability of a pixel belonging to each of a predefined set of m-classes is calculated, and the pixel is then assigned to the class for which the probability is the highest. Figure 3.16 shows the example of on-screen selection of polygonal training data (i.e. ROI: Region Of Interest) in maximum likelihood classification.

3.7. Change Detection from Multi-temporal Images

Change detection is a technology ascertaining the changes of specific features within a certain time interval. It provides the spatial distribution of features and qualitative and quantitative information of features changes. The quantitative analysis and identifying the characteristics and processes of surface changes is carried through from the different periods of remote sensing data. There is change detection based on elevation change information of digital surface models apart from the change detection using multi-spectral remote sensing images.

Change-detection images provide information about seasonal or other changes. The information was extracted by comparing two or more images of the study area that were acquired at different times. To get higher-quality change detection results, any other noise factors have to be minimized by selecting multi-temporal image pairs that have similar photographing conditions, such as atmospheric conditions, variation in the solar illumination angles, and sensor calibration trends. It is, however, very difficult to maintain radiometric consistencies between images due to these different photographing conditions. Therefore, radiometric co-registration should be done to remove these noise effects between multi-temporal images [02Yon]. One prerequisite for successful change detection is an accurate registration of satellite imagery, so the overlaid pixels represent the same location.

There are many types of change detection methods of multi-spectral image data. They can be classified as three categories: characteristic analysis of spectral type, vector analysis of spectral changes and time series analysis. In this chapter, the method of time series analysis will be described, where the aim is to analyze the process and trend of changes by monitoring ground objects based on remote sensing continuous observation data. Three methods will be followed up; Image subtraction, Image ratio and method of

change detection after classification.

3.7.1. Image Subtraction Method

It is a method with the most extensive application that can be applied to a wide variety of types of images and geographical environments. It is generally conducted on the basis of gray values. The changed region and unchanged region is determined by selecting the appropriate threshold values of gray levels in the subtraction image. The gray value of the subtraction image shows the differences of corresponding pixels of two images. Its advantage is that in the subtraction image the threshold selecting operation needs to be applied only once. Choosing a suitable threshold value can best separate the areas of real change and the change areas due to random factors. The gray values of the subtraction image are often approximating a Gaussian distribution, the unchanged pixels are grouped around the average value and the changed pixels are in the two tails of the distribution.

It is beneficial for collecting change information at areas such as the beach zones, estuaries and water channel ditches. It is widely used in detecting coastal environmental changes, tropical forests changes, temperate forests changes, and desertification and crop analysis. The main disadvantage of this method is that it does not reflect changes in categories. The value of subtraction image does not always show the change of the objects because of a variety of factors such as atmospheric conditions, the sun illumination, sensor calibration, and ground water conditions, and so on. In actual applications, the choice of threshold is quite difficult. Therefore, it is not suitable for change detection of urban areas and change detection of natural images, because some information will be lost. So, it is difficult to determine the nature of changes and further analysis is needed.

3.7.2. Image Ratio Method

A pixel value of a time series image divides the corresponding pixel of another time series image. In this method, we calculate the ratio of corresponding pixels in each band from two images of different periods after image co-registration. A threshold value selects significant changes regions in the ratio image. The choice of threshold value must be based on the characteristics of the regional research targets and the surrounding environment. A threshold value will vary in different regions, different times and different images. The threshold value of 'change' and 'no change' pixels is often chosen using the histogram of the ratio image.

The image ratio method is useful for the extraction of vegetation and texture. The

influence of the slope and aspect, the shadow or sun angle, radiation changing caused of strong seasonal variations and multiplicative noise can be eliminated or reduced. It can highlight different slope features between the bands. It has higher accuracy and can be applied to estimate change detection in cities. A drawback of this method is also that the type of feature changes can't be analyzed. The choice of threshold value is difficult. Different features of the same slope are easy to be confused and the ratio synthesized image is often compensated for in the analysis.

3.7.3. Change Detection after Classification

This method is the most simple change detection analysis technique based on the classification. Each image of multi-temporal images is classified separately and after that we compare the classification result images. If the corresponding pixels have the same category label, the pixel has not changed, or else the pixel has changed. There are supervised classification methods and non-supervised classification methods. Non-supervised classification is also known as cluster analysis or point cluster analysis. That is the process of searching and defining the natural spectrum cluster group in the multi-spectral image where the computer automatically composes cluster groups according to pixel spectral values or space position. And then each group and the reference data will be compared and divided into certain categories. The type of change of each changed pixel is determined in the change detection matrix.

The advantage of this method is that it does not only ascertain the spatial distribution of changes but also gives the nature of changes, in other words the information on the transition from one class to another. One shortcoming of this method is the high requirements for a reasonable classification of categories. Secondly, when the classification and change detection become two relatively independent processes, the amount of information may be reduced and the accuracy also. Finally, this method is sensitive to classification errors. Therefore, the accuracy of this method depends on the accuracy of the classification results. This method is not suitable for change detection of details of urban areas because of the generally low-resolution of multispectral images and the complex spectral characteristics of cities.

From the application point of view, the image subtraction method and the method of change detection after classification do not apply to the change detection of details of urban areas, while the image ratio method can be used for change detection in cities, particularly analysis of vegetation and soil. The image subtraction and image ratio methods

are capable only of detecting the position and degree of changes but cannot provide information about the type of changes, such as what class was changed to what, which can be provided by change detection after classification.

Among the three methods, post classification method was applied for the present study. The post classification method is the most widely used and has been adopted here for following reasons:

- The accuracy of change detection is dependent on the accuracy of individual classification which can be reclassified or updated easily whenever necessary.
- Pre-classification method provides the change information by attribute of "change or no change" only.
- To avoid the problems those arise due to different properties of multi-source images and due to co-registration since each image have been classified independently.
- Individual classification of time-series images produced a historical set of land cover data which can be used for some other applications as well.

The method of post classification consists in overlaying the classified images, using the cross operation, to be compared for change detection. The cross operation using two classified images from different time allows the interpreter to know the extent and nature of changes in land cover transition between different land cover classes and corresponding area of change.

Since the final change classes resulting from cross operation are quite numerous and time consuming as well as slight difference in co-registration between data might result misinterpretation of changes, it has been decided to confine the change analysis to the perspective of area change for each class where area of each class have been calculated individually to show the area change for each class. Moreover, the study is more focused on suitability of applied change detection method instead the result of change detection.

3.7.4. Percentage of Changes

The comparison of the land cover statistics assisted in identifying the percentage of change, rate of change between 1987 to 2011 for study area-1 and rate of change between 1988 and 2009 for study area-2. In achieving this, the first task was to develop a table showing the area in meter and the percentage change for each year (1987, 1996, 2001 and 2011 for study area-1 and 1988, 1996 and 2009 for study area-2) measured against each land cover type. Percentage change to determine the trend of change can then be calculated

by dividing observed change by sum of changes multiplied by 100.

$$Percentage\ of\ change = \frac{Observed\ change}{Sum\ of\ change} \times 100$$

<div align="right">3.2</div>

In obtaining annual rate of change, the percentage change is divided by 100 and multiplied by the number of study years; 1987-1996 (9 years), 1996-2001 (5 years) and 2001-2011 (10 years) in study area-1 and 1988-1996 (8 years) and 1996-2009 (13 years) in study area-2.

3.8. Deriving Land Surface Temperature

Land Surface Temperature (LST) of Mandalay city was retrieved from Landsat TM/ETM+ data in the thermal infrared band (10.4-12.4 μm). The normalized difference vegetation index (NDVI) and land emissivity were estimated from visible and near infrared bands, while the effective satellite temperature was estimated from the thermal infrared band. The emissivity of the surface is controlled by such factors as water content, chemical composition, structure, and roughness. The emissivity of vegetated surfaces can vary significantly with plant species, area density, and growth stage. Emissivity as a function of wavelength is commonly referred to as spectral emissivity [00Sob]. Surface emissivity based on the conventional land classification method was used in this study. The following methods were adopted:

NDVI were computed from the reflectance of Band 3 and Band 4 data using the formula:

$$NDVI = \frac{B4 - B3}{B4 + B3}$$

<div align="right">3.3</div>

The following equation was used to convert the digital number (DN) of Landsat TM thermal infrared band into spectral radiance.

$$L_\lambda = 0.0370588 \times DN + 3.2 \qquad\qquad 3.4$$

The next step is to covert the spectral radiance to at satellite bright near temperature (i.e, blackbody temperature, TB, under the assumption of uniform emissivity [93Pra]. The

conversion formula, effective Satellite temperature T_s:

$$T_s = \frac{K_2}{\ln\left(\frac{K_1}{L_\lambda}\right) + 1}$$

3.5

Satellite thermal infrared sensors measure radiance at the top of the atmosphere (also known as blackbody radiance), from which brightness temperatures T_B can be derive by using Planck's law [86Mar]:

$$T_B = \left(\frac{hc}{k\lambda}\right)\left(\frac{1}{\ln\left(\frac{2hc^2\lambda^{-5}}{B_\lambda} + 1\right)}\right)$$

3.6

where L_λ is the spectral radiance at the sensor ($Wm^{-2}sr^{-1}\mu m^{-1}$), h is Planck's constant (6.63×10^{-34} J/sec), c is the speed of light (2.998×10^8 m·sec^{-1}), k is the Boltzmann constant (1.38×10^{-23} J/K^{-1}), λ= wavelength of emitted radiance (11.5μm) [86Mar] and $\underline{B_\lambda}$ is the blackbody radiance ($Wm^{-2}\mu m^{-1}$). The flowchart of estimating land surface temperature is shown as follow.
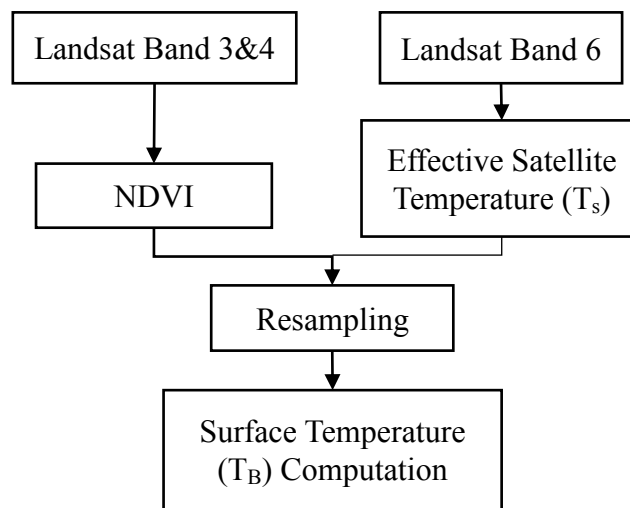

Figure 3.17. Flowchart for Estimating Surface Temperature [07Ifa]

CHAPTER 4
DATA ANALYSIS AND RESULTS

4.1. Satellite Remote Sensing

Increasing concern over how human activities interact and influence the global environment have led to the initiation and formulation of a number of environment assessment programs, treaties and agreements which call for increased, systematic observation of Earth systems. Such systematic observations require consistent, geographically referenced data that can be acquired over large areas repeatedly and at a reasonably low cost, using remote sensing technology. Since the launch of the first Meteorological Satellite in 1960, satellite remote sensing has emerged to be a cost-effective method for conducting time-series, large-scale observations of the Earth's systems. Satellite images can be used to map the entire world and to generate a number of global datasets needed for various thematic applications as well as detecting the environmental changes occurred in passage of time and natural disaster.

The objective of this study forms the basis of all the analysis carried out in this chapter. The results are presented inform of images, charts and statistical tables. They include the static, change and projected land cover of each class.

4.2. Steps in Analysis of Satellite Images for Land Cover Change

Landsat TM and ETM+ images on 1987, 1996, 2001 and 2011 for Hino city (area-1) and 1988, 1996 and 2009 for Mandalay city (area-2) were chosen to be same season to minimize the differences of land features for land cover classification and change detection included land surface temperature (LST). In study area-1, almost all images were taken in April but there was only one image available for 1987 taken in May. In order to detect changes over years, Landsat images availability is very limited to get same season and same month due to the percentage of cloud cover free in the satellite orbit (16 days cycle for Landsat). In the case of study area-2, the images were in December and January which is the same season for this area. Steps for data analysis were approached as following.

4.2.1. Data Acquisition

First of all, Landsat images of for both study areas were downloaded from the USGS website and saved [6]. There are 7 bands for Landsat TM and 8 bands for ETM+ images with 30m resolution except thermal band (Band 6) with 120m resolution for TM

image, and 60m resolution for ETM+. There is an extra 15 m band for Landsat ETM+ which is panchromatic band. Following are the original downloaded scenes in 107/35 (Path/Row) of 1987/5/21 shown in Figure 4.1for study area-1 and Figure 4.2 is the scenes of study area-2 taken in 1988/5/21 with 133/45 (Path/Row).
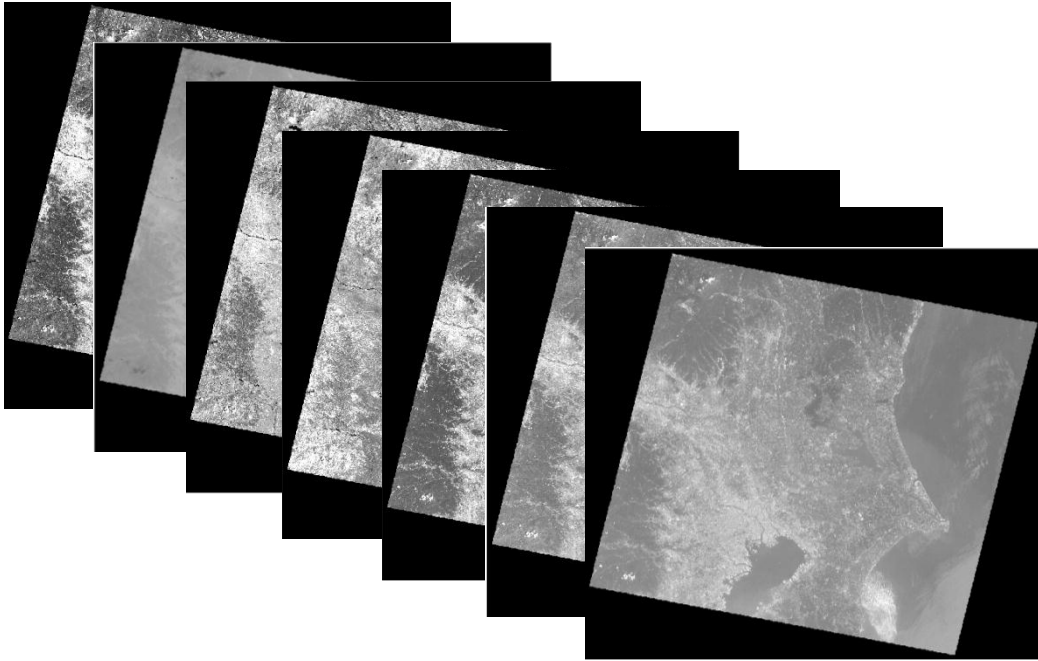

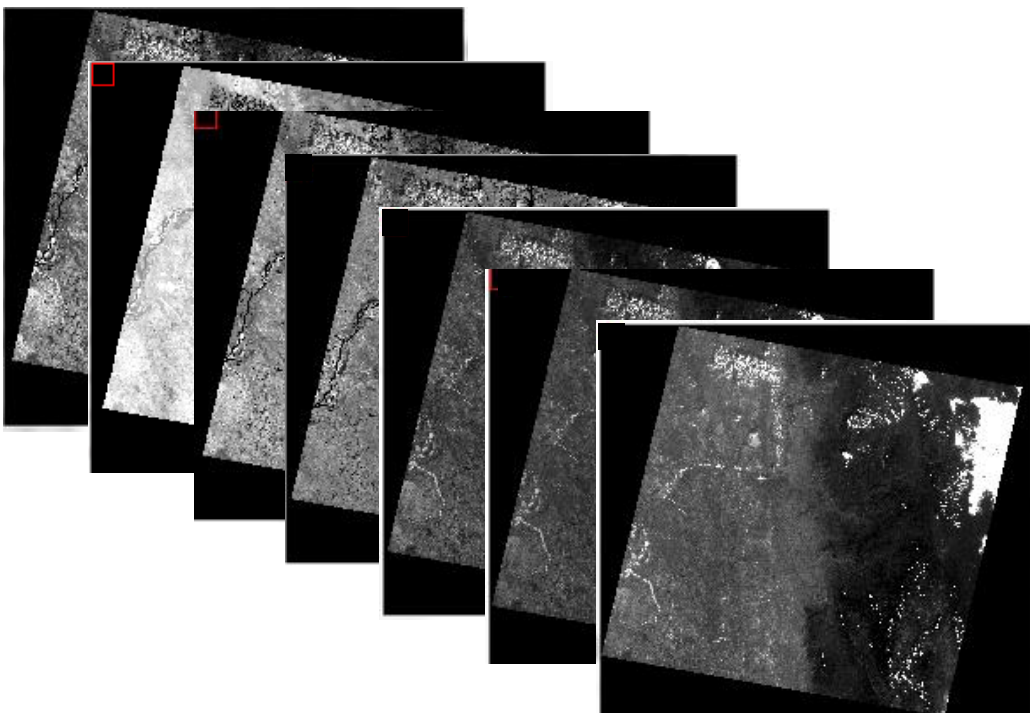Figure 4.1. Seven Bands of Satellite Image on Tokyo Region (1987/5/21)

Figure 4.2. Seven Bands of Satellite Image on Mandalay Region (1988/12/31)

4.2.2. Pre-processing

Preprocessing of satellite images prior to image classification and change detection is essential. Preprocessing commonly comprises a series of sequential operations, including atmospheric correction or normalization, image registration, geometric correction, and masking (e.g., for clouds, water, irrelevant features). Geometric correction was performed for all bands of the image of 1996 using image to image registration method whereas other images are not necessary for this correction. Geometric correction is necessary to preprocess remotely sensed data and remove geometric distortion so that individual picture elements (pixels) are in their proper plain metric (x, y) map locations. This allows remote sensing-derived information to be related to other thematic information in GIS. Geometrically corrected imagery can be used to extract accurate distance, polygon area, and direction (bearing) information. Landsat scenes are much larger than study area. In these instances it is beneficial to reduce the size of the image file to include only the area of interest. This not only eliminates the extraneous data in the file, but it speeds up processing due to the smaller amount of data to process. This is important when utilizing multiband data such as Landsat TM imagery.

After the geometric correction was done for scenes of 1996 image, color composition process for all images was applied to create true color images and false color images. True color composition image (Band 3, Band 2 and Band 1), which is useful to classify water boundary and type of ground, resembles closely what would be observed by the human eyes. False color composition or infrared composition image (Band 4, Band 3 and Band 2) was used to classify vegetation from other contents because vegetation appears in different shades of red depending on the types and conditions of the vegetation, since it has a high reflectance in the NIR band. Figure 4.3 is represented the composited images of Tokyo scene, taken on 1987/5/21.

4.2.3. Extracting Study Areas

The area of Tokyo region is about 35049 square km and the study area, Hino city is 27.53 square km. It is necessary to extract out study area from Tokyo scene composition. In order to extract Hino city from each scene, shape file of study area or Hino city was created in ArcMap (ArcGIS) with referencing to GIS map of Japan which acquired from Economic and Social Research Institute, Japan (ESRIJ) as shown in Figure 4.4.

New shape file of polygon was created in ArcCatalog projecting in UTM-54. Then the polygon of Hino city was edited in ArcMap by getting along with Japan GIS map

(Figure 4.5). After the shape file was done, the extraction process was applied to extract image of Hino city from Tokyo scene by using spatial analysis tools in ArcGIS. The extracted images are shown in Figure 4.6.

In consequence, the study area-2, Mandalay city which is 506.36km^2, was also extracted from the area of Mandalay region, which is 37,021.29km^2, by referencing to the digital format of Mandalay region map which acquired from local government office as shown in figure 4.7. The extraction was done in both ArcCatalog and ArcMap in the same way as in study area-1.

Figure 4.3. True Color and False Color Composition of Tokyo Scene on 1987/5/21
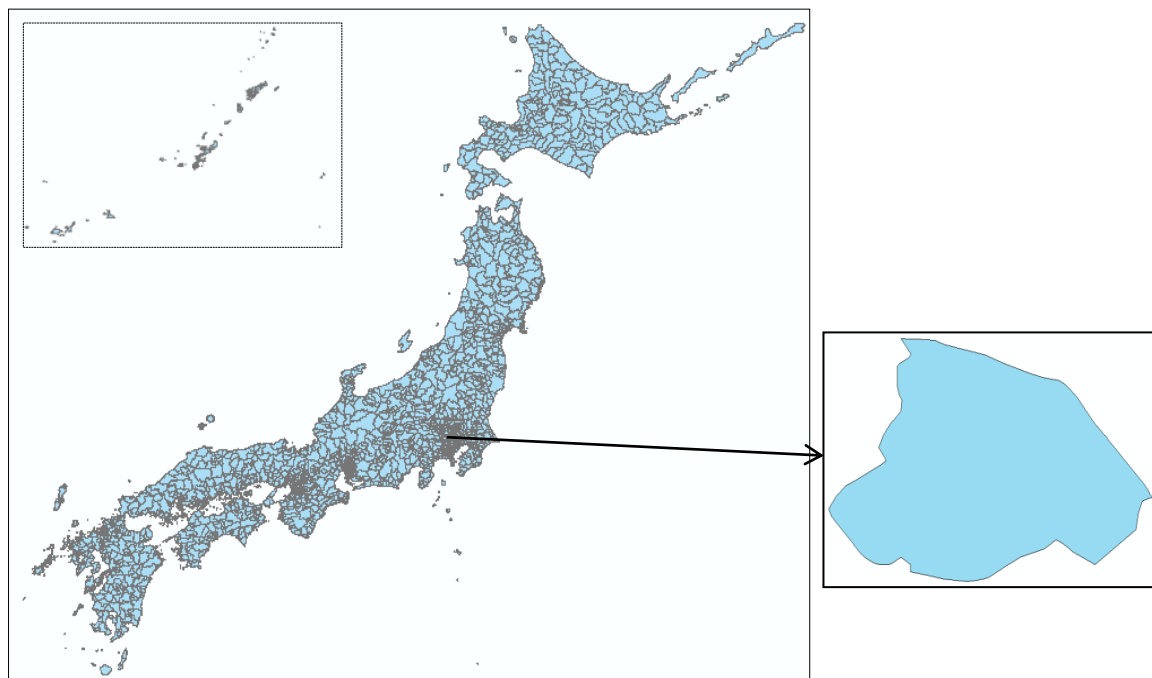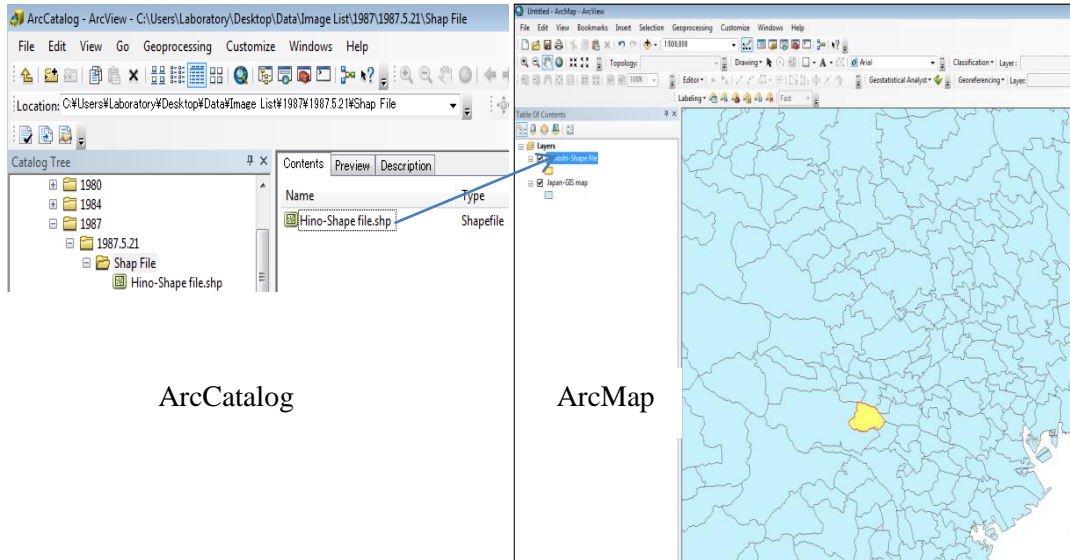

Figure 4.4. Japan GIS Map and Shape File of Hino City

Figure 4.5. Shape file of Hino City Created in ArcCatalog and ArcMap

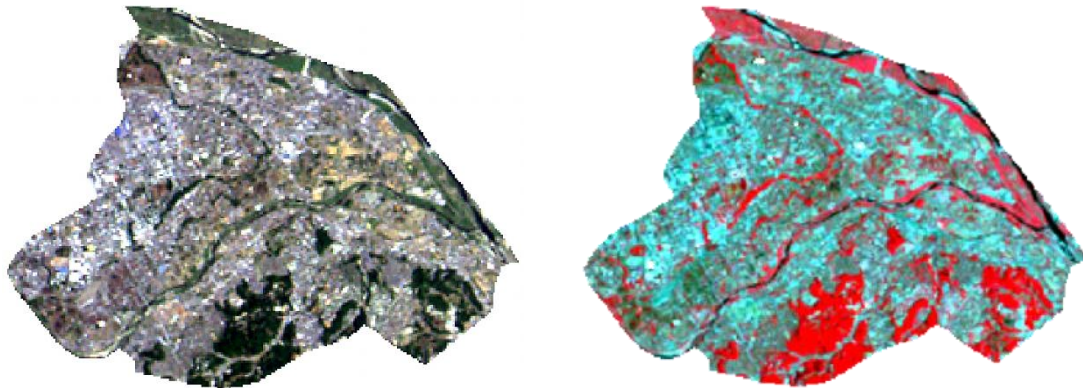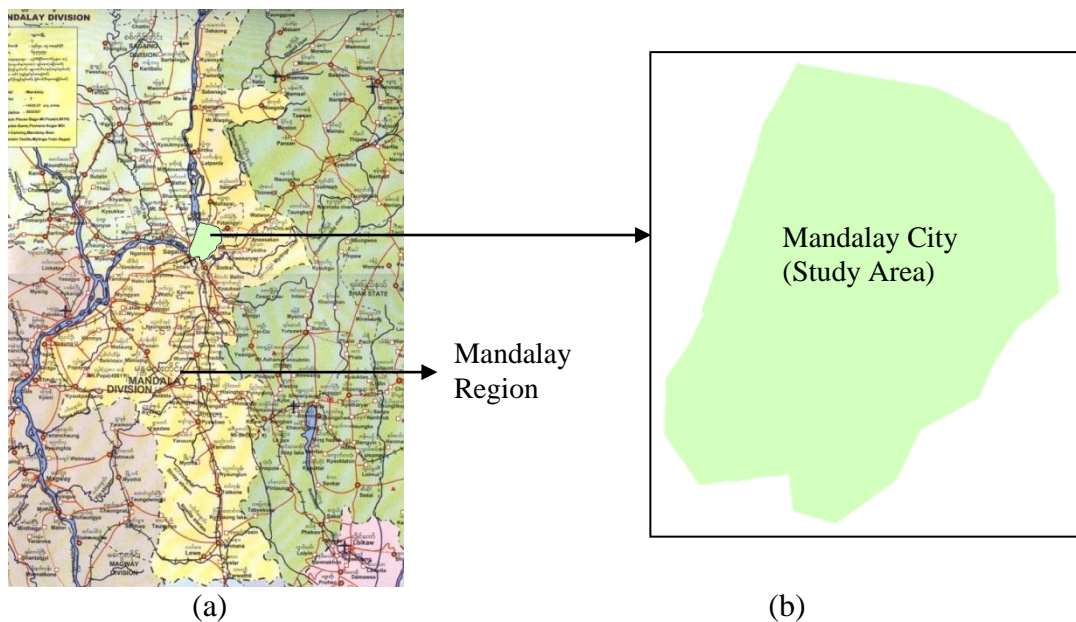

Figure 4.6. Extracted Study Area from True Color and False Color Images (1987/5/21)

(a)   (b)

Figure 4.7. (a) Map Mandalay Region and (b) Shape File

4.2.4. Image Enhancement

　　　　Almost all image processing softwares have the facility of performing contrast stretching and those are nearly the same with some subtle differences in the way they follow the procedure. ENVI has been used in this case for having interactive stretching which allows real-time visualization of the image and its histogram together. All images for both study areas have been enhanced and 'Linear 2%' method was applied. After that, histogram equalization was applied which improved the image significantly (Figure 4.8).

Figure 4.8. Enhancement of True Color and False Color Image of Hino City (1987/5/21)

4.3. Classification Scheme, Statistics and Results

　　　　Different land cover types in an image can be discriminated using image classification algorithms and using spectral features, i.e. the brightness and color information contained in each pixel. Classification is a complex process that may affect by many factors and still remained challenge. In this study, a classification process was developed to avoid the common problems in classification; mixed pixel problem, effect of shadows due to topography and misinterpreted classes.

　　　　Firstly, the classification scheme was developed, mainly based on the image resolution as it was difficult to classify if two or more land cover types fell within 30 square meters. Basically, 5 classes of land covers were chosen to be classified from Landsat images of Hino city; forest, lawn/grass, water, bare ground and built up or other. By referencing to Hino city GIS map, pixels of some areas of known land cover types for each class were selected from the corresponded composited images (Figure 4.9). These pixels are known as the training pixels with different values. After the training pixels were collected, the minimum and maximum values in each band for each class were determined (Table 4.1). The selected training pixels were plots to confirm if they were clearly scattered to use as samples for other else pixels (Figure 4.10). If they are scattered clearly, a pixel

from another location was compared to the range of training pixels and assign to each corresponded class. This process was repeated until the total pixels numbers for Hino city were assigned to each class (Table 4.2). The classification process was the same for all images of Hino city and the classified images area shown in figure 4.11.

Figure 4.9. Know Locations of Training Areas in Hino City

Table 4.1. The Range of Training Pixels' values (1987/5/21)

Land Cover Categories	No. of Training Pixels	Mini ~ Maxi pixel value			Mean		
		Green	Red	NIR	Green	Red	NIR
Forest	121	85~135	63~95	208~255	104.92	71.97	243.22
Lawn/Grass	9	127~170	109~137	150~222	155.88	127	197.25
Water	23	85~120	68~105	10~59	99.95	81.09	29.45
		Blue	Green	Red	Blue	Green	Red
Bare Ground	4	29~32	30~35	32~44	30.56	32.88	38.31
Built-up/other	44	36~44	39~52	36~56	40.15	46.08	49.10

Table 4.2. The Numbers of Classified Pixels (1987/5/21)

Land cover categories	No. of Pixels
Forest	6584
Lawn/Grass	4246
Water	224
Bare ground	1254
Built up or other	18158
Total Pixels	30466
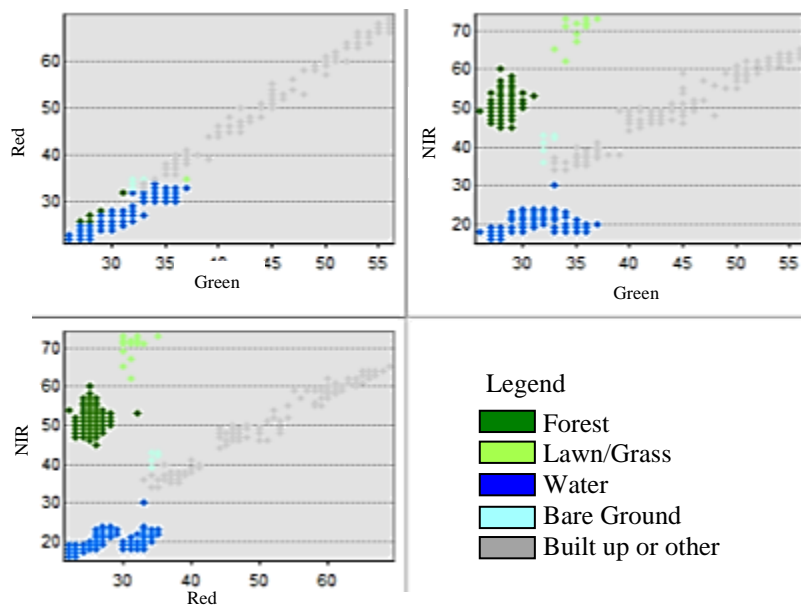
Figure 4.10. Scatter Plots of Training Pixels (1987/5/21)

(a) 1987/5/21

(c) 2001/4/1

(b) 1996/4/5

(d) 2011/4/5
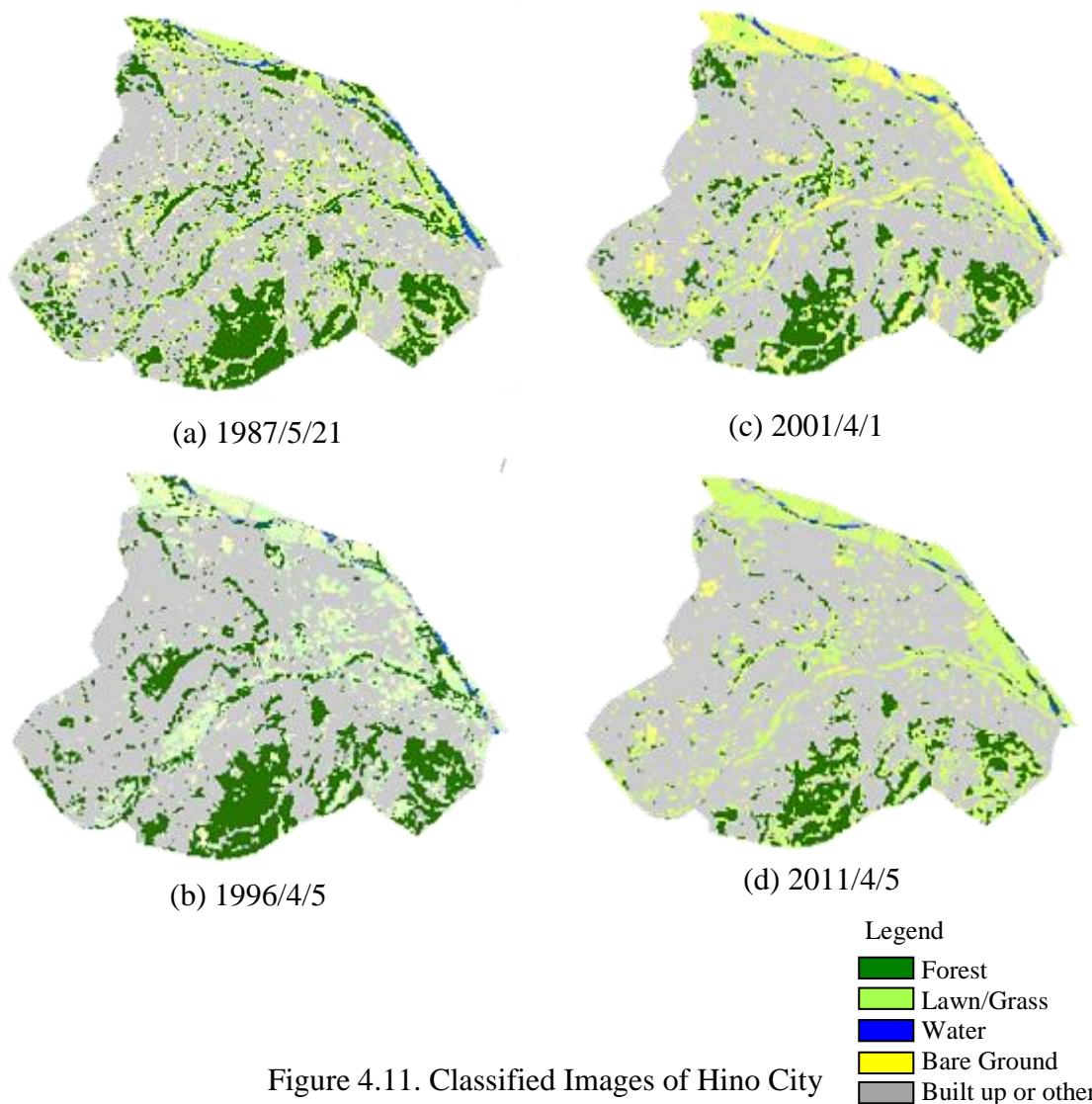
Figure 4.11. Classified Images of Hino City

68

After that, 5 classes of land covers were also chosen for Mandalay city; forest, lawn/grass, water, agriculture mixed land and built up or other. By referencing to map of Mandalay city, training pixels were selected from the corresponded composited images (Figure 4.12).The minimum and maximum values in each band for each class were determined (Table 4.3). The selected training pixels were plots to confirm if they were clearly scattered to use as samples for other else pixels (Figure 4.13). If they are scattered clearly, a pixel from another location was compared to the range of training pixels and assign to each corresponded class. This process was repeated until the total pixels numbers for Mandalay city were assigned to each class (Table 4.4). The classification process was the same for all images of Mandalay city and the classified images area shown in Figure 4.14.
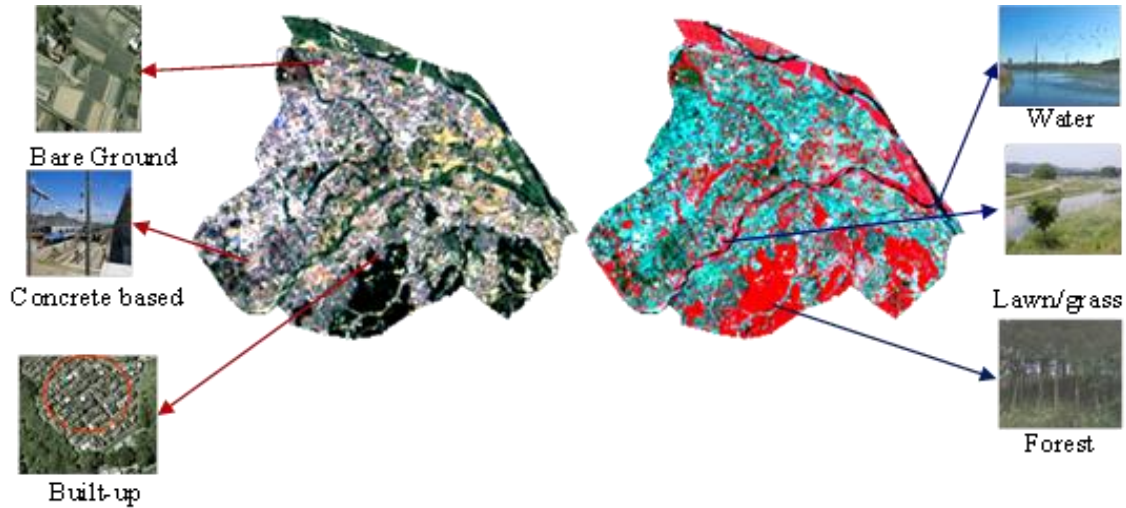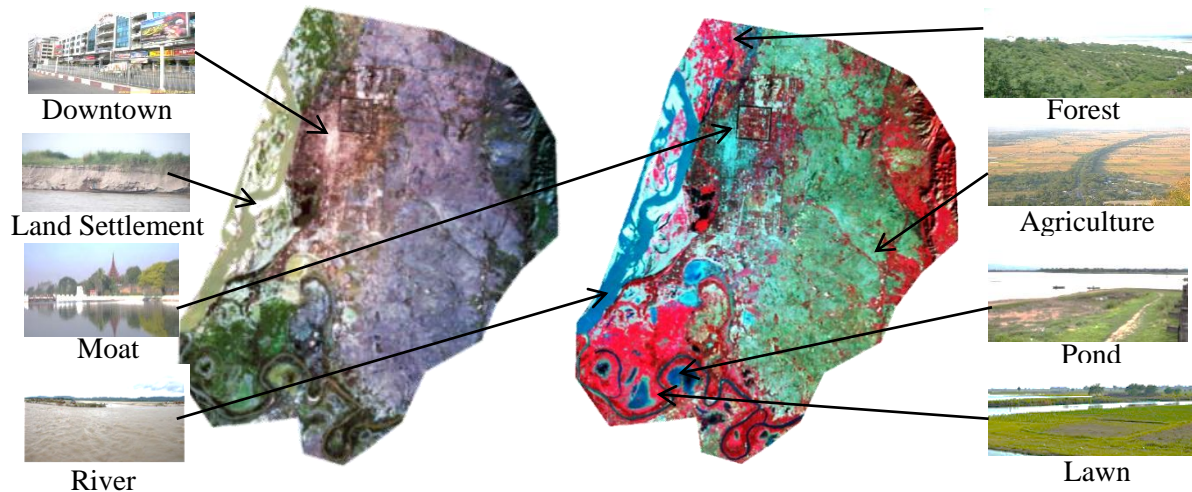

Figure 4.12. Know Locations of Training Areas in Mandalay City

Table 4.3. The Range of Training Pixels' values (1988/12/31)

Land Cover Categories	No. of Training Pixels	Mini~Maxi pixel value			Mean		
		Green	Red	NIR	Green	Red	NIR
Forest	199	23~28	19~26	46~113	26.34	21.52	64.47
Lawn/Grass	31	31~32	26~28	67~77	31.13	27.29	72.35
Water	1161	23~39	17~40	11~28	33.20	29.89	16.55
Agriculture Mixed Land		Blue	Green	Red	Blue	Green	Red
	16	29~32	30~35	32~44	30.56	32.88	38.31
Built-up/ other	84	36~44	39~52	36~56	40.15	46.08	49.10
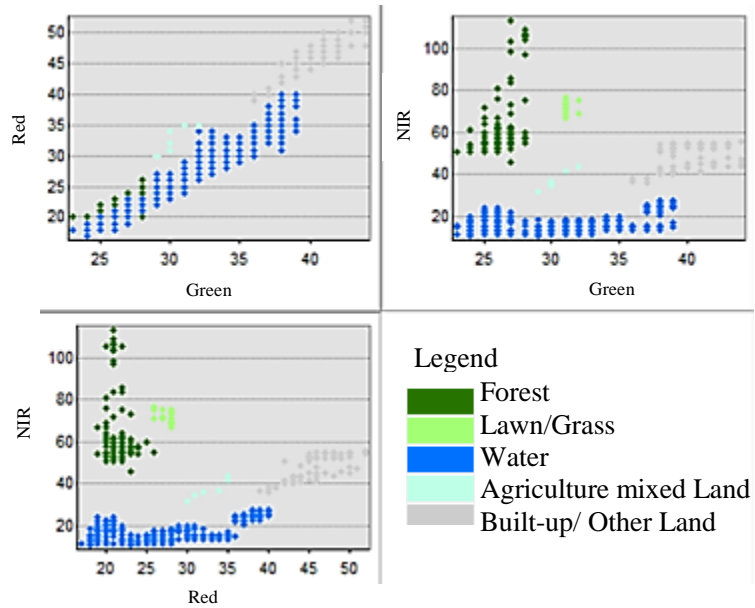
Figure 4.13. Scatter Plots of Training Pixels (1988/12/31)

Table 4.4. The Numbers of Classified Pixels (1988/12/31)

Land Cover Categories	No. of Pixels
Forest	231211
Lawn/Grass	51754
Water	50753
Agriculture Mixed Land	107147
Built-up/other Land	123064

(a) 1988/12/31   (b) 1996/1/12

(c) 2009/1/15

Legend
◼ Forest
◼ Lawn/Grass
◼ Water
◼ Agriculture mixed Land
◼ Built-up/ Other Land
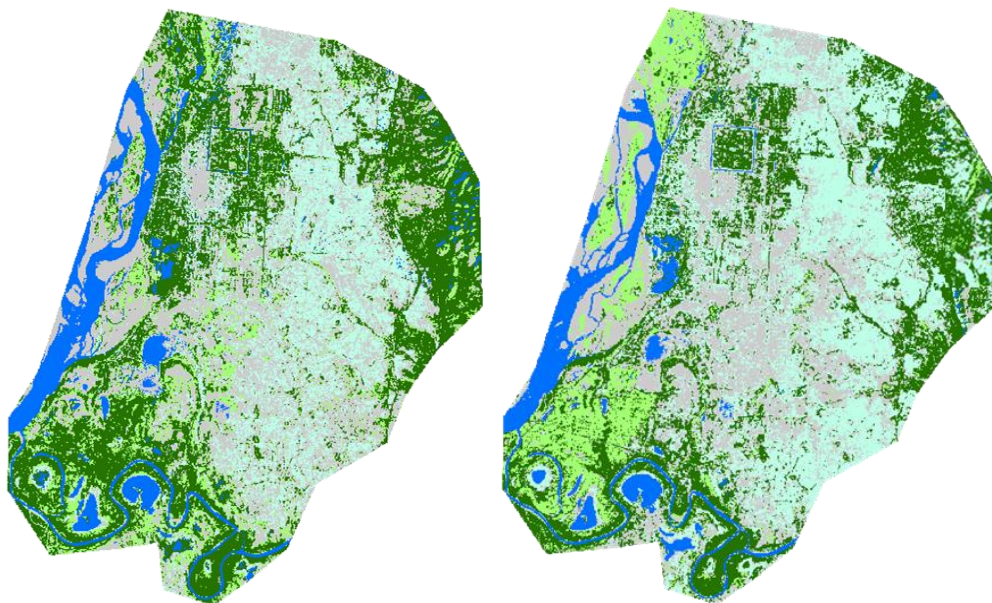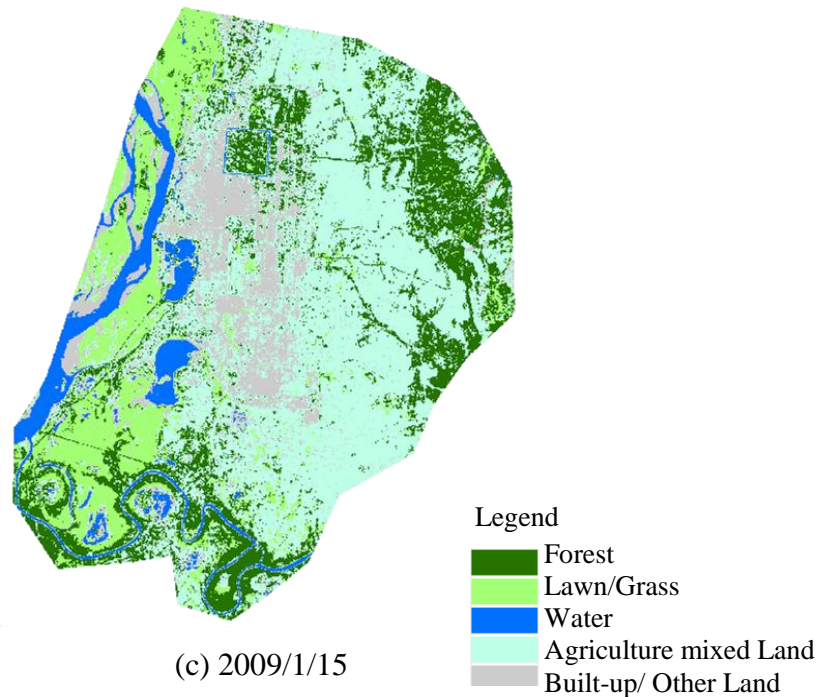
Figure 4.14. Classified Images of Mandalay City

The classification result of study area-1 shows that it mostly covered by built-up land. The result in study area-2 indicates that the area is mostly covered by arable land as the main stay of majority of the region is farming. The area-2 covers by a relatively higher amount of forest, settlement (urban fabric) and mixed agriculture. Most importantly, it is to be noted that the classification results in both study areas do not classify classes which are below the minimum mapping unit. This is also true for road and transport network which have been considered under the class of urban fabric. So, it is quite obvious the change detection in relatively smaller class was not considered in the study.

4.4. Change Detection Analysis

An important aspect of change detection is to determine what is actually changing to what and which land cover class is changing to the other. This information will reveal both the desirable and undesirable changes and classes that are "relatively" stable overtime. This information will also serve as a vital tool in management decisions. This process involves a pixel to pixel comparison of the study year images through overlay. Change detection tries to identify changes in the distribution of a stochastic process or time series. In general the problem concerns both detecting whether or not a change has occurred, or whether several changes might have occurred, and identifying the times of any such changes. Specific applications may be concerned with changes in the mean, variance,

71

correlation, or spectral density of the process.

4.4.1. Analysis in Study Area-1

The static land cover distribution for each study year as derived from the land cover classification for Hino city is presented in the table 4.5 followed by its graph, figure 4.15. From the results of classified TM images of Hino city, in 1987, green cover occupied about 36% of the total class while it was 33% in 1996, 29% in 2001 and 28% in 2011. In Hino city, green cover is essential to balance the environment of urban. Water was the least percentage in the classes and the river areas are so small to detect clearly in Landsat images. Bare ground was not significant in 1987, but seemed increased in the following years 1996 to 2011. It is considered the images were taken in April when there was still less vegetation. Built up or other land increased from 60% in 1987 to 69% in 2011 while it was 62% and 63% in 1996 and 2001 respectively.

Forest has a loss of 3% between 1988 and 1996, by 5% between 1996 and 2001 and by 5% between 2001 and 2011. On the other hand lawn/grass gained by 1% between 1996 and 2001 and 5% between 2001 and 2011 but there seemed no changes between 1987 and 1996. Water area looked less than 30 square meters and it's difficult to detect the changes. Bare ground gained by 3% between 1996 and 2001 but lessen by 6% between 2001 and 2011 while it relatively stable between 1987 and 1996. Built-up or other land increased slightly between 1987 and 2001 which is 3% but gained by 6% between 2001 and 2011.

The green cover percentage of Hino city in 2001 is about 30% of the area. When comparing this result to the GIS data which classified from IKONOS image with 1m resolution, it was found that the green cover percentage is almost the same which is 29.57% though the data sources are different (Table 4.6). Therefore, it is considered that the developed method of classification is suitable for Hino city by using Landsat images.

In terms of location of change, the emphasis is on vegetation cover. Table 4.7 shows this change in three trends, 1987-1996, 1996-2001 and 2001-2011 and also the annual rate of change was also calculated. Forest was lost about 3% in 1987-1996 trends while the lost was 5% in both trends; 1996-2001 and 200-2011. So, the annual rate of change (lost) was 0.23, 0.27 and 0.47 respectively. The noticeable growth was built-up land, where it increased annually by 0.17%, 0.06% and 0.63% for all trends. Another increased area was lawn/grass due to forest lost, which were 0.04% in the first two trends and 0.49% in the third trend. However, bare ground was changed instability-loss or gain for all trends.

Table 4.5. Land Cover Distributions of Hino City (1987, 1996, 2001, 2011)

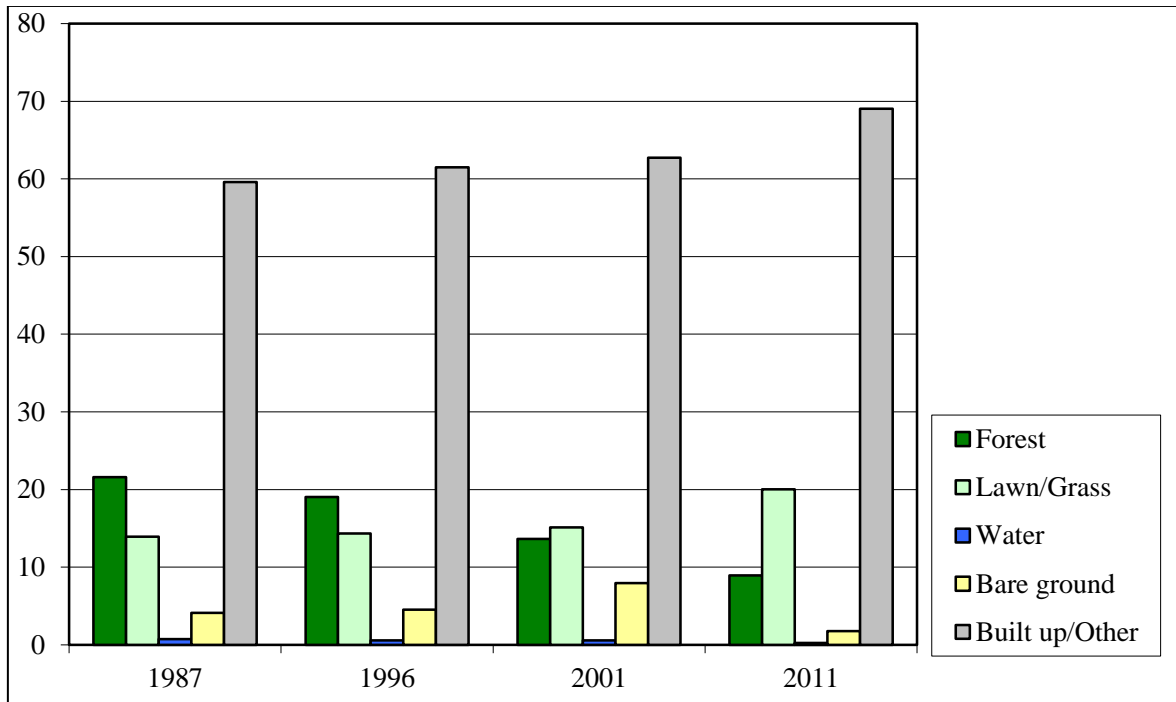| Land Cover Categories	1987 (Area)		1996 (Area)		2001 (Area)		2011 (Area)	
	km^2	%	km^2	%	km^2	%	km^2	%
Forest	5.9256	22	5.2236	19	3.7413	14	2.4498	9
Lawn	3.8214	14	3.9357	14	4.1463	15	5.4909	19
Water	0.2016	1	0.1575	1	0.1557	1	0.0657	1
Bare Ground	1.1286	4	1.2375	5	2.1789	8	0.486	2
Built-up/Other	16.3422	60	16.8651	62	17.1972	63	18.927	69
Total	27.4194	100	27.4194	100	27.4194	100	27.4194	100

Figure 4.15. The Graph of Classified data of Hino City

Table 4.6. Classified Data of Hino City from IKONOS (2008/9/9)

2008/9/9	Percentage
Green Cover	29.57%
Rice Field	6.86%
Water	2.97%
Bare Ground	2.57%
Other	58.08%

Table 4.7. Land Cover Change of Hino City

Land Cover categories	1987-1996 Change area		1996-2009 Change area		2001-2011 Change area		Annual Rate of Change (%)		
	km^2	%	km^2	%	km^2	%	87-96 (9yrs)	96-01 (5ys)	01-11 (10yrs)
Forest	-0.70	-3	-1.48	-5	-1.29	-5	-0.23	-0.27	-0.47
Lawn/grass	0.11	0	0.21	1	1.34	4	0.04	0.04	0.49
Water	-0.04	0	-0	0	-0.09	0	-0.01	0	-0.03
Bare Ground	0.11	0	0.94	3	-1.69	-6	0.04	0.17	-0.61
Built-up/Other	0.52	2	0.33	1	1.73	6	0.17	0.06	0.63

4.4.2. Analysis in Study Area-2

The static land cover distribution for each study year as derived from the land cover classification is presented in the table 4.8 followed by its graph, figure 4.16. From the results of classified TM images of Mandalay city, in 1988, forest still occupied the highest class with 41.7% of the total class while it was 35.4% in 1996 and 20.3% in 2009. In Mandalay region, the fire wood and charcoal are mainly used for cooking, which must be the main reason of losing forest every year. The forest in this tropical low land is essential to balance the environment of urban and it should be monitored to provide affective environmental management, which also forms the main objectives of this study.

Water area took up the least percentage in the total class. It also seemed to be arbitrarily exaggerated due to the land settlement as the region is the low land. Especially, the several work sites in northern part of Myanmar throw the waste into the river which forced to form land. Lawn or grass land percentage seemed increased due to the land forming in the river but variable according to the climate.

Also, agriculture mixed land seems to be practiced moderately, occupying 18% of the total classes in 1988 but it increased to 22% and 24% in 2009. This may be due to the fact that the agriculture seems to form the basis for living. Apart from this, new farming are created every year to the highland to get new top soil fertility and to the need of increasing population could also be major contributing factors to the observed classification, contributing to the high percentage of waste land and the low percentage of forest. Built-up or other concrete based area in 1988 occupies the least with just 21% of total classes but the built up area increased in 1996 and 2009. The reasons may be the new

industrial forming and city expanding.

Forest had a loss of 7% between 1988 and 1996 and by 15% between 1996 and 2009. On the other hand lawn/grass gained by 5% between 1988 and 1996 but just 1% between 1996 and 2009 while water body exist a relative stability between 1988 and 1996 as evident in the 0% increased shown in the table. But this class lost by 2% between 1996 and 2009 due to the river settlement. Built-up or other land increased i.e. gained by 1% between 1988 and 1996 but 11% between 1996 and 2009. Agricultural mixed land gained by 1% between 1988 and 1996 and 5% between 1996 and 2009.

Table 4.8. Land Cover Distributions (1988, 1996, 2009)

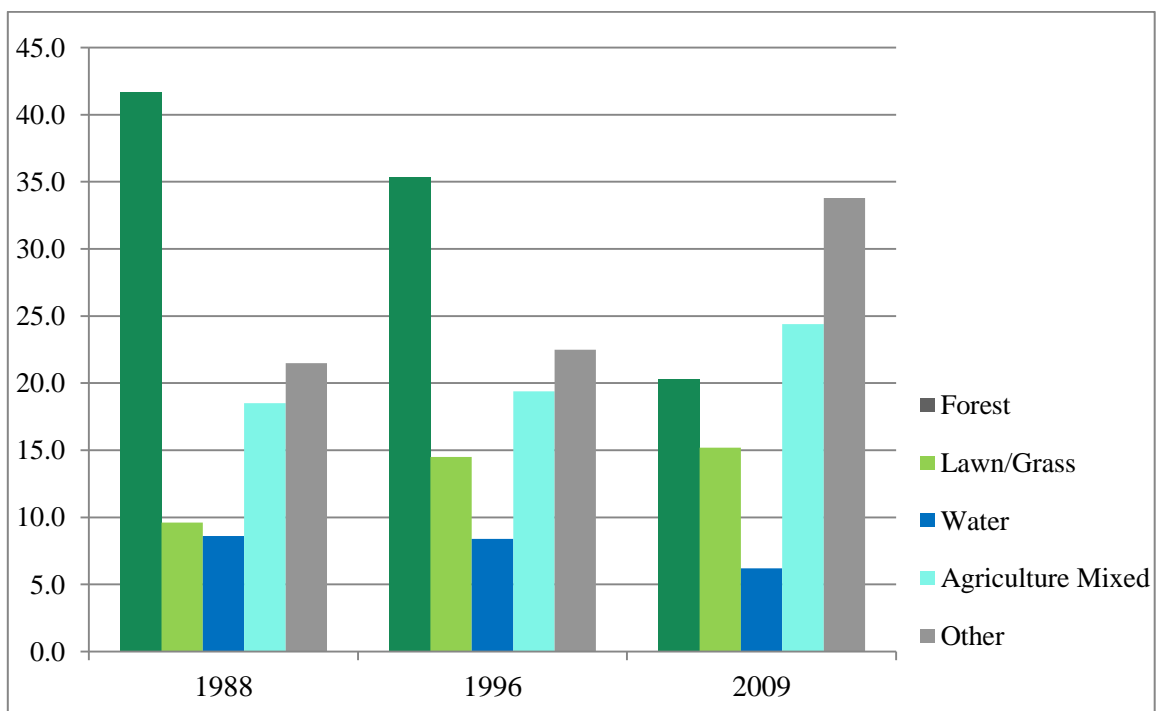| Land Cover Categories	1987 (Area)		1996 (Area)		2009 (Area)	
	km^2	%	km^2	%	km^2	%
Forest	161.14	41.7	214.49	35.4	103.08	20.3
Lawn	48.78	9.6	51.63	14.5	77.09	15.2
Water	43.65	8.6	40.58	8.4	31.67	6.2
Agriculture mixed Land	93.85	18.5	142.15	19.4	225.41	24.4
Built-up or Other Land	160.12	21.5	58.68	22.5	70.28	20.3
Total	507.54	100	507.54	100	507.54	100

Figure 4.16. Graph of Classified Land Cover Data

75

In terms of location of change, the emphasis is on forest (vegetation). Table 4.9 shows this change in two trends, 1988-1996 and 1996-2009 and also the annual rate of change was also calculated. Forest was lost about 6.3% in 1988-1996 trends while the lost was -15.1% in 1996-2009. So, the annual rate of change (lost) was 0.5 and 1.2 respectively. The only noticeable growths are the river settlement (land forming), where the water body lost annually by 0.016% and 0.176% for both trends. Due to land forming and forest lost, it was observed that lawn or grass area seemed increased 4.9% for the first trend and 0.7% for the second trend. However, the agriculture mixed land and other area changed instability-loss or gain by each class in both trends.

Table 4.9. Land Cover Change of Mandalay City

Land Cover category	1988-1996 Change area		1996-2009 Change area		Annual Rate of Change (%)	
	km^2	%	km^2	%	88-96 (8yrs)	96-09 (13yrs)
Forest	59282	-6.3	-123792	-15.1	-0.504	-1.208
Lawn	3172	4.9	28286	0.7	0.392	0.056
Water	-3412	-0.2	-9902	-2.2	-0.016	-0.176
Agriculture mixed Land	53668	0.9	92517	5	0.072	0.4
Built-up Land	-112710	1	12891	-2.2	0.08	-0.176

4.4.3. Accuracy Assessment

In this study, the developed classification method is considered worked well with Landsat images to solve the common problems in image classification as it was found to be potentially satisfied to the GIS data of Hino city. When comparing this method to object oriented method which still has unclassified-pixels [04Wan], the classification rate becomes higher and every pixel of Landsat image was assigned to its corresponded class as shown in figure 4.17. This developed method is based on training pixels selected from the composited images where every feature of images is clearly highlighted, so misinterpreted classes problem has been solved while neural network approach still can't do [89Ers]. Besides, a mixed pixel problem is one of the commonly found problems in classification of satellite image and it can be ignored this problem in this study as Landsat image just captures only one features in a pixel even though there may include one or more features (Figure 4.18).
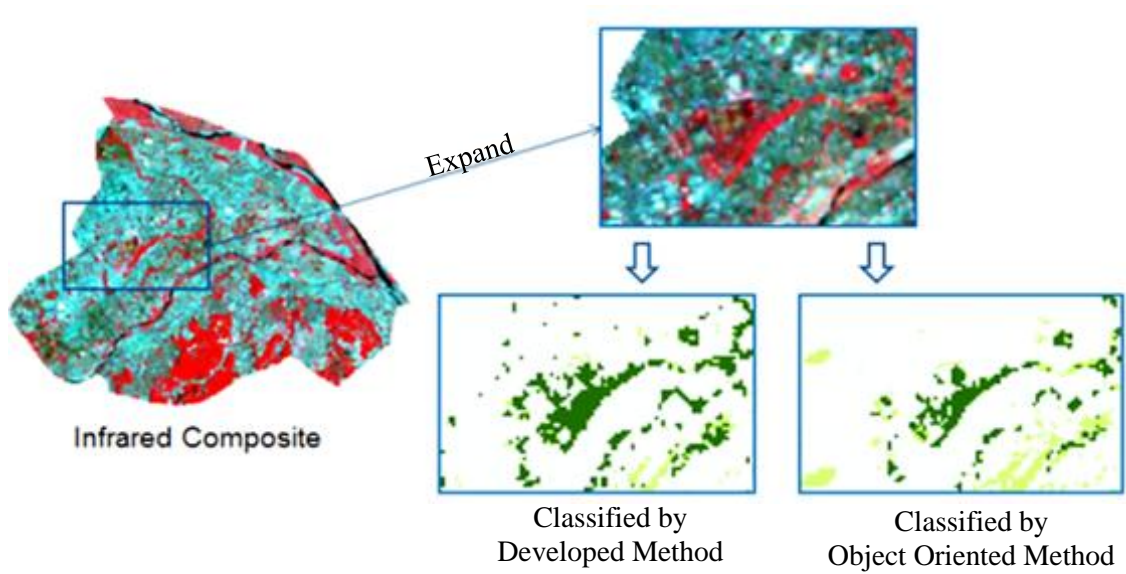
Figure 4.17. Comparison Results between Developed Method and Object Oriented Method
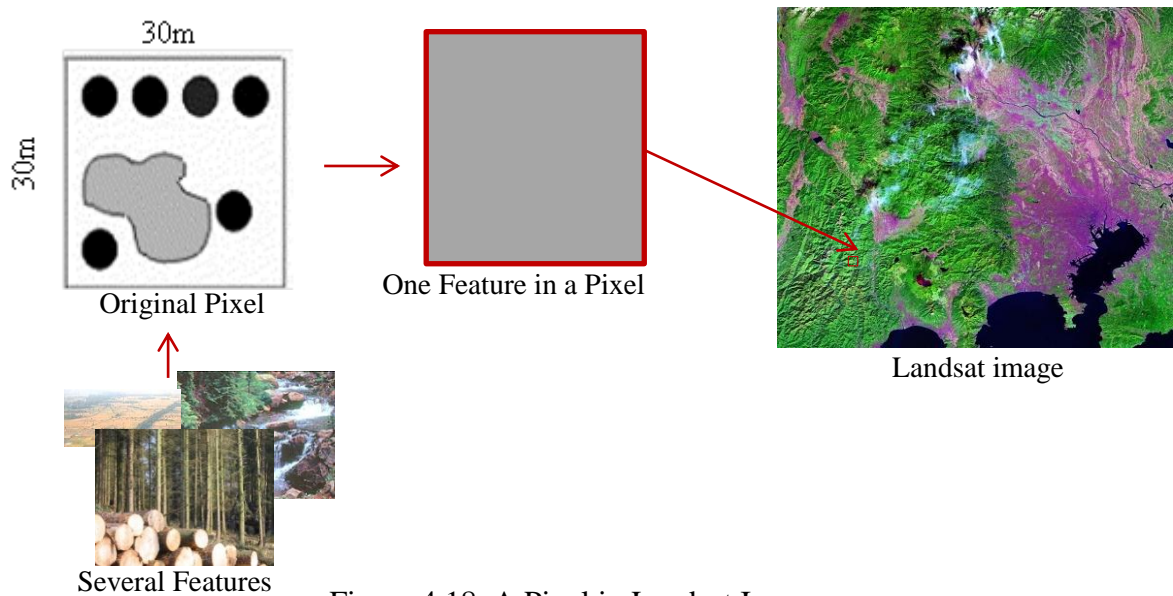
Figure 4.18. A Pixel in Landsat Image

4.4.4. Maps of Land Cover

Maps of land cover are fundamental tools for natural resource management and planning. These land cover maps provide a standard system by which units of land can be categorized. These serve to assess the area and distribution of individual land cover, categories (such as cropland and pasture), show the diversity of the landscape, contrast the land diversity of different regions, and monitor changes in land cover over time.

The land cover data files describe the vegetation, water, natural surface, and cultural features on the land surface. Landsat images of Hino city and Mandalay city

images were classified to be created land cover maps. The maps of land cover were created as following where all land cover data conform to the Universal Transverse Mercator (UTM) projection, Zone 54N and plotted in every 1° for study area-1 and to the UTM-47 projection and plotted in every 3° with scaling 1-inch equals 8627 meters.

Figure 4.19. Land Cover Map of Hino City in 1987/5/21

Figure 4.20. Land Cover Map of Mandalay City in 1988/12/31

78

4.5. Deriving Land Surface Temperature and NDVI

The knowledge of surface temperature is important to a range of issues and themes in earth sciences central to urban climatology, global environmental change, and human-environment interactions. In this study an attempt has been made 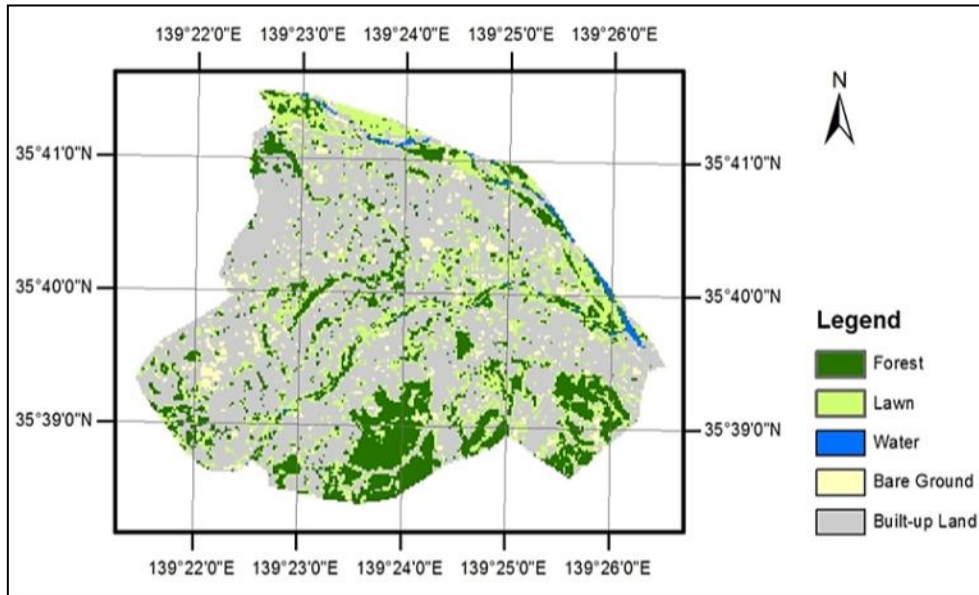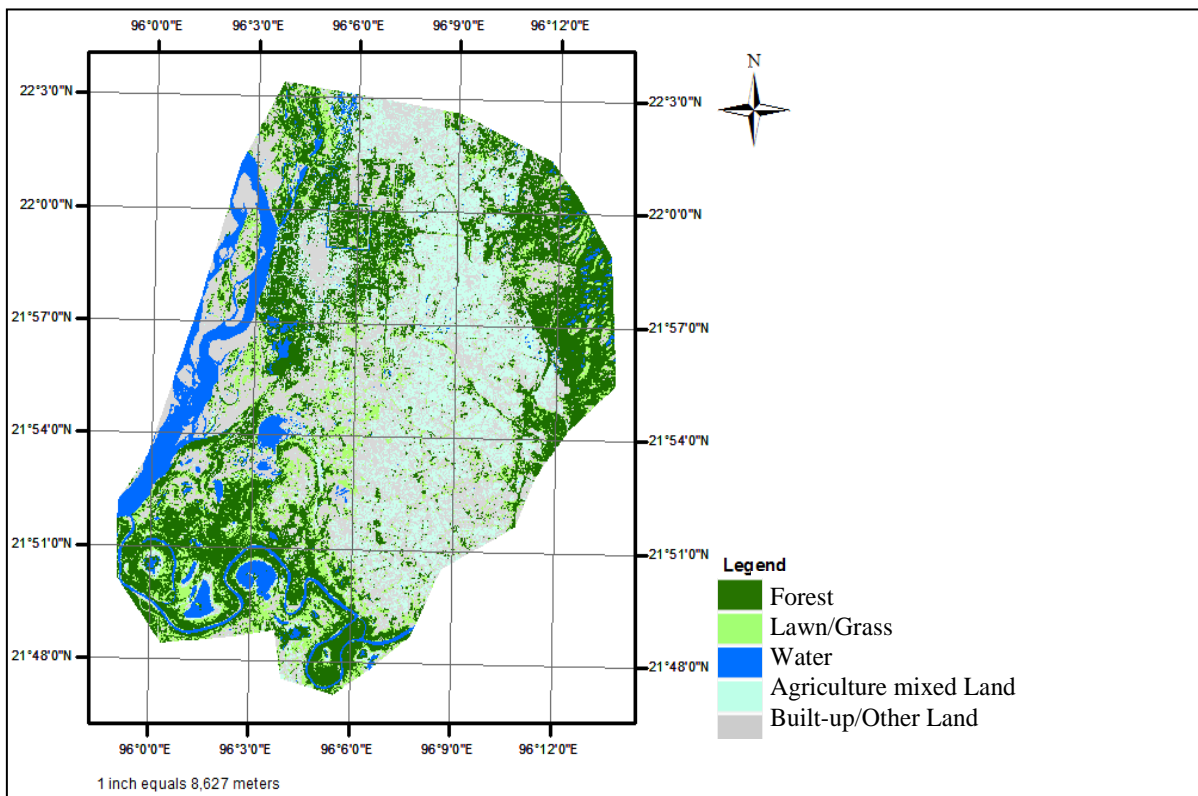to estimate surface temperature over Hino city area and Mandalay area using Landsat TM and ETM+ data. The variability of these retrieved LSTs had been investigated with respect to different land cover types determined from the Landsat visible and NIR bands. This provides an effective fact in evaluating the environmental influences of zoning in urban ecosystems with remote sensing and geographical information systems.

In the present study, LSTs were derived by taking the fraction of vegetation cover per pixel in conjunction with NDVI which has been widely used to monitor vegetation changes since the early eighties. The resulted images are shown below in figure 4.21 and 4.22.

It was observed that estimated temperature was the highest at bare ground and agriculture mixed land while it supposed to be at built up or other land class. But it seems that the emissivity were controlled by a mixed of housing, garden and trees in the city. The highest temperature was about 28°C in study area-1 and 30°C in study area-2, and followed by the built up land about 22°C in study area-1 and 28°C in study area-2. The lowest temperature was found at water body which was about 10°C and about 15°C at the forest for study area-2. But it was less than 10°C in study area-1 as the images were taken in early spring. The temperature of agriculture mixed land was varied depending on its features, planted or bare ground.

4.5.1. Derivation of Normalized Difference Vegetation Index (NDVI)

NDVI were also calculated to estimate the relation between LST and NDVI. To determine the density of green on land, the distinct colors (wavelengths) of visible and near-infrared sunlight reflected by the plants must be observed. NDVI was calculated from the visible red band and near-infrared light (band 4) reflected by vegetation.

Calculations of NDVI for a given pixel always result in a number that ranges from minus one (−1) to plus one (+1), and the NDVI for a pixel with no green leaves is close to zero. A zero means no vegetation and a value close to +1 (0.8–0.9) indicates the highest possible density of green leaves. The calculated images are shown in figure 4.23 and 4.24. Green color represents NDVI value close to +1 and Yellow and red colors show NDVI value is 0 and -1.

For overall, the density of green area was decreased according to the calculation of images in both study areas. Especially, NDVI in the built up area of Hino city greatly decreased from 1987 to 2011. It might be due to the difference of early spring and late spring where vegetation starts to change in this season. Moreover, NDVI of the downtown area of Mandalay city reduced during 1988 to 2009 which were in same season. At the same time, the LST at built-up areas in both study areas were also increasing according to the figure 4.21 and 4.22. Accordingly, the surface temperature significantly low where NDVI value was close to 1, plus the agriculture mixed land and built up land has high surface temperature while NDVI value was -1 and close to 0. Therefore, the strong correlation between NDVI and LST was also found significantly different in this study.

(a) 1987/5/21   (c) 2001/4/1

(b) 1996/4/27   (d) 2011/4/5

LST Bar in °C

10   15   20   25   30°C
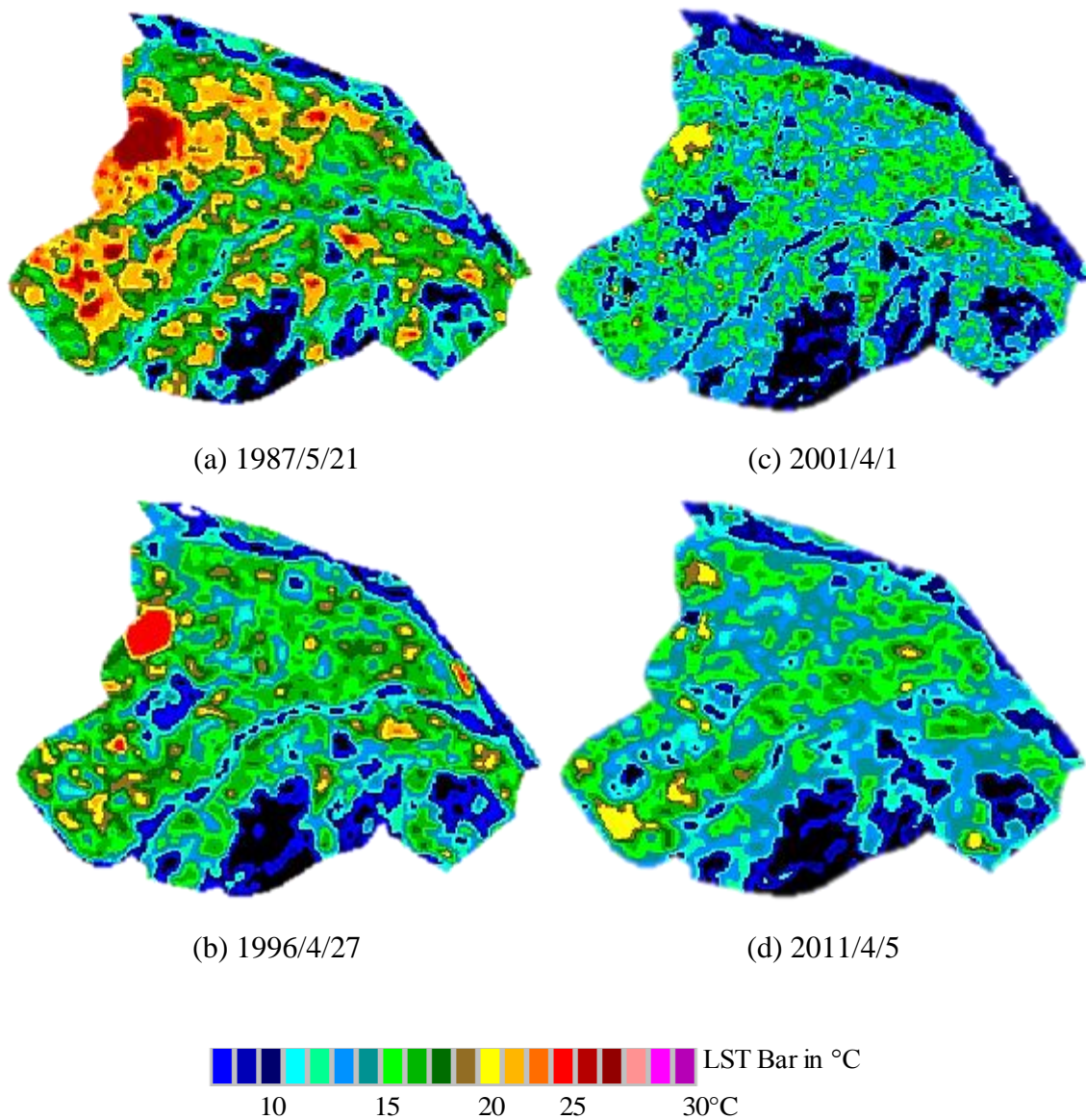
Figure 4.21. LST Estimation Derived from Hino City Images

(a) 1988/12/31   (b) 1996/1/12

(c) 2009/1/15

LST Bar in °C

10   15   20   25   30°C
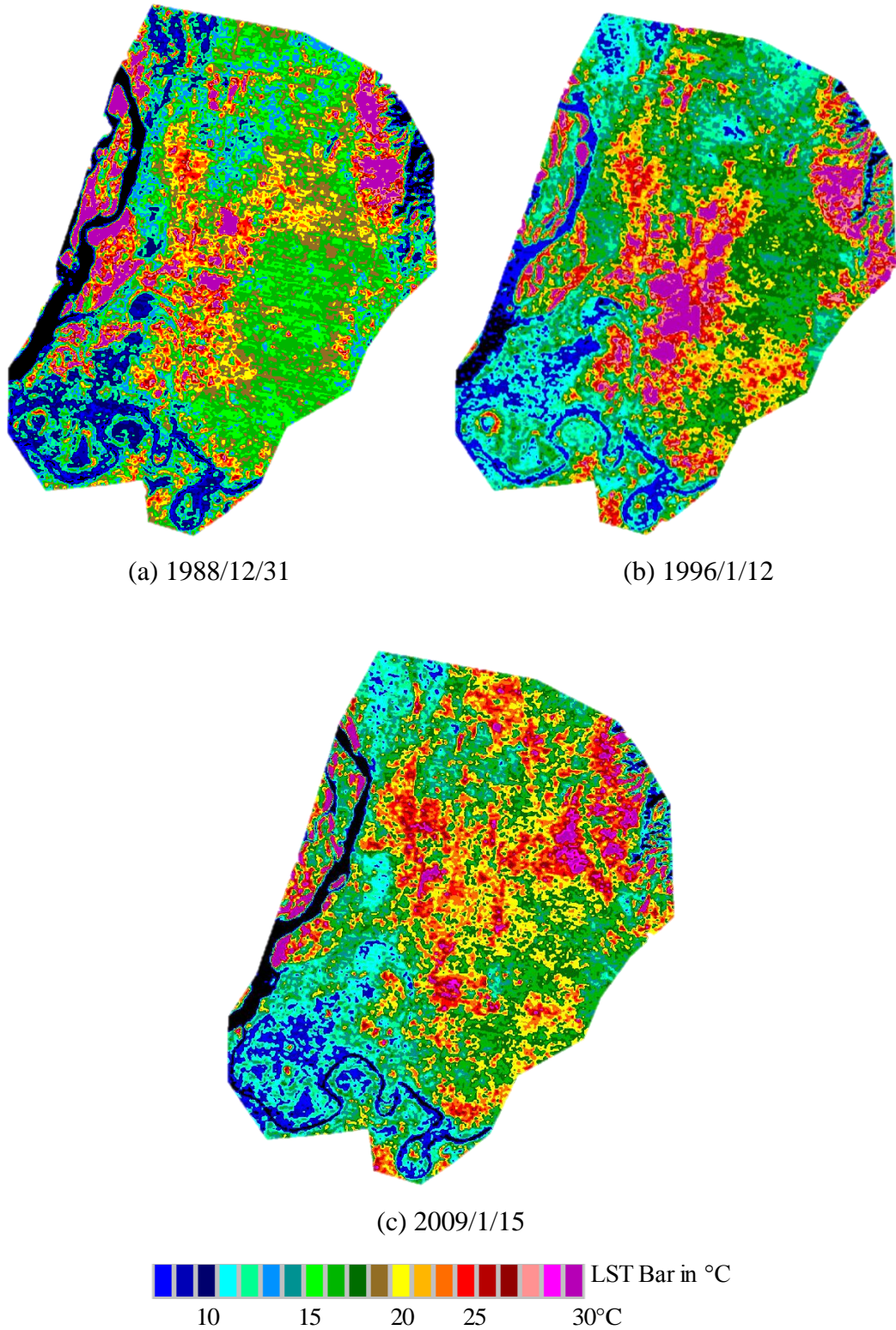
Figure 4.22. LST Estimation Derived from Mandalay City Images

(a) 1987/5/21   (c) 2001/4/1

(b) 1996/4/27   (d) 2011/4/5

-1   +1
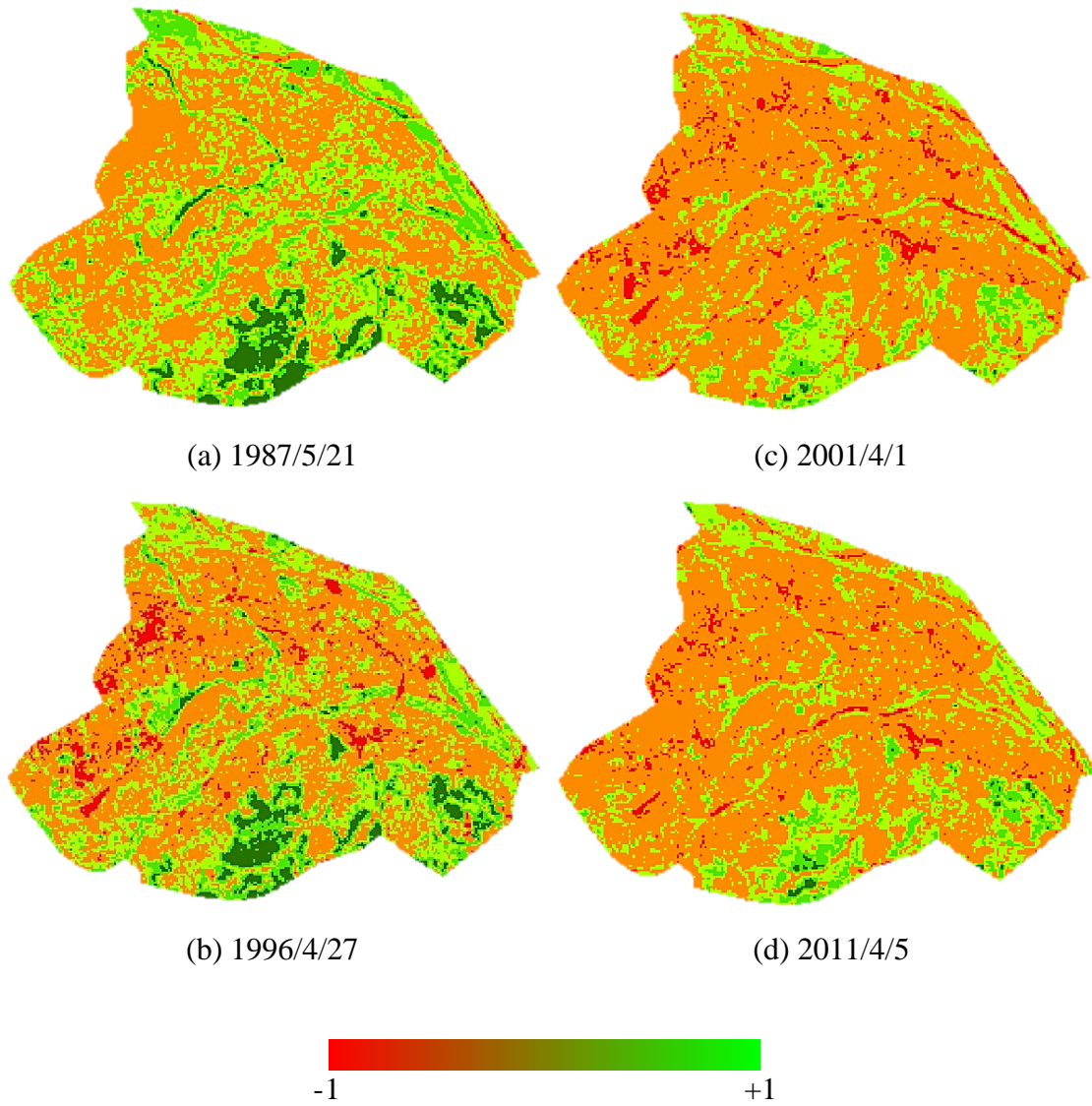
Figure 4.23. Calculation of Normalized Difference Vegetation Index for Hino City

(a) 1988/12/31   (b) 1996/1/12

(c) 2009/1/15

-1   +1
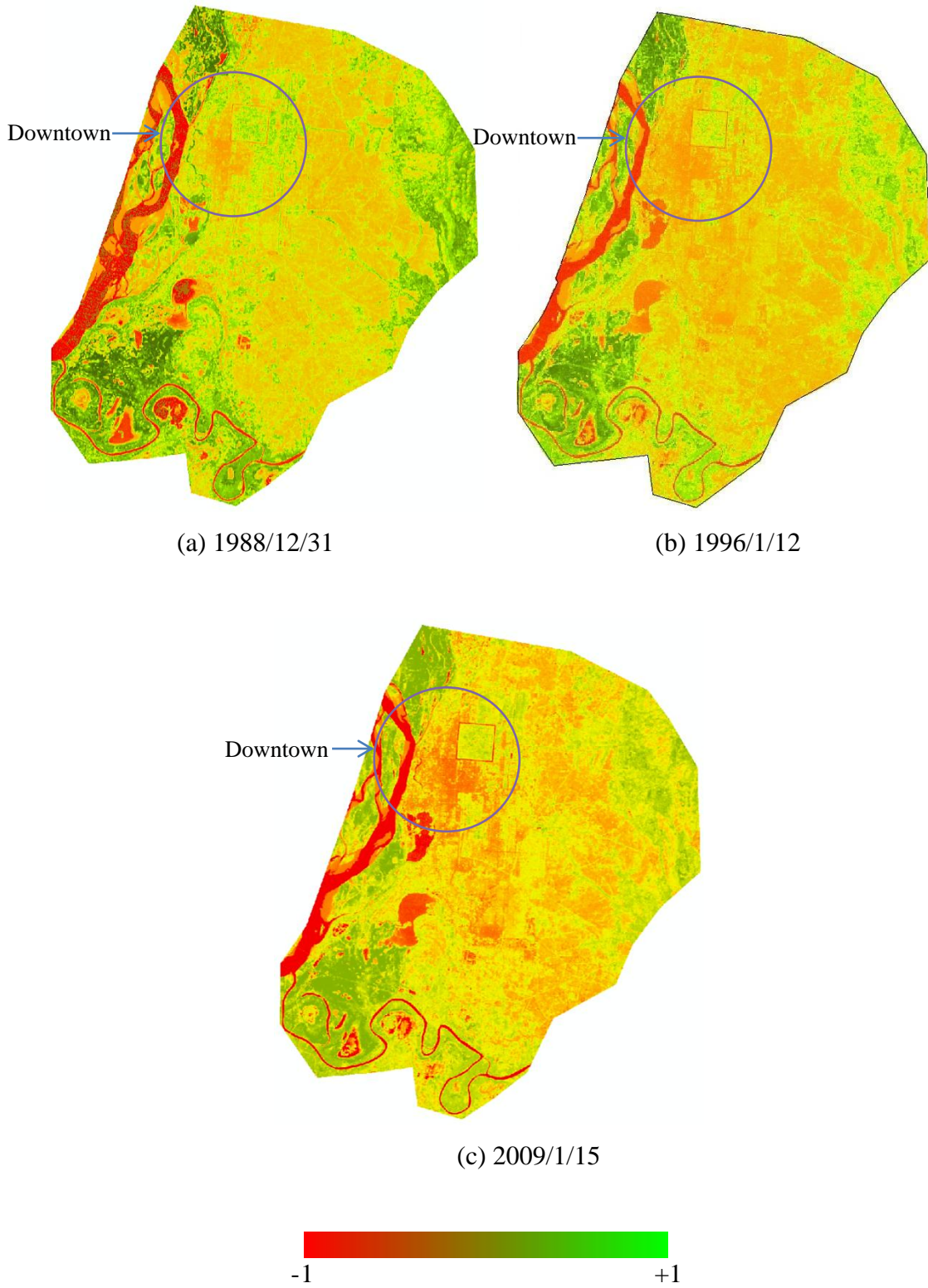
Figure 4.24. Calculation of Normalized Difference Vegetation Index for Mandalay City

CHAPTER 5
CONCLUSIONS

5.1. Summary and Conclusions

This research work demonstrates the ability of GIS and Remote Sensing in capturing spatial-temporal data. A classification scheme and a process of classification were developed simply based on "training pixel values" and then classify the other else pixels of the images. Attempt was made to capture as accurate as possible five classes of land cover for both study areas as they change through years. By utilization the classified data, the maps of land cover were created with projections to UTM to identify the unit of classified data. In addition to the analysis of land cover, land surface temperature (LST) and normalized difference vegetation index (NDVI) were also calculated to provide an effective fact in evaluating the environmental influences of zoning in urban ecosystems by using remote sensing and geographical information systems.

Landsat TM and ETM+ images of study areas, Hino city and Mandalay city were mainly used and the scenes of 1996 image were geometrically corrected. After the classification scheme were created, the five classes were distinctly produced for each study year but with more emphasis on forest land as it is the one that affects the environmental status. LSTs were calculated from the thermal band of Landsat and it was found that environmental changed impacts on the climate, where the reduced of forest and extended built-up area highly affected on increased surface temperature.

In classification process, the commonly occurred problems can be solved by using "training pixels" based classification. Mixed pixel problem was ignored as Landsat image recognized only one feature in a pixel even though there may two or more features included. As every pixel are matched with the range of "training pixels" and assigned to each corresponded class, this classification process also solved the problem of misinterpreted classes. The "training pixels" can be collected from known locations, so the problem caused by shadows of topography can be solved easily. Therefore, the accuracy of classification is considered to be highly improved after solving the common problems and probably suitable for studying land cover to manage environmental changes by utilizing with Landsat images.

5.2. Problems and Challenges

In this study, some problems are also found while doing change detecting,

classification the contents of image and doing image registration that there is inadequate database to access and acquire images with various spectral and texture information existed at different scales and resolutions. The main problem comes out due to the resolution of the images. Therefore this brought into being less accuracy in directly comparison of multi-temporal images.

Classification of low resolution imagery tends to present problems and challenges that may or may not be typical while performing similar work with very high resolution imagery. Some of these difficulties are described here simply to raise awareness for other image analyst. How to deal with the difficulties depends on one's level of competency, familiarity with software capabilities and other resources available.

With low resolution image, it is not easy discriminating between light colored built-up land and agriculture mixed land or not. These are largely comprised of the same materials (built up land or bare ground on agriculture mixed land) and thus yield a similar spectral signature. Classifying built up is sometimes further complicated at such low resolution images.

It is also difficult to classify at low resolution when shadows from tall features (cloud, buildings, and trees) cast shadows on the plain surface. These shadows also have different characteristics depending on the transparency of the obstruction (building vs. tree).

Transitions between classes are always difficult, but are much more common in low resolution imagery. The problem is exacerbated by the fact that low resolution sensors have low spectral resolution. One of the most commonly encountered transitions pertains to discriminating between grass and bare soil. The problem is even greater in winter or early spring imagery with senesced grass. Confusion is common for this leaf-off scene because grass is the most commonly used variety for residences, commercial property and golf courses. Public parks are typically covered with a fescue variety of grass that remains green year-round. If grass on river settlement is still senesced, where it is thin or sparse, it may be spectrally indistinguishable from ground. In wintertime imagery, there is often also difficulty in discriminating between senescent grass and deciduous trees, largely because significant contribution to overall radiance from the underlying grass passes through the tree crown when there are no leaves.

Hence, as a major limitation, 30m resolution image is still difficult to classify the area which is less than 30×30m. Therefore, classification results are required to improve by utilizing very high resolution (VHR) satellite imagery in future.

Another problem in this study is that there is no ground truth data which the surveys to the study areas haven't done due to time limitation. Therefore, the source data were referenced to the digital form of maps. The accuracy of classification result will be varying with no ground truth data.

However, results of this work could be helped researchers to monitor environmental changes that could affect urban ecosystem in the future conditions like pollution, climate change, natural disaster affected environmental changes, natural resource management, urban growth, and it would be useful much more and trend across large geographic areas.

REFERENCES

[76And] Anderson, et al., (1976), *A Land Use and Land Cover Classification System for Use with Remote Sensor Data,* Geological Survey Professional Paper No.964, U.S. Government Printing Office, Washington D.C., 28.

[96Ace] Acevedo W., Foresman T.W. & Buchanan J.T., (1996), *Origins and Philosophy of Building a Temporal Database to Examine Human Transformation Processes*, Proceedings of ASPRS/ACSM Annual Convention and Exhibition, Baltimore, MD, April 22-24, Vol. I, 148-161.

[99Abu] Abuelgasim A.A., Ross W.D., Gopal S., & Woodcock C.E., (1999), *Change Detection Using Adaptive Fuzzy Neural Networks: Environmental Damage Assessment after the Gulf War,* RS of Environment, 70, 208–223.

[99Ade] Adeniyi P.O. & Omojola A., (1999), *Landuse and landcover Change Evaluation in Sokoto Rima Basin of North Western Nigeria,* Archival of the Environment (AARSE) on Geo-information Technology Applications for Resource and Environmental Management in Africa, 143-172.

[02Aga] Agarwal C., Green G.M., Grove J.M., Evans T.P., & Schweik C.M., (2002), *A Review and Assessment of Land-Use Change Models: Dynamics of Space, Time, and Human Choice,* General Technical Report NE-297, Newtown Square, Pennsylvania, U.S. Department of Agriculture, Forest Service, Northeastern Research Station.

[06Arv] Arvind C. Pandy & M.S. Nathawat, (2006), *Land Use Land Cover Mapping Through Digital Image Processing of Satellite Data: A case study from Panchkula*, Ambala and Yamunanagar Districts, Haryana State, India.

[80Byr] Byrne G.F., Crapper P.F. & Mayo K.K., (1980), *Monitoring Land-cover Change by Principle Component Analysis of Multi-temporal Landsat Data,* RS Environment, 10,175-189.

[90Bec] Becker F., & Li Z.L., (1990), *Toward a Local Split Window Method over Land Surface*, International Journal of Remote Sensing, 11(3), 369-393.

[00Bru] L. Bruzzone & D.F. Prieto, (2000), *Automatic Analysis of the Difference Image for Unsupervised Change Detection,* IEEE Transactions on Geoscience and Remote Sensing, vol. 38, 3, 1171-1182.

[03Bar] Barbara Z. & Jan F., (2003), *Image Registration Methods: A Survey*, Image Processing Press, Institute of Information Theory and Automation, Prague, 8.

[81Col]   Colwell J.E. & E.P. Weber., (1981), *Forest Change Detection,* Proceedings of the 15th International Symposium on Remote Sensing of Environment held in Ann Arbor, 839-852.

[89Coo]   Cooper D., & G. Asrar, (1989), *Evaluating Atmospheric Correction Models for Retrieving Surface Temperature from the AVHRR over a Tallgrass Prairie,* RS Environment, 27, 93-102.

[95Cop]   P.R. Coppin & M.E. Bauer, (1995), *The Potential Contribution of Pixel-based Canopy Change Information to Stand-based Forest Management in Northern U.S.,* Journal of Environmental Management, 44:69-82.

[96Cop]   Coppin P. R., & Bauer M. E., (1996), *Digital Change Detection in Forest Ecosystems with Remote Sensing Imagery,* Remote Sens. Rev. 13:207–234.

[00Che]   Chen H. & Varshney P. K., (200), *A Pyramid Approach for Multimodality Image Registration Based on Mutual Information*, Proceedings of Fusion, Paris (International Society of Image Fusion), MoD 3-9–MoD3-15.

[02Cha]   Chan et al., Chan, S., Sio M., Volgelgesang T., Yik T. F., Hengst B., Pham S. B., & Sammut C., (2002), *The UNSW Robo Cup 2001 Sony Legged Robot League Team,* [Birk et al.], 39-45.

[02Cla]   Clarke & Keith C., (2002), *Land Use Change Modeling Using SLEUTH,* Workshop report in Proceedings of Advanced Training Workshop on Land Use and Land Cover Change Study, December 9-20th, Taiwan, National Taiwan University, 525-573.

[95Dim]   Dimyati, et al.(1995), *An Analysis of Land Use/Land Cover Change Using the Combination of MSS Landsat and Land Use Map- A case study of Yogyakarta, Indonesia*, International Journal of Remote Sensing 17(5): 931-944.

[02Dan]   Daniel, et al, (2002), *A comparison of Landuse and Landcover Change Detection Methods,* ASPRS-ACSM Annual Conference and FIG XXII Congress, 2.

[05Den]   Deng, J., K. Wang, et al., (2005), *Integration of SPOT-5 and ETM+ images to detect land cover change in urban environment,* Proceedings, Geoscience and Remote Sensing Symposium, IGARSS'05, July 25-29, Seoul, South Korea.

[08Den]   Deng J., K., Wang, et al., (2008), *PCA-based land-use change detection and analysis using multitemporal and multisensor satellite data,* International Journal of Remote Sensing 29(16): 4823-4838.

[89Ers]   O.K. Ersoy & D. Hong, (1989), *A hierarchical neural network involving non-linear spectral processing*, presented at IJCNN '89, Washington, DC.

[90Ehl]   Ehlers M., Jadkowski A.M., Howard R. & Brostuen D., (1990), *Application of Spot Data for Regional Growth Analysis and Local Planning,* Photogrammetric Engineering and Remote Sensing 56(2):175-180.

[92ERDAS]   ERDAS, Inc. 1992. ERDAS Production Services Map State for Georgia DNR in the Monitor, Vol. 4, No 1, ERDAS, Inc, Atlanta, GA.

[92EOSAT]   EOSAT 1992. Landsat TM Classification International Georgia Wetlands in EOSAT Data User Notes, Vol. 7, No 1, EOSAT Company, Lanham, MD.

[94EOSAT]   EOSAT 1994. EOSAT, Statewide Purchase Plan Keeps South Carolina Residents, in EOSAT Notes, Vol. 9, No 1, EOSAT Company Lanham, MD.

[99ERDAS]   ERDAS Field Guide, (1999), Earth Resources Data Analysis System. ERDAS Inc. Atlanta, Georgia, 628.

[87Fit]   Fitzpatric-lins, et al., (1987), *Producing Alaska Interim Land Cover Maps from Landsat Digital and Ancillary Data*, Proceedings of the 11th Annual William T. Pecora Memorial Symposium, Satellite Land Remote Sensing, 339-347.

[88Fun]   Fung, T. & E. LeDrew, (1988), *The determination of optimal threshold levels for change detection using various accuracy indices,* Photogrammetric Engineering and Remote Sensing 54(10): 1449-1454.

[98Gil]   Gillespie A.R., Rokugawa S., Matsunaga T., Cothern J.S., Hook S.J. & Kahle A.B., (1998), *A temperature and emissivity separation algorithm for advanced space borne thermal emission and reflection radiometer (ASTER) images*, IEEE Trans. Geosci. Remote Sens. 36 1113–1126.

[81How]   Howarth P.J., Wickware G.M., (1981), *Procedures for change detection using Landsat digital data,* International Journal of Remote Sensing, 2: 277-291.

[00Hol]   Holden M., Hill D.L.G., Denton E.R.E., Jarosz J.M., Cox T.C.S., Rohlfing T., Goodey J., & Hawkes D.J., (2000), *Voxel Similarity Measures for 3-D serial MR Brain Image Registration*, IEEE Transactions on Medical Imaging, 16, 287-298.

[03Hua]   Hua-mei Chen, Manoj K. Arora & Pramod K, (2003), *Mutual Information Based Image Registration for Remote Sensing Data*, NY 13244, USA.

[07Ifa]   Ifatimehin O.O., (2007), *An Assessment of Urban Heat Island of Lokoja Town and Surroundings Using Landsat ETM Data.* FUTY Journal of the Environment, Volume2 (1): 100-108.

[96Jen]   Jensen J. R, (1996), *Introductory digital image processing*, A remote sensing perspective, Second edition, New Jersey, U.S.A: Prentice Hall, 257-278.

[01Jen]   Jensen L. & B. Gorte, (2001), *Principle of remote sensing, Chapter 12 Digital image classification,* ITC, Enchede, Netherlands.

[81Key]   Keys R.G., (1981), *Cubic Convolution Interpolation for Digital Image Processing*, IEEE Transactions on Acoustics, Speech and Signal Processing, ASSP-29, 1153-1160.

[94Kah]   Kahru M., U. Horstmann & O. Rud, (1994), *Satellite Detection Of Increased Cyanobacteria Blooms In The Baltic Sea: Natural Fluctuation Or Ecosystem Change*, Ambio, 23 (8), 469-472.

[99Kho]   Khorram S., Biging G.S., Chrisman N.R., Congalton R.G., Dobson J.E. & Ferguson R.L., (1999), *Accuracy assessment of remote sensing-derived change detection,* Bethesda: Am. Soc. Photogrammetry and Remote Sensing.48-68.

[06Kra]   V.I. Kravtsova & E.A. Baldina, (2006), *Study of Natural and Economical Objects Dynamics By Color composition of Multi-temporal images*, Faculty of Geography Moscow state University,Russia, Moscow, 119992, Leninskie Gory.

[72Lil]   Lillestrand R.L., (1972), *Techniques of Change Detection*, IEEE Transactions on Computers, Vol. C-21, 7, July.

[97Lam]   Lambin E.F. & Ehrilich D., (1997), *Land-cover changes in sub-Saharan Africa (1982-1991)*, Application of a change index based on remotely-sensed surface temperature and vegetation indices at a continental scale, Remote Sensing of Environment, vol.61, 2, 181-200.

[98Lun]   Lunetta R.S., & Elvidge C.D., (1998), *Remote Sensing Change Detection: Environmental Monitoring Methods and Applications*, Ann Arbor Press: Michigan USA.

[98Lun]   Lunetta V.N. & P. Fensham (Ed.), (1998), *Developments and dilemmas in science education,* The school science laboratory: historical perspectives and centers for contemporary teaching, 169-188, London, Falmer Press.

[02Lov]   Loveland T.R., Sohl T.L., Stehman S.V., Gallant A.L., Sayler K.L. & Napton D.E., (2002), *A strategy for estimating the rates of recent United States landcover changes,* Photogramm Eng Remote Sens 68:1091-1099.

[04Lew]   Lewinski S., & K. Zaremski, (2004), *Examples Of Object-Oriented Classification Performed On High-Resolution Satellite Images*, Miscellanea

Geographic Warszawa, 11:259 - 358.

[78Mul]   M. J. Mulcahy, (1978), *An Investigation into the Use of Maximum Likelihood Classifiers, Decision Trees, Neural Networks and Conditional Probabilistic Networks for Mapping and Predicting Salinity*, Mapping Technology Workshop.

[80Mal]   Malia W., (1980), *Change vector analysis- An approach for detecting forest changes with Landsat,* Machine processing of remotely sensed data and soil information systems and remote sensing and soil survey, 326-336.

[86Mar]   Markham B.L., & Barker, J.L., (1986), *Landsat MSS and TM post-calibration dynamic ranges, Exoatmospheric reflectance and at satellite temperature*s, Earth Observation Satellite Co., Lanham, MD, Landsat Tech. Note 1.

[90Mea]   Meaille R. & L. Wald, (1990), *Using geographic information system and satellite imagery within a numerical simulation of regional urban growth,* International Journal of Geographic information Systems 4:445-456.

[94Muc]   Muchoney, D.M. & Haack, B.N., (1994*), Change Detection for Monitoring Forest Defoliation,* International Photogrammetric Engineering & Remote Sensing, October, ASPRS, Vol. 60, 10, 1243-1251.

[95Mey]   Meyer W.B., (1995*), Past and Present Land-use and Land-cover in the U.S.A.,* Consequences, 24-33.

[97Mae]   Maes F., Collignon A., Vandermeulen D., Marchal G. & Suetens P., (1997), *Multimodality Image Registration By Maximization Of Mutual Information,* IEEE Transactions on Medical Imaging, 16, 187-198.

[98Mac]   Macleod & Congalton, (1998), *A Quantitative Comparison of Change detection, algorithms for Monitoring Eelgrass from Remotely Sensed Data,* Photogrammetric Engineering & Remote Sensing Vol. 64. No.3, 207-216, Environmental Management 59, 47–69.

[99Mar]   Marcel J. Castro, (1999), *Color Image Classification*, Computing Research Conference, December, Pub- 00681.

[99Mos]   Moshen A., (1999), *Environmental Land Use Change Detection and Assessment Using with Multi-temporal Satellite Imagery*, Zanjan University.

[02Mal]   Maldonado, F., J. Santos, et al., (2002), *Land use dynamics in the semi-arid region of Brazil (Quixaba, PE); characterization by principal component analysis (PCA).* International Journal of Remote Sensing 23(23), 5005-5013.

[04Mau]   Lu D., P. Mausel, et al., (2004), *Change detection techniques*, International Journal of Remote Sensing 25(12), 2365-2407.

[90Nor]   Norman P.M., Kjelbom P., Bradley D.J., Hahn M.C. & Lamb C.J., (1990), *Immune-affinity purification and biochemical characterization of plasma membrane arabinogalactan rich glycoproteins of Nicotiana glutinosa,* 181, 365-373.

[94Nic]   Nichol J.E., (1994), *A GIS-based approach to microclimate monitoring in Singapore's high rise housing estates,* Photogramm. Eng. RS. 60, 1225-1232.

[95Nez]   Nezry E., Genovese G., Rémondiére S. & Solaas G., (1995), *Mapping of next season's crops during the winter using ERS SAR*, ESA Earth Observation Quarterly,50, 1-5, Dec.

[05Owo]   Owojori A. & H. Xie, (2005*), Landsat Image-Based Landuse landcover Changes Of San Antonio, Texas Using Advanced Atmospheric Correction And Object-Oriented Image Analysis Approaches*, 5th International Symposium on Remote Sensing of Urban Areas, Tempe, AZ.

[88Pil]   Pilon et al., (1988), *An enhanced Classification Approach to Change Detection in Semi-Arid Environments*, Photogramm. Eng. Rem. Sens. 45 (12), 1709-1716.

[93Pra]   Prata A.J., (1993), *Land surface temperatures derived from the advanced very high resolution radiometer and the along-track scanning radiometer*, Journal of Geophysical Research.

[98Poh]   Pohl C. & Van Genderen J.L., (1998), *Multi-sensor Image Fusion In Remote Sensing: concepts, methods and applications*, International Journal of Remote Sensing, 19, 823-854.

[07Pee]   Peel M. C., Finlayson B. L., & McMahon T. A., (2007), *Updated world map of the Köppen-Geiger climate classification,* Hydrol. Earth Syst. Sci., 11, 1633-1644.

[97Qua]   Lo C.P., Quattrochi D.A., & Luvall, J.C., (1997), *Application of high-resolution thermal infrared remote sensing and GIS to assess the urban heat island effect,* International Journal of Remote Sensing, 18, 287– 304.

[99Qua]   D.A. Quattrochi & J.C. Luvall, (1999), *Thermal infrared remote sensing for analysis of landscape ecological processes: Methods and applications,* Land Science Ecology, vol. 14, 6, 577–598, Dec.

[04Qua]   D.A. Quattrochi & J.C. Luvall, (2004), *Thermal Remote Sensing in Land Surface Processes,* Boca Raton, FL: CRC Press, 440.

[94Rie]   Riebsame W.E., Meyer, W.B., & Turner, B.L.II., (1994), *Modeling Land-use and Cover as Part of Global Environmental Change,* Climate Change. Vol. 28, 45.

[04Rog]   Rogan J. & D. Chen, (2004), *Remote sensing technology for mapping & monitoring landcover and land-use change*, Progress in Planning, 61, 301-325.

[06Ric]   Richards J. & X. Jia, (2006), *Remote Sensing Digital Image Analysis,* An Introduction, 4th Ed., Springer.

[07Rym]   Rymasheuskaya M., (2007), *Land cover change detection in northern Belarus,* ScanGIS'2007-11th Scandinavian Research Conference on Geographical Information Science, Norway, Department of Mathematical Sciences and Technology, UMB, Postbooks 5003, N-1432, Norway.

[89Sin]   Singh A., (1989), *Digital Change Detection Techniques Using Remotely Sensed Data,* International Journal of Remote Sensing. Vol. 10, 6, 989-1003.

[94Sho]   Shoshany, M, et al., (1994), *Monitoring Temporal Vegetation Cover Changes in Mediterranean and Arid Ecosystems Using a Remote Sensing Technique*, Case study of the Judean Mountain and the Judean Desert. Journal of Arid Environments, 33, 9-21.

[96Sob]   Sobrino J.A., Li Z., Stroll M.P., & Becker F., (1996), *Multichannel and multi-angle algorithm for estimating sea and land surface temperature from ASTER data*, Int. J. Remote Sens. 17 2089–2114.

[97Sab]   F. Sabins, (1997), *Remote Sensing, Principles and Interpretation,* W.H. Freeman and Company, New York.

[99Ser]   Serpico S.B., Bruzzone L., (1999), *Change detection, In: Information Processing for Remote sensing,* Eds C.N.Chen, World Scientific Publishing Co.: Singapore, Ch. 15, 319-336.

[00Sob]   Sobrino J. & N. Raissouni (2000*). Toward remote sensing methods for land cover dynamic monitoring; application to Morocco,* International Journal of Remote Sensing 21(2):353-366.

[09Tan]   Tanmoy Das, (2009), *Land Use/Land Cover Change Detection: an Object Oriented Approach, Münster, Germany,* Master Thesis of Science in Geospatial Technologies, Institue for geoinformatics, Univeristy of Munster, Germany, March.

[01Tso]   Tso B. & P. Mather (2001). Classification Methods for Remotely Sensed Data, CRC Press.

[77Wei]   Weismiller R. A., Kristof, S. J., Scholz, D. K., Anuta, P. E., & Momen, S. A., (1977), *Change detection in coastal zone environments,* Photogrammetric Engineering and Remote Sensing, 43, 1533–1539.

[89Wuk]   Wukelic G.E., Gibbons D.E., Martucci L.M. & Foote H.P., (1989), *Radiometric Calibration of Landsat Thematic Mapper Thermal Band Data*, Remote Sens. Environ. 28, 339-347.

[96Wil]   Wilkie D.S., & Finn J.T., (1996), *Remote Sensing Imagery for Natural Resources Monitoring,* Columbia University Press, New York, 295.

[01Wen]   Weng Q., (2001), *A remote sensing-GIS evaluation of urban expansion and its impact on surface temperature in the Zhujiang Delta, China,* International Journal of Remote Sensing 22 (10), 19992014.

[04Wen]   Weng Q., Lu D. & Schubring J., (2004), *Estimation of land surface temperature vegetation abundance relationship for urban heat island studies,*Remote sensing of Environment 89 (4), 467483.

[04Wan]   Wang L., Biging G.S. & Gone P., (2004), *Integration of object-based and pixel-based classification for mapping mangroves with IKONOS imagery*, International Journal of Remote Sensing, 25, 5655–5668.

[08Wen]   Weng Q. & Lu D., (2008), *A sub-pixel analysis of urbanization effect on land surface temperature and its interplay with impervious surface and vegetation coverage in Indianapolis, United States,* International Journal of Applied Earth Observation and Geoinformation 10 (1), 6883.

[99Xia]   Xiaomei Y & Ronqing L.Q. Y, (1999), *Change Detection Based on Remote Sensing Information Model and its Application to Coastal Line of Yellow River Delta,* Earth Observation Center, NASDA, China.

[99Yeh]   Yeh A.G.O. & Li X., (1999), *A Decision Support System for Sustainable Land Development: A Case Study in Dongguan, Kersten, Gregory, Mikolajuk, Zbigniew, Rais, Mohammand and Yeh, Anthony (eds.), Decision Support System for Sustainable Development, Ottawa*, International Development Research Centre (IDRC), 73-98.

[02Yan]   Yang X. & Lo C., (2002), *Using satellite imagery to detect land use land cover changes in Atlanta, Georgia metropolitan area,* International Journal of Remote Sensing. 23, 1775-1798.

[02Yan]   Yannis S. Avrithis & Stefanos D. Kollias, (2002), *Fuzzy Image Classification Using Multiresolution Neural Networks with Applications to Remote Sensing*, Proceeding of 5th Remote Sensing of Environment, 82, 123-134.

[02Yon]   Yong Du, et al, (2002), *Radiometric Normalization of Multitemporal High-Resolution Satellite Images with Quality Control for Land Cover Change Detection,* Proceeding of 5th Remote Sensing of Environment, 84, 138-140.

[04Zha]   W. Zhang, M. Liao, Y. Wang, L. Lu & Y. Wang, (2004), *Robust Approach to the MAD Change Detection Method*, Proceeding of the 11th SPIE International Symposium on Remote Sensing X, vol. 5574 September, 184–193.

[06Zha]   Zhang C.L., Pearson A., Li Y.-L., Mills G. & Wiegel J., (2006), *A thermophilic temperature optimum for crenarchaeol and its implication for archaeal evolution,* Appl. Environ. Microbiol. 72: 4419-4422.

[06Zub]   Zubair Ayodeji, (2006), *Change Detection in Land Use and Land Cover Using Remote Sensing Data and GIS (A case study of Ilorin and its environs in Kwara State*, Thesis for MSc Degree in Geographical Information Systems, Department of Geography, University of Ibadan, October.

Web References

[1]   http://www.esri.com/software/arcgis

[2]   http://www.exelisvis.com/ProductsServices/ENVI.aspx

[3]   http://www.restec.or.jp/?page_id=10666

[4]   http://www.kankyo.metro.tokyo.jp/en/greenery/fund.html

[5]   NASA Web, (http://www.nasa.gov/audience/forstudents/index.html)

[6]   USGS website, (http://glovis.usgs.gov/)

[7]   Mandalay City, (http://en.wikipedia.org/wiki/Mandalay)

[8]   Climate Information for Mandalay City, (http://worldweather.wmo.int/180/c00588.htm)

[9]   Hino City official Website, (http://www.city.hino.lg.jp)

[10]   Tokyo, (http://en.wikipedia.org/wiki/Tokyo)

[11]   http://www.crisp.nus.edu.sg/~research/tutorial/intro.htm